

**ÇUKUROVA UNIVERSITY
INSTITUTE OF NATURAL AND APPLIED SCIENCES**

MSc THESIS

Zeynep DEMİRAY

**HYDROGEOLOGY OF VALCO SAN PAOLO (ROME-ITALY):
GROUNDWATER MODELLING APPROACH WITH
MODFLOW-2005**

DEPARTMENT OF GEOLOGICAL ENGINEERING

ADANA, 2010

ÇUKUROVA UNIVERSITY
INSTITUTE OF NATURAL AND APPLIED SCIENCES

**HYDROGEOLOGY OF VALCO SAN PAOLO (ROME-ITALY):
GROUNDWATER MODELLING APPROACH WITH MODFLOW-2005**

Zeynep DEMİRAY

MSc THESIS

DEPARTMENT OF GEOLOGICAL ENGINEERING

We certify that the thesis titled above was reviewed and approved for the award of degree of the Master of Science by the board of jury on 21/12/2010.

.....
Assoc. Prof. Dr. Sedat TÜRKMEN
SUPERVISOR

.....
Asist.Prof.Dr. Hakan GÜNEYLİ
MEMBER

.....
Assist.Prof.Dr. Zübeyde HATİPOĞLU
MEMBER

.....
Assoc. Prof. Dr. Cüneyt GÜLER
MEMBER

.....
Assoc. Prof. Dr.İ.Altay ACAR
MEMBER

This MSc Thesis is written at the Department of Institute of Natural And Applied Sciences of Çukurova University.

Registration Number:

Prof. Dr. İlhami YEĞİNGİL
Director
Institute of Natural and Applied Sciences

Not: The usage of the presented specific declarations, tables, figures, and photographs either in this thesis or in any other reference without citation is subject to "The law of Arts and Intellectual Products" number of 5846 of Turkish Republic

ABSTRACT

MSc THESIS

HYDROGEOLOGY OF VALCO SAN PAOLO (ROME-ITALY): GROUNDWATER MODELLING APPROACH WITH MODFLOW-2005

Zeynep DEMİRAY

**ÇUKUROVA UNIVERSITY
INSTITUTE OF NATURAL AND APPLIED SCIENCES
DEPARTMENT OF GEOLOGICAL ENGINEERING**

Supervisor	: Assoc. Prof. Dr. Sedat TÜRKMEN
2nd supervisor	: Dr. Francesco LA VIGNA
Year	: 2010, Pages : 109
Jury	: Assoc. Prof. Dr. Sedat TÜRKMEN : Assoc. Prof. Dr. Cüneyt GÜLER : Assoc. Prof. Dr. İ. Altay ACAR : Asst. Prof. Dr. Hakan GÜNEYLİ : Asst. Prof. Dr. Zübeyde H. BAĞCI

The Valco S. Paolo site may be regarded as representative of the main Tiber valley in the urban area of Rome, which is located 2 km south of the city center. In recent years, as per level, temperature and electrical conductivity measurements conducted in gravel and sand aquifers have notable variations. For this purpose, heads observed from 15 piezometers and physical characteristic data of sand and gravel aquifers were monitored in 5 piezometers in the Tiber river by dataloggers during 4 months and integrated with available geological and hydrogeological information to develop a conceptual model of the system. These fundamental information are required to characterize the existing groundwater system in this area in order to establish a groundwater flow model.

The validation of the conceptual model by a steady-state numerical groundwater flow model reveals that minimum change occur in the center. Trial and Error calibration method has been applied to this model. Before and after the model calibration the average of residuals were 0,6 m and 0,15 m, respectively. After the calibration stage; the model verified with additional measurements and the average of residuals reduced to 0,18 m. The calibrated model had been used to simulate a different set of field measurements and the verification showed a good degree of confidence.

Key Words: Tiber river, groundwater, modeling, Modflow-2005, calibration

ÖZ

YÜKSEK LİSANS TEZİ

VALCO SAN PAOLO (ROMA-İTALYA) BÖLGESİNİN HİDROJEOLOJİSİ: MODFLOW-2005 İLE YERALTI SUYU MODELLEMESİ

Zeynep DEMİRAY

ÇUKUROVA ÜNİVERSİTESİ FEN BİLİMLERİ ENSTİTÜSÜ JEOLOJİ MÜHENDİSLİĞİ ANABİLİM DALI

Danışman : Doç. Dr. Sedat TÜRKMEN
II. Danışman : Dr. Francesco LA VIGNA
Yıl : 2010, Sayfa: 109
Jüri : Doç. Dr. Sedat TÜRKMEN
: Doç. Dr. Cüneyt GÜLER
: Doç. Dr. İ. Altay ACAR
: Yrd. Doç. Dr. Hakan GÜNEYLİ
: Yrd. Doç. Dr. Zübeyde H. BAĞCI

Roma şehir merkezinin 2 km güneyinde bulunan Valco San Paolo bölgesi, Tiber vadisini temsil edecek örnek yerlerden biridir. Son yıllarda, taban konglomerası ve kum akiferinde ölçülen seviye, sıcaklık ve elektriksel iletkenlik değerlerinde dikkate değer değişimler gözlenmiştir. Bu nedenle bölgede 15 adet piyezometrede ölçümler yapılmış ayrıca Tiber nehri ile birlikte bu kuyulardan 5 tanesi 4 ay boyunca izlenmiş sonuç olarak ise elde bulunan veriler, jeolojik ve hidrojeolojik veriler ile birleştirilerek sistemin bir kavramsal modeli oluşturulmuştur. Bu temel veriler, bölgedeki yeraltı suyu sistemi karakterinin geçerli bir sayısal akış modelini oluşturmak için gerekli görülmüştür.

Kavramsal modelin geçerliliği açısından, dengeli durumda çalıştırılan model, minimum değişimlerin çalışma alanı merkezinde, bölgedeki maksimum düşümlerin ise düşük hidrolik iletkenlikli bölgelerde meydana geldiği ortaya çıkmıştır. Kalibrasyon aşamasında deneme - yanılma metodu uygulanmıştır. Kalibre edilmeden önce ve edildikten sonraki hata ortalaması sırasıyla 0,6 m ve 0,15 m ölçülmüştür. Model sağlamasında, kalibrasyonu yapılmış simülasyon, farklı bir güne ait arazi ölçümleriyle tekrar çalıştırılıp karşılaştırılması yapıldığında benzer sonuçlar verdiği görülmüştür.

Anahtar Kelimeler: Tiber nehri, yeraltı suyu, modelleme, Modflow-2005, kalibrasyon

ACKNOWLEDGEMENTS

I would like to thank to my research supervisor, Assoc. Prof. Dr. Sedat TÜRKMEN, for his support during my graduate education.

I am truly grateful to my 2nd supervisor, Dr. Francesco LA VIGNA for his guidance, support from all points of view and devotion of invaluable time throughout my research activities and the preparation of this thesis.

I would like to express my special thanks to Prof. Dr. Guiseppe CAPELLI and Dr. Roberto MAZZA on their allowance to work in the laboratory and to use all sorts of documents and data in order to develop this thesis.

I am thankful to all MSc and PhD students at the Numerical and Quantitative Hydrogeology Laboratory (LinQ) of Geological Sciences Department of Roma TRE University for their helps during the work.

Special thanks to my dear friends Aslihan KISACIK, Tolga RUŞEN and project assistants at Geological Engineering Department of Çukurova University for their continuous support and motivation.

Another point that should be emphasized here is the all spiritually and materially support including continuous moral, motivation, encouragement and patience of my mother E. Piraye DEMİRAY and my father R. Erdoğan DEMİRAY and my sister Ayşen YILMAZ throughout my scientific efforts.

CONTENTS	PAGE
ABSTRACT	I
ÖZ	II
ACKNOWLEDGEMENTS	III
CONTENTS	IV
LIST OF TABLES.....	VI
LIST OF FIGURES	VIII
ABBREVIATIONS AND NOMENCLATURES.....	XIV
1. INTRODUCTION	1
1.1. Geological Setting of Roman Area	2
1.2. General Hydrogeological Setting of Rome.....	8
1.3. Specific Geology of Valco San Polo.....	11
1.4. Hydrogeological Setting of Valco San Paolo	14
1.5. Groundwater modelling	16
2. PREVIOUS STUDIES.....	17
3. MATERIALS AND METHODS	21
3.1. MATERIALS	21
3.1.1. Collection of thematic maps	21
3.1.2. Groundwater monitoring instruments – dataloggers.....	24
3.2. METHODS.....	26
3.2.1. Compilation of data.....	28
3.2.2. Conceptual model	29
3.2.3. The computer code.....	29
3.2.3.1. Groundwater flow equation	29
3.2.3.2. Finite-difference approach for groundwater flow equation	30
3.2.3.3. Derivation of finite-difference equation	31
3.2.3.4. River - aquifer interaction.....	34
3.2.3.5. Construct a steady-state groundwater flow model - Defining boundary conditions	35

3.2.4. Calibrating the model and perform a sensitivity analysis.....	35
3.2.5. Making predictive simulations and perform a postaudit.....	36
4. RESULTS AND DISCUSSION.....	37
4.1. Geological interpretation	37
4.1.1. Sediment survey of Tiber valley in Valco San Paolo	37
4.1.2. Creating surfaces with ArcMap 9.2	56
4.2. Hydrological and hydrogeological survey.....	69
4.2.1. Monitoring results in Valco San Paolo	69
4.2.2. Physical analysis of groundwater	72
4.3. Hydrogeological Conceptual Model	83
4.4. Numerical Model.....	86
4.4.1. Grid construction and layer discretization.....	86
4.4.2. Boundary conditions	90
4.4.3. Steady-state model calibration	94
5. CONCLUSION.....	101
REFERENCES	103
CURRICULUM VITAE.....	109

LIST OF TABLES	PAGE
Table 4.1. Attributes of boreholes	56
Table 4.2. Static level measurements of wells in sand aquifer	77
Table 4.3. Static level measurements of wells in gravel aquifer	78
Table 4.4. Head observations of the piezometers in sand.....	91
Table 4.5. Head observations of the piezometers in gravel	91
Table 4.6. Pumping rates of wells	92
Table 4.7. Calibration parameters used in model and intervals	95

LIST OF FIGURES	PAGE
Figure 1.1. Location map of the study area.....	2
Figure 1.2. Central coastal Latium paleogeography, about in the late Pliocene time (view northward)	3
Figure 1.3. Pleistocene evolution of the Roman area.....	5
Figure 1.4. Geological map of Rome.....	6
Figure 1.5. Lithostratigraphic units of the study area.....	7
Figure 1.6. Hydrogeologic map of the Roman area	9
Figure 1.7. Geological section of the Tiber valley at Valco S.Paolo and location of hole S1	12
Figure 1.8. Geological sketch of Grottaperfetta valley.....	13
Figure 1.9. Lithotypes in the study area	14
Figure 1.10. Hydrogeological units of the area.....	15
Figure 3.1. Topographic map of the study area no° 374102.....	20
Figure 3.2. Visualization of the Excel file including borehole properties.....	21
Figure 3.3. Depth of bedrock in the study area	22
Figure 3.4. General water table of Rome	22
Figure 3.5.a. Multiparametric instrument (with pH, Cond, T° probe), b. Measuring the depth of piezometer manually with line	23
Figure 3.6. Measurement from a piezometer in Science Geology Department	23
Figure 3.7. CTD-diver dataloggers used in the study.....	24
Figure 3.8. Flow chart of the modeling process.....	26
Figure 3.9. A discretized hypothetical aquifer system	30
Figure 3.10. Indices for the six adjacent cells surrounding cell i,j,k.	31

Figure 3.11. Flow into cell i,j,k from cell i,j-1,k	32
Figure 4.1. Holocene alluvium limit in the area with location of selected boreholes.....	37
Figure 4.2.a. Location of recent boreholes drilled by private companies, b. A view from drillings no° SA, SB, SC.....	38
Figure 4.3. Location of the cross sections and the ancient Tiber River's left-bank tributary; Grotta Perfetta stream.....	39
Figure 4.4. Cross section No°1.....	41
Figure 4.5. Cross section No°2.....	43
Figure 4.6. Cross section No°3.....	45
Figure 4.7. Cross section No°4.....	47
Figure 4.8. Cross section No°5.....	49
Figure 4.9. Cross section No°6.....	51
Figure 4.10. Cross section No°7.....	53
Figure 4.11. Terrain elevation contour map.....	58
Figure 4.12. Boreholes displayed with bottom elevation values (asl) of lithotypeR.....	59
Figure 4.13. Contoured IDW map of bottom of lithotype R.....	60
Figure 4.14. Boreholes displayed with top elevation values of lithotype B	61
Figure 4.15. Additional with original boreholes for lithotype B.....	61
Figure 4.16. Contoured IDW top elevation map of lithotype B.....	62
Figure 4.17. Boreholes displayed with top elevation values of lithotype C	63
Figure 4.18. Additional with original boreholes for lithotype C.....	63
Figure 4.19. Contoured IDW top elevation map of lithotype C.....	64

Figure 4.20. Boreholes displayed with top elevation values of lithotype G	65
Figure 4.21. Additional with original boreholes for lithotype G	65
Figure 4.22. Contoured with IDW method top elevation map of lithotype G	66
Figure 4.23. Boreholes displayed with top elevation values of Monte Vaticano Unit	67
Figure 4.24. Additional with original boreholes for Monte Vaticano Unit	67
Figure 4.25. Contoured with IDW method top elevation map of Monte Vaticano Unit	68
Figure 4.26. Location of (a) piezometers (b) Tiber datalogger.....	69
Figure 4.27. Installing datalogger in Tiber River.....	70
Figure 4.28. Monitoring wells.....	71
Figure 4.29. Hourly groundwater level variation in gravel.....	72
Figure 4.30. Hourly water temperature variation in gravel.....	72
Figure 4.31. Hourly conductivity variations of the piezometer in gravel.....	73
Figure 4.32. Log profile of well P4; a. T(oC), b. pH and c. EC(mS/cm) measurement (Department of Geological Sciences, RomaTRE University 16/07/2009)	74
Figure 4.33. Hourly Tiber river level variation.....	75
Figure 4.34. Hourly level variations of the piezometers in sand compared with Tiber river variations	75
Figure 4.35. Hourly temperature variations of the piezometers in sand compared with Tiber variations.....	76
Figure 4.36. Hourly electrical conductivity variations of the piezometers in sand..	76
Figure 4.37. River stage gradient along the Tiber River	79

Figure 4.38. Water table map of sand aquifer	80
Figure 4.39. Potentiometric level map of gravel aquifer	81
Figure 4.40. The Hydrogeological conceptual model	84
Figure 4.41. 3D visualization of top model topography	85
Figure 4.42. Displayed active domain limit of the model	86
Figure 4.43. Formula for “Sand_Bottom” data set.....	86
Figure 4.44. Modflow layer groups tab	87
Figure 4.45. The values shown above were defined as HK parameters under LPF package in MODFLOW	88
Figure 4.46. a. Schematic view of vertical grid discretization, b. initial general hydraulic conductivity values of the starting simple Valco S.Paolo model	89
Figure 4.47. Constant head boundaries of convertible aquifers from Layer 1 to 4.....	90
Figure 4.48. Constant head boundary of confined basal gravel aquifer	90
Figure 4.49. Head observation locations with Tiber river head change	92
Figure 4.50. Water budget of the steady-state model without pumping.....	93
Figure 4.51. PCG Pane dialog box	94
Figure 4.52. Water budget of the steady-state model with pumping.....	94
Figure 4.53. Comparison between observed and simulated heads of first model execute before calibration with pumping rates.....	96
Figure 4.54. Calibrated Valco S. Paolo model fitting	96
Figure 4.55. Calibrated observed-simulated values and residuals	97

Figure 4.56. Observed and simulated hydraulic heads distribution of sand aquifer	97
Figure 4.57. Observed and simulated hydraulic heads distribution of gravel aquifer	98
Figure 4.58. Observed-simulated head values and residuals with measurings of date 28.05.2010 to verify the model.....	99

ABBREVIATIONS AND NOMENCLATURES

m	: meter
km	: kilometer
SMVD	: Sabatini mountains volcanic district
AHVD	: Albani hill volcanic district
a.s.l.	: above sea level
UMV	: Monte Vaticano unit
k	: permeability
L	: liter
GW	: groundwater
MODFLOW	: MODular groundwater FLOW model

1. INTRODUCTION

The study area, Valco San Paolo district, is located in the south of Rome urban area along the Tiber River, and the development of a groundwater model has made necessary to study the groundwater circulation because of the new construction of important buildings. The aim is to analyse the hydrogeological setting of the Valco San Paolo area and to realize a preliminary steady state groundwater model in order to verify the goodness of the conceptual model of circulation.

The proposed preliminary model can be used as a starting point for projects to be conducted in the Tiber River alluvium or for defining a specific approach to technical problems linked to these projects. Moreover, recently the Department of Geology of RomaTRE University is working on an important low enthalpy geothermal project, and the Valco San Paolo has been selected as a test-site.

Valco S. Paolo area, which is crossed by the Tiber River, is located about 2 km southwest of Rome's historical centre. The ~6,5 km²-large study area; 3 km long and 1.5 km wide, at most is situated between 41°50'35,761"N and 41°50'38,2"N latitudes and 12°27'23,855"E and 12°27'27,277"E longitudes (Figure 1.1) The main alluvial deposits lie in an area with smoothly undulating topography together with deposits of a left-bank tributary of Tiber valley.

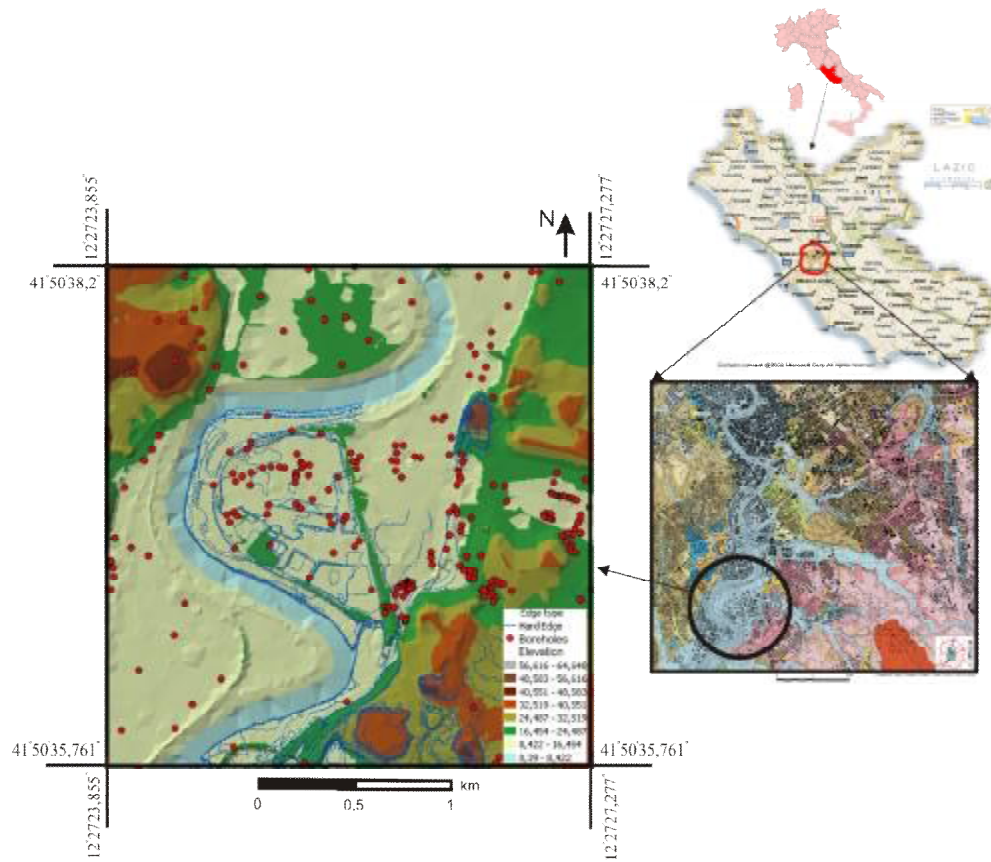


Figure 1.1. Location map of the study area

1.1. Geological Setting of Roman Area

The oldest sediments outcropping in the city are represented by the “Monte Vaticano Unit”, which is characterised by Middle-Upper Pliocene grey-blue clays (Marra and Rosa 1995; Carboni and Iorio 1997) with decimetric-scale intercalations of sands. The Monte Vaticano Unit affects the whole structural setting of the city of Rome and outcrops predominantly in the right bank of the Tiber River, at the base of the hills of Monte Mario, Vaticano and Gianicolo and represents the continuous bedrock of the Rome area (Bozzano et al, 2000).

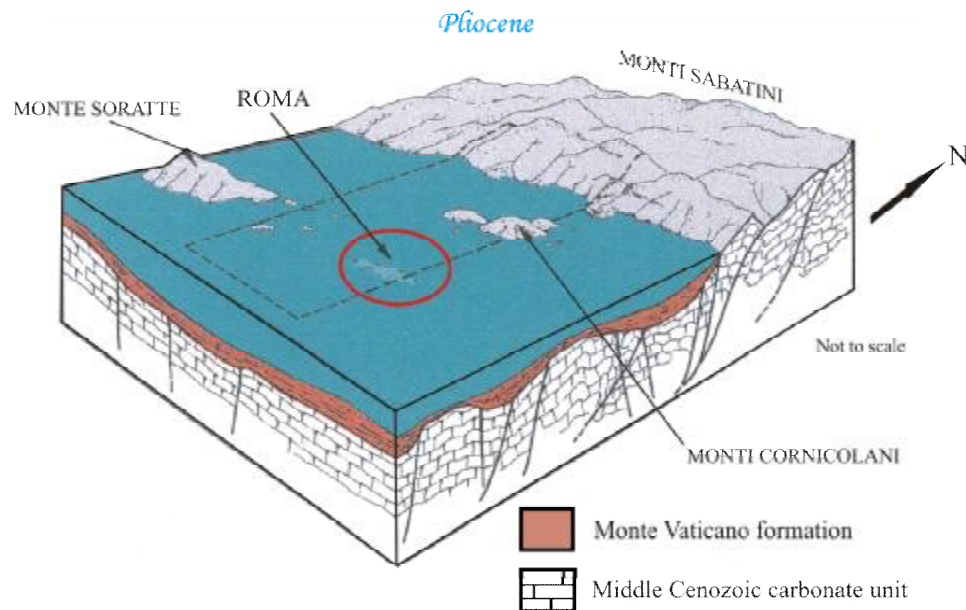


Figure 1.2. Central coastal Latium paleogeography, about in the late Pliocene time (view northward) (Progetto strategico Roma capitale. C.N.R., Design of M.Parotto, 1990)

Lower Pleistocene “Monte Mario”, “Monte Ciocci” and “Monte delle Piche” Units are overlying this substratum (Fig.1.2). The first and last units are marine sediments, whereas the middle is a 10- to 20-m-thick epicontinental deposit of gravels and sands whose stratigraphical unit is still being debated in the literature (Ambrosetti and Bonadonna, 1967; Marra,1993; Bellotti et al. 1994). The dominant feature on the Tiber River's right bank is the “Monte Mario” ridge. It lies parallel to the Tiber valley and reaches nearly 140 m a.s.l.; to the south, it is 60 m a.s.l. Monte Mario is made up of Plio-Pleistocenic marine deposits pertaining to the “Monte Vaticano” and “Monte Mario” Units (Funicciello et al., 2004).

These marine deposits are exposed at the base of the “Monte Mario” ridge. To the east and west of the ridge the Monte Vaticano Unit lies at various depths in paleogeomorphologic depression in tectonically deformed bedrock (Campolunghi et al, 2007). Above those marine sequences, can be followed the change from marine to coastal, then to continental sedimentation. This is an effect of the Apennine and its Tyrrhenian margin uplift.

The continental and coastal facies trace the flow of an old river called Paleotiber, which was parallel to the coast running SE along a continuously subsiding belt, producing conglomerate deposits tens of metres thick. From the Middle Pleistocene pyroclastic deposits erupted from an intense volcanic activity of the SMVD (Sabatini mountains volcanic district-30 km north west of Rome) and AHVD (Albani hill volcanic district-25 km south east of Rome) reached the area of Rome and overlie the sediments. The city of Rome has been developed in an area of the lower Tiber River valley between the Alban Hills Volcanic District (AHVD) to the southeast and the Sabatini Mountains Volcanic District (SMVD) to the northwest (Campolunghi et al., 2007).

The geomorphological and hydrogeological setting was deeply modified by this volcanic activity. The Paleotiber's course was deviated until arrived the present-day position within the boundary between the Albani and Sabatini products. The last glacial lowstand was 120 m below today's level. This event produced a deepening of the Tiber's course and its tributaries' as they eroded first the volcanic deposits, followed by the continental Paleotiber's deposits then, carving deeply into the underlying and well-consolidated "MonteVaticano" Unit (Campolunghi et al., 2007).

When the sea level rose, the deep gorges were infilled by alluvial deposits (Funciello, 1995), which are the main units of our study area. (Figure 1.3.)

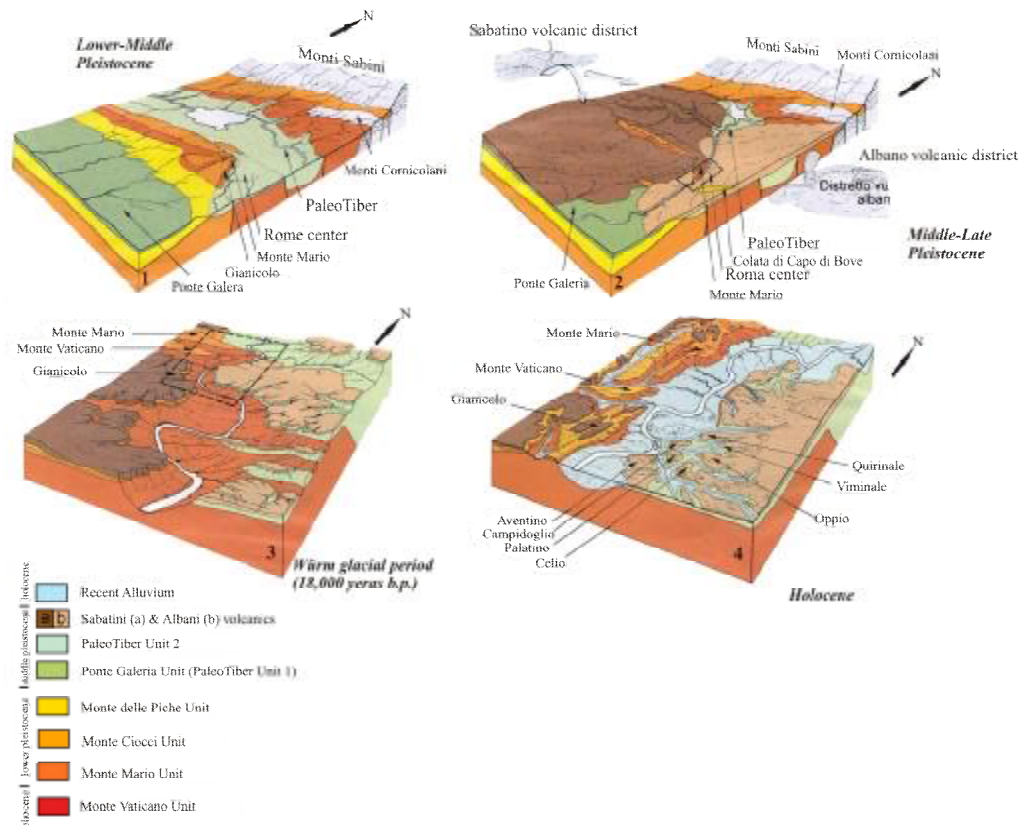


Figure 1.3. Pleistocene evolution of the Roman area (Progetto strategico Roma capitale. C.N.R.,M.Parotto, 1990)

As a consequence, the Lower Pleistocene sediments are absent on the left bank of the Tiber River in the Roman area and the Middle Pleistocene continental deposits (Paleo-Tiber unit 2) directly overlie the erosional surface of the Pliocene substratum (i.e. the Monte Vaticano Unit) (Bozzano et al., 2000).

The succession of these events created the present-day terrain of the city of Rome: the area consists of a central plain, which is the Tiber's alluvial plain; the relief on the river's right bank is the “Monte Mario”-“Monte Vaticano” structural high; at the Tiber's left bank lies an articulated area that, in the historical city center, corresponds to the famous “Seven Hills” of Rome (Funicello et al., 2004).

The urban area of Rome is therefore characterised on the left bank of the Tiber River alluvial plain by volcanic products overlying the continental deposits of the Paleo-Tiber and on the right bank almost exclusively by marine Pliocene-Pleistocene deposits (Figure 1.4).

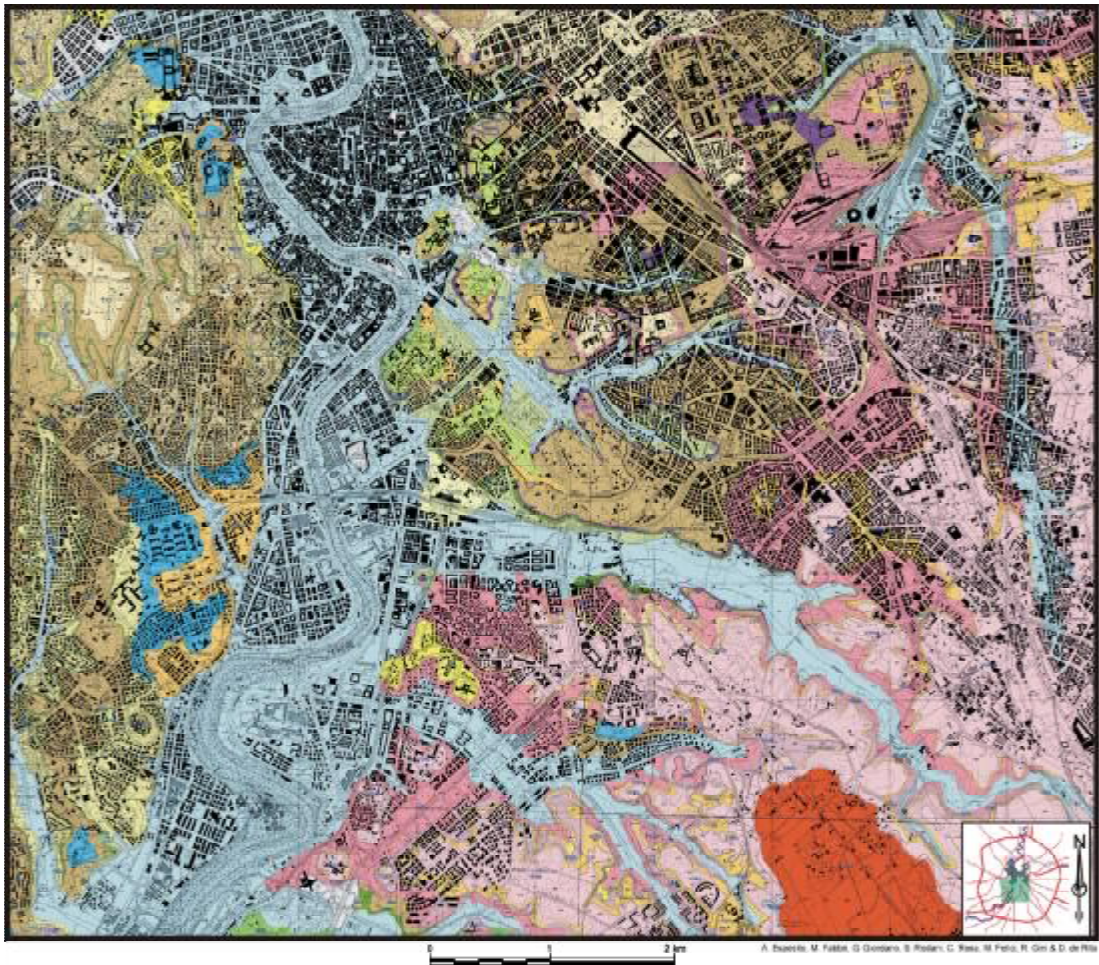


Figure 1.4. Geological map of Rome (Giordano et al.,2004)
(for legend see Fig.1.5)

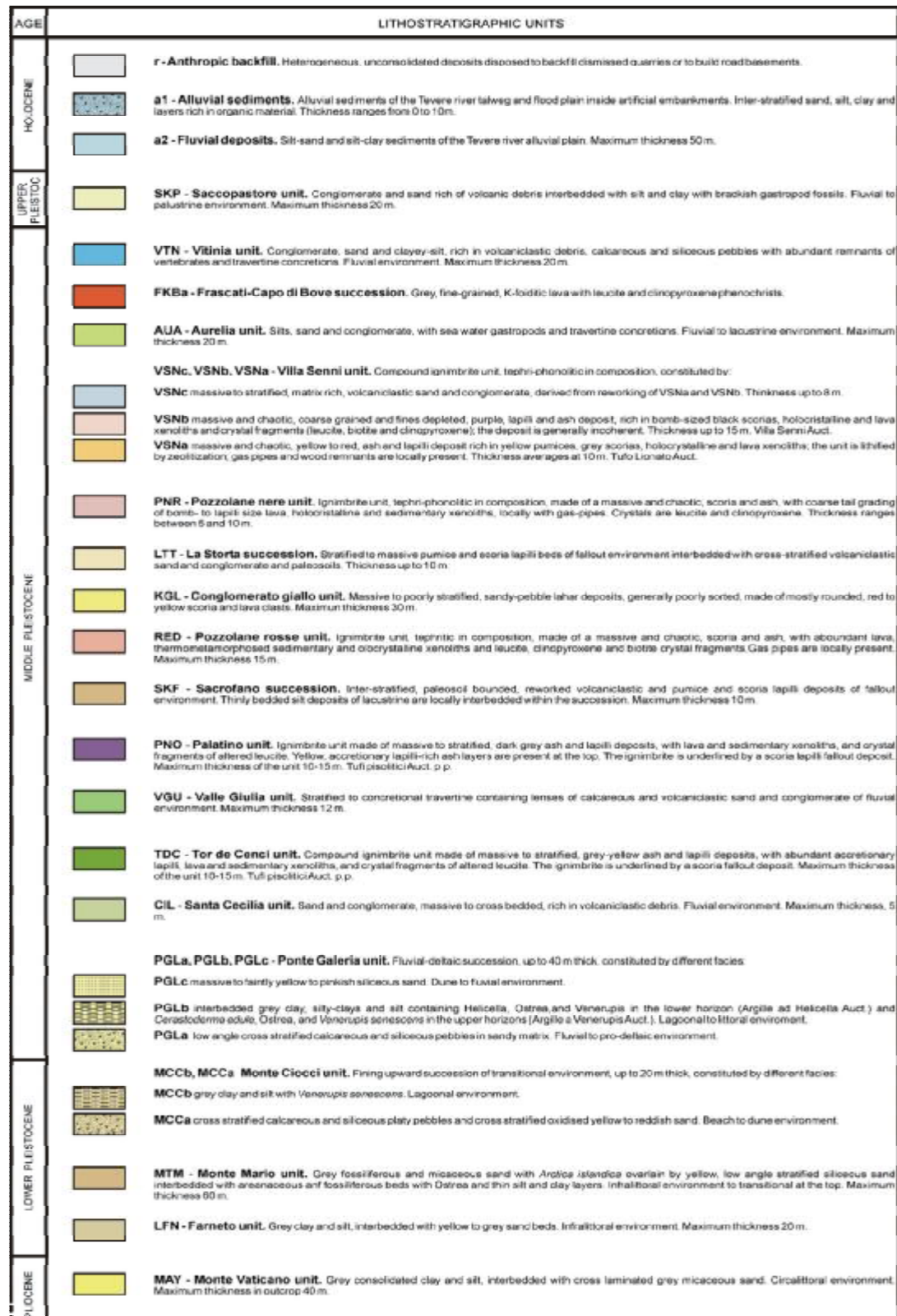


Figure 1.5. Lithostratigraphic units of the study area

1.2. General Hydrogeological Setting of Rome

The hydrogeologic framework of the Monte Vaticano Unit, which is the major regional aquiclude underlying the shallow hydrogeologic units, is hundreds of meters thick and has a very low permeability (Ventriglia, 1971, 1990, 2002; Albani et al., 1972; Boni et al., 1988; Corazza and Lombardi, 1995; Funicello and Giordano, 2005; Capelli et al., 2005). The nearly impermeable bedrock is overlain by Lower to Middle Pleistocene marine to continental sediments (claystones, sandstones, and thick sequences of conglomerates), which are in turn overlain by and partly interfingered with Middle to Upper Pleistocene volcanic deposits from the Sabatini volcanic complex to the north and the Colli Albani volcanic complex to the south (Funicello and Giordano, 2005; Capelli et al., 2005).

Moreover on a regional scale, the Pliocene - Lower Pleistocene marine claystone aquiclude overlies a deep aquifer in highly deformed Mesozoic - Cenozoic carbonates (Boni et al., 1988), which is recharged from the Apennine region. Tectonic and volcano-tectonic discontinuities control groundwater flow on a local scale, as well as gas and fluid leakage from the deeper Mesozoic - Cenozoic carbonate reservoir, as evidenced by the presence of several low - to medium - enthalpy hydrothermal springs in Rome's surroundings (eg., Tivoli) (Funicello et al., 2003; Carapezza et al., 2003; Tuccimei et al., 2006).

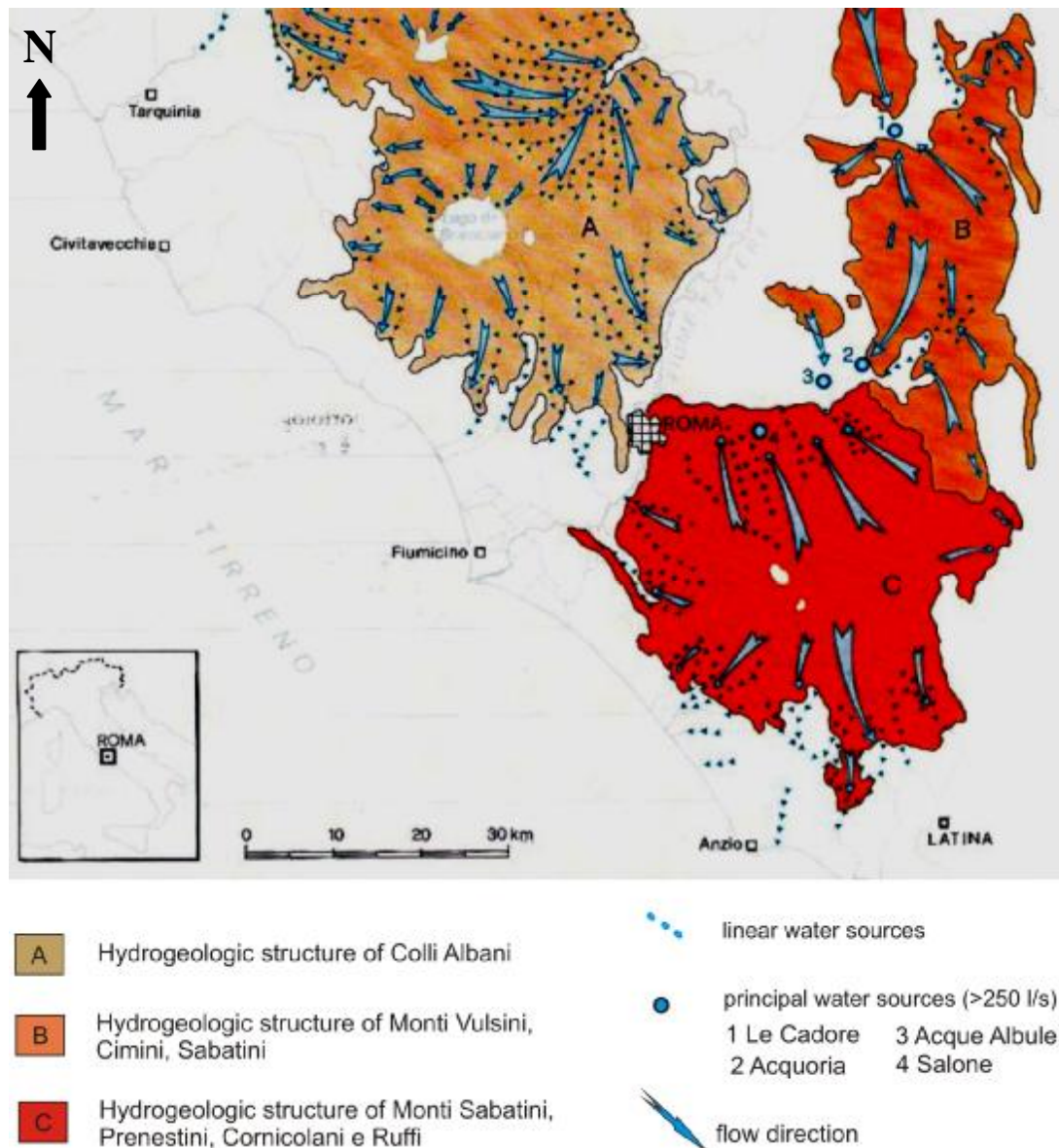


Figure 1.6. Hydrogeologic map of the Roman area (Boni et al, 1986)

Major aquifers around Rome can be found in interbedded pyroclastic deposits (ignimbrites, surge and fall deposits, and reworked pyroclastic materials) and lavas. The volcanic aquifers are characterised by good permeability as a whole (primary permeability in tuffs and secondary in lavas, although considerable variation in permeability may be found among different deposits (Capelli et al., 2000; 2005). Fractured lavas embedded in generally lower-permeability tuffs represent preferential groundwater drainage pathways.

The volcanic deposits host many aquifers at different depths. The main aquifer is located at the base of the volcanic pile, and is confined by either the oldest low-permeability volcanic products or by the Pliocene - Pleistocene marine sediments. Above the main aquifer, many local perched aquifers can be found confined at the base by low-permeability pyroclastics and thick paleosoils. Aquifers are generally unconfined because of the lateral discontinuity of impermeable layers, although confined aquifers, especially thick lava-flow units, can be found locally (Capelli, et al., 2005).

To the east and south of the Tiber River, volcanic deposits belong to the Colli Albani volcanic complex, and the main aquifer flows radially outward from the volcano reaching the southern and eastern suburbs of Rome. The river system and springs in the area, which supply much of the potable water in the Roman area, gain water from the main aquifer. Examples include the Acqua Vergine spring, which presently has a discharge of 600 L/s (and was 1200 L/s during classical Roman times) and drains water from lavas, or the many springs utilized by the Appio and Augusto aqueducts of the ancient Romans, which discharged more than 1000 L/s (presently ~600 L/s). In the city center, a number of small springs are fed by water from a localized shallower aquifer (important for the local history and economy) (Coppa et al., 1984; Pisani Sartorio and Liberati, 1986; Corazza and Lombardi, 1995). North of the Aniene River, some springs with few liters per second of discharge gain water from the aquifer that flows toward the Tiber and Aniene Rivers.

West of the Tiber River, volcanic deposits mainly belong to the Sabatini volcanic complex, and thin southward toward Rome. The aquifer flows radially away from the volcanic complex, i.e., from the northwest (where it reaches the surface at the Bracciano and Martignano lakes) to the south-southeast (Boni et al., 1988; Ventriglia, 1990; Capelli et al., 2005). Some important springs are located in the northern sector of the Roman area, where the volcanic pile is thickest and the main aquifer is more substantial. Smaller springs (<0,5 L/s) are related to perched, local aquifers. Many water wells have been drilled in the area that drain water from the main aquifer, with resulting specific capacity of up to tens of liters per meter of water-table drawdown.

In the western sector of the city, the structural high of M. Mario can be observed which is NW-SE oriented and influences the underground circulation. This structural high is composed of sandy-clay sediments having low hydraulic conductivity, and it obstructs the natural drainage of the M. Sabatini, oriented towards the Tyrrhenian Sea and R. Tiber deflecting to the southwest towards the F. Arrone (discharge 300 l/s) and to east towards F.della Mola-Cremera-Valchetta basins (total discharge 770 l/s).

On the contrary, the recharge of Galeria and Magliana streams is principally due to the supplies of the gravely-sandy aquifers belonging to the PaleoTiber Unit 1.

Holocene alluvial sediments cap the stratigraphic sequence along the present-day river systems (Corazza et al., 1999; Funicello and Giordano, 2005). Holocene eolian sand dunes cover a narrow area along the present-day Tyrrhenian coastline.

All rock sequences overlying the Monte Vaticano Unit have different permeabilities, the geometry and circulation of which are controlled by both the evolution of the paleotopographic setting and the vertical - lateral variations of lithologies (Capelli et al., 2005).

The Tiber river basin can be divided into four sectors (carbonate, volcanic, alluvial and flysch) where circulation networks behave in different ways depending on hydrogeological characteristics, groundwater- surface water interaction (Di Domenicantonio et al, 2009).

Other locally important hydrogeologic units, only present in the urbanized areas are backfill deposits accumulated during 3000 years of human civilization in the Roman area.

1.3. Specific Geology of Valco San Polo

Above the alluvial unit, about 1.5 m of man-made filling (level R) is present; below this unit, about 7.5 m of historical alluvial sediments, i.e., clay silt evolving into sandy silt and into weakly silty sand with diffuse organic matter (level A); roughly 10 m of yellowish to black sand with a gravelly basal layer having millimeter-scale elements in a sandy matrix (level B); approximately 30 m of silty

clay with diffuse organic matter and scarce sandy intercalations (level C); gray sand gradually passing to gravel downwards (level D); about 12.5 m of prevalently calcareous-marly gravel with heterometric centimeter-scale elements (level G) (Bozzano et al, 2008). Starting from about 63 m from ground level, this alluvial succession of Holocene age (14,000 a to present) rests, with erosional contact, on consistent clay of Pliocene age (Monte Vaticano Unit); these clays represent the geological bedrock of the Roman area (Figure 1.7).

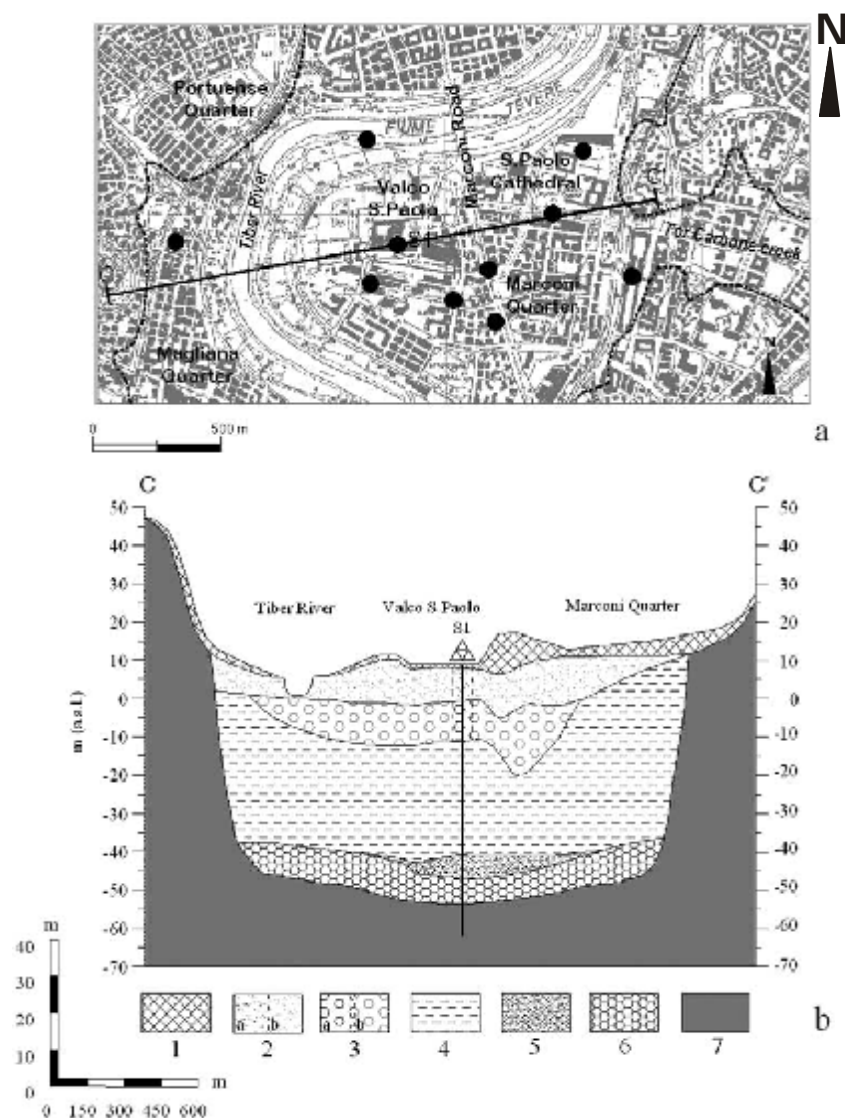


Figure 1.7. Geological section of the Tiber valley at Valco S. Paolo and location of hole S1. 1) man-made fills; 2) level A; 3) level B; 4) level C; 5) level D; 6) level G; 7) Plio-Pleistocene bedrock (Bozzano et al, 2008)

The Grottaperfetta valley is a left bank stream of the Tiber River (Figure 1.8.). The alluvial plain reaches a maximum width of 300 m in the section proximal to the junction with the Tiber River (Cinti et al., 2008). It is 8.5 km long and 2 km wide, at most and nowadays the original stream-bed is no more visible, since it has been completely channelled and connected to the sewer system of the city (Campolunghi et al., 2007). The alluvial plain itself is mostly urbanized and covered by buildings and roads. The valley, like most of the Tiber River's hydrographic network, originated since the times of upward movement and continentalization of the area of Rome, and was deepened during each glacial epoch until the last one (Würm, 18-20 ka) (Marra, 2001).

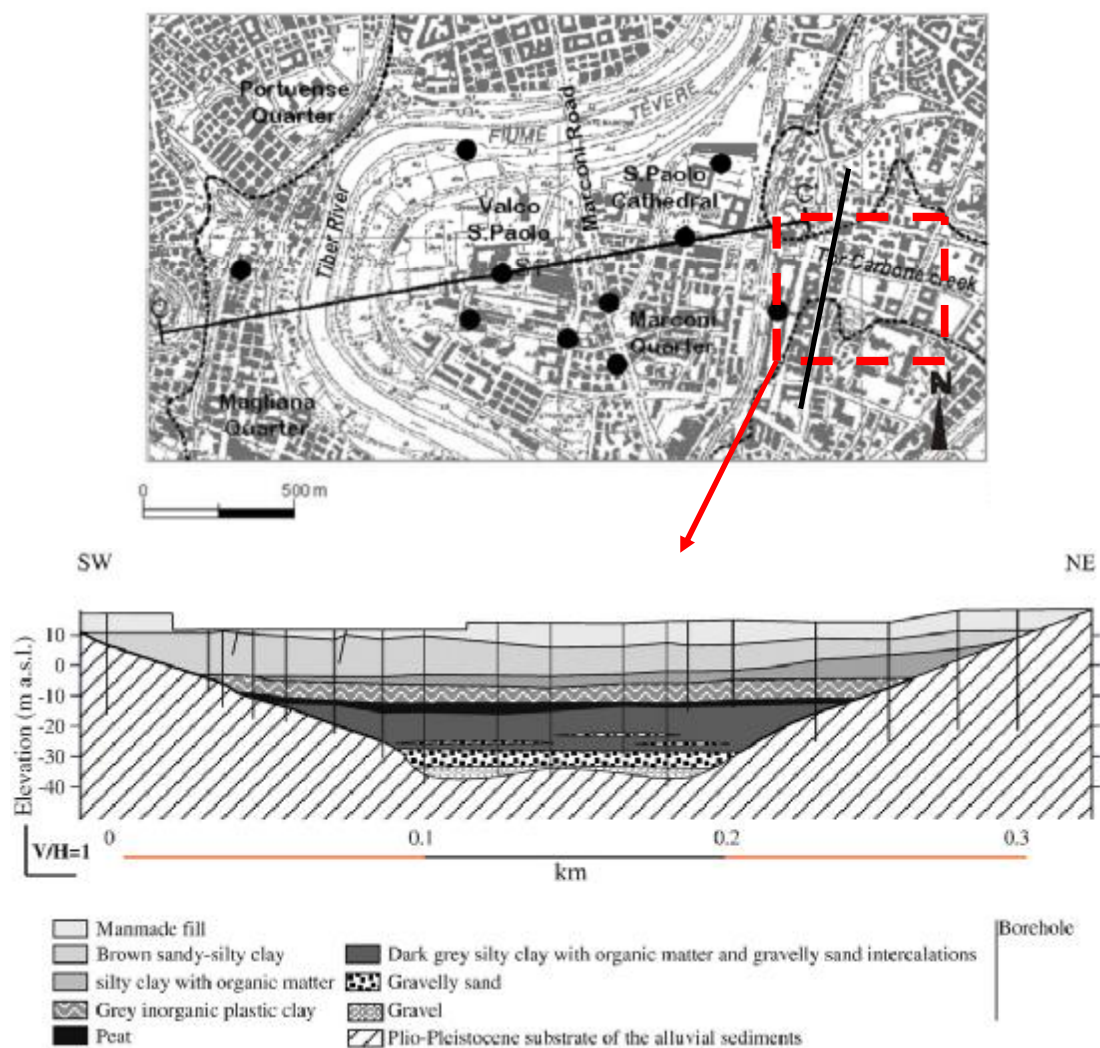


Figure 1.8. Geological sketch of Grottaperfetta valley (Stramondo et al, 2008)

1.4. Hydrogeological Setting of Valco San Paolo

The Valco San Paolo area is characterized by the alluvial series of the Tiber River. The base of the local hydrogeological system is formed by the clayey Pliocene sediments of the Monte Vaticano Unit, which acts as a very low-permeability ($k=10^{-10}$ m/s) substratum throughout the entire Rome area. Characteristic with its low permeability, this unit has been considered as “Aquiclude” under all aquifer formation. The principal aquifer of the area occurs in the basal gravel (lithotype G), with flows towards the south of the highly mineralised water (Corazza and Lombardi 1995) occurring from a recharge area north of Rome. In the overlying alluvial deposits it is possible that bodies of lithotypes B and D ($k = 10^{-6}$ and 10^{-7} m/s, respectively) may represent local aquifers within the low-permeability lithotypes A and C ($10^{-6}/10^{-8}$ and 10^{-10} m/s, respectively) (see Figure 1.7).

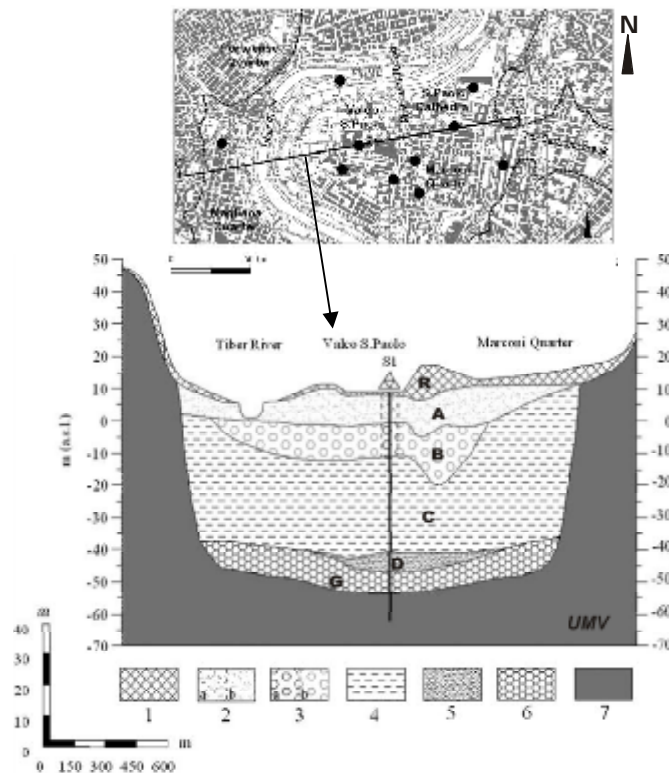


Figure 1.9. Lithotypes in the study area 1) Lithotype R; 2) Lithotype A; 3) Lithotype B; 4) Lithotype C; 5) Lithotype D; 6) Lithotype G; 7) Monte Vaticano Unit (UMV) (Bozzano et al, 2008)

This framework is more complicated on the north side of the section due to the presence of more frequent, relatively coarser levels (lithotypes B and D). It is probable that the nearby hills provide the recharge for these aquifers, at least since urbanisation of the alluvial plain began to impede direct infiltration.

Regarding the connections with the Tiber River, the aquifer within lithotype B appears to feed the river when the Tiber is in a low to normal flow regime, but during high flow periods the gradient is reversed and the river recharges the aquifer (Bozzano et al, 2008). Data regarding the surface anthropic fill sediments (lithotype R) indicate an unconfined aquifer bounded by a low permeability base formed of lithotypes A and C. Given the high level of urbanisation in the area, this aquifer is more likely to be fed by loss from the sewer and aqueduct systems and/or by ancient, buried springs than by direct infiltration (Bozzano et al., 2000).

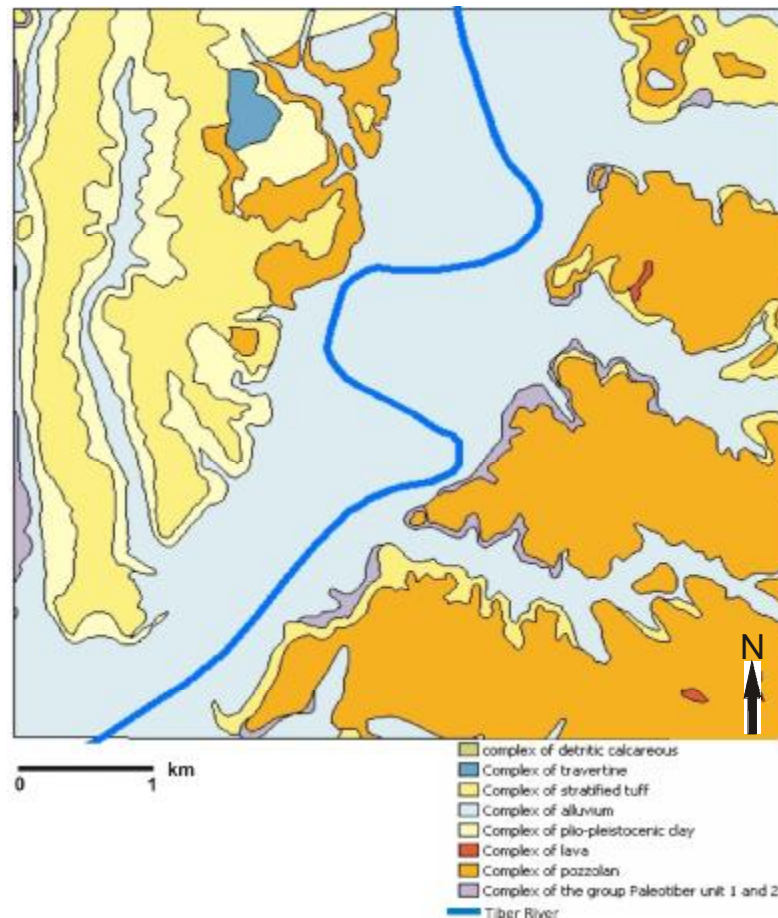


Figure 1.10. Hydrogeological units of the area

1.5. Groundwater modelling

Groundwater modelling is one of the main tools used in the hydrogeological sciences for the assessment of the resource potential and prediction of future impact under different circumstances/stresses (Spits and Moreno, 1996). Its predictive capacity makes it the most useful tool for planning, design, implementation and management of the groundwater resources. Application of existing groundwater models include water balance (in terms of water quantity), gaining knowledge about the quantitative aspects of the unsaturated zone, simulating of water flow and chemical migration in the saturated zone including river-groundwater relations, assessing the impact of changes of the groundwater regime on the environment, setting up/optimising monitoring networks, and setting up groundwater protection zones (Spits and Moreno, 1996).

The term “groundwater model” is used equivalently to the term “numerical model”, which is the combination of the mathematical description, the numerical computer code, and its application to the specific groundwater problem. Today numerical models dominate the study of complex groundwater problems. In particular numerical models solve the equations describing water flow through a porous medium by means of discretization (Spits and Moreno, 1996).

By means of numerical modelling the results of a case study concerning the Holocene alluvial deposits of the Tiber River valley, in the city of Rome is presented. In the case of alluvial aquifers the simulation target consists of the piezometric heads within a reasonable estimate of the balance and of the range of the hydrodynamic parameters.

It is important to note that around 35% of the historical centre of Rome is built on the alluvial plain of the Tiber River or its tributaries and that several new structures are being built, or will soon be built, on or within these deposits, sometimes affecting the groundwater circulation (personal communication with La Vigna, 2009).

2. PREVIOUS STUDIES

The selected studies from the large quantity of bibliography concentrate on Tiber river sediments dealing with mostly geotechnical, geomorphological and hydrogeological characteristics of these deposits.

Bonini (1997), presented the chronology of deformation and analogue modelling of the Plio-Pleistocene Tiber basin; implications for the evolution of the Northern Apennines. The data presented, provide some important insights for the Plio-Quaternary evolution of the Northern Apennines, since the Tiber basin extends in the central part of the chain and allows to date the main deformational phases

Bozzano et al. (2000), presented a geological model of the buried Tiber River valley beneath the historical centre of Rome from a multidisciplinary approach including a detailed geological, hydrogeological, mineralogical and defining the geomechanical behaviour of Tiber alluvial system lithotypes by means of information regarding the geology, geomorphology, climate, hydrographic network, urban development and history of the Rome area.

Campolunghi et al. (2007), identified the highly compressible units, which may be responsible for subsidence and settlement phenomena below urban structures and a yield hazard zoning for urban structures related to recent alluvial deposits has also been defined related with Grotta Perfetta tributary.

Bozzano et al. (2008), presented the engineering-geology and geophysical study of the Valco S. Paolo test site by the analysis of seismic noise records then simulations were made with the SHAKE1D software to reconstruct the vertical trends of the maximum shear deformations that could be obtained in the Tiber alluvium in response to the maximum expected earthquake for the city of Rome.

Cinti et al. (2008), focused on chronostratigraphic study of the Grottaperfetta alluvial valley (left bank tributary of Tiber river) in the city of Rome and investigating possible interaction between sedimentary and tectonic processes.

Calvo and Savi (2008), proposed an adaptive, conceptual model for real-time flood forecasting of the Tiber river in Rome. The model simulates both rainfall-

runoff transformations, to reproduce the contributions of 37 ungauged sub-basins that covered about 30% of the catchment area, and flood routing processes in the hydrographic network. The adaptive component of the model concerns the rainfall-runoff analysis: at any time step the whole set of the model parameters is recalibrated by minimizing the objective function constituted by the sum of the squares of the differences between observed and computed water surface elevations (or discharges).

Stramondo et al. (2008), described subsidence induced by urbanisation in the city of Rome detected by advanced InSAR technique and geotechnical investigations. The velocity maps evidenced that a general subsidence affects the buildings that are founded over the alluvial terrains of the Tiber River hydrographic network.

Barberi et al. (2008), showed that the aquifer contained in the basal gravels of Tiber river represents an important geothermal resource for a kind of direct heat utilization in the city of Rome. The study includes Valco San Paolo and Vasca Navale zone. Maps describing the variation along the river course of the top, bed and hence thickness of the base gravels have been obtained by processing the stratigraphic data of 216 wells drilled in the past in the Tiber alluvial deposits.

Capelli et al. (2008), the goal of the authors of this study was to update the knowledge about the aquifers that are belonging to different hydrogeological units. By means of numerical modelling using “Modflow” (Harbaugh, 2005), they correlated georeferred stratigraphic information, the surfaces of the main hydrogeological complexes of the Ablan Unit, on which the city of Rome lays.

La Vigna et al. (2008), proposed a model of groundwater circulation in the Aniene river basin area, which lies in the northeastern part of Rome, on the left bank of the Tiber river.

La Vigna et al. (2009), presents a model calibration experience on a complex groundwater system located in central Italy, in the subsiding Acque Albule Plain near Rome (Italy). The calibration process applied to this model consisted in three main steps, including numerical and trial and error methods, and also new data collection suggested from sensitivity analysis. The model fitting shows clearly the importance

of applying not only automatic estimation methods for calibration processes but also the need to be prepared to change the conceptual model starting from sensitivity analysis and from collecting new data to better understand the system.

Raspa et al. (2009), described the spatial variability of geotechnical characterization in the upper Pleistocene-Holocene alluvial deposits in Rome by means of multivariate statistics of geotechnical parameters by means of multivariate statistics.

Di Domenicantonio et al. (2009), described the quantitative hydrogeology in the Tiber river basin management planning in central Italy. The first step was the hydrogeological structures' delimitation upon which the hydrogeological balance can be elaborated. For each hydrogeological structure a conceptual model is then defined. From this scale it was possible to extrapolate single aquifer detail.

Preziosi and Romano (2009), discussed the regional aquifers of central Italy from a hydrostructural analysis to the mathematical modelling. A comparison was made among models referring to two aquifers that differ in type of permeability, hydrogeological framework and in the field data available for their characterization and calibration. The aim of the present note was to show how, the different approaches followed in reconstructing the hydrogeological configuration of the two described aquifers, based essentially in one case on a knowledge of the water budget, and in the other of the piezometric field, the reliability of the described numerical model was comparable.

3. MATERIALS AND METHODS

3.1. Materials

Interpreted geological data of the subsoil of the study area were collected from Department of Geological Sciences of RomaTre University and from public administrations and private companies. The collected information were archived in a geodatabase, selecting boreholes with a reliable location, a detailed lithologic description was made and filtered according to specific criteria.

3.1.1. Collection of thematic maps

During the data collection, a modified 1:5000-scale topographic map of Rome has been scanned to make available on a GIS visualization (Figure 3.1).

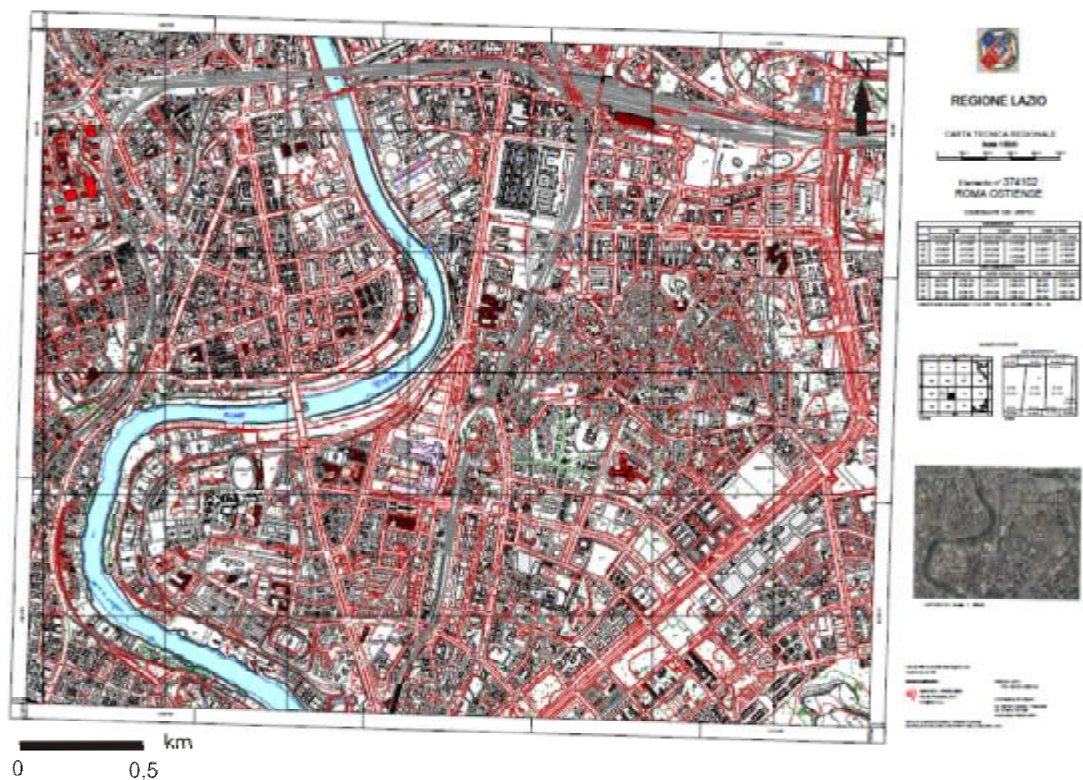


Figure 3.1. Topographic map of the study area no° 374102

Using the properties of several boreholes within and around the study area which documented in Excel files under headings about name, x_ and y_ coordinates, terrain elevation (slm), stratigraphic unit depths (m) with lithologic description had been examined and imported in a new Excel file with modified terrain elevation values and new drilled boreholes (Figure 3.2).

Borehole ID	Elevation (m)	Name	Depth (m)	Description	
15011512	14		0	toroso di spata	
212519	14	Monte-Vaticano	4	Non stratigrafica	
212519	14	Monte-Vaticano	41	argille limose con intercalazioni calcaree argillose	
15	15.5	Via G. Sacco	0	4.2	Materiale di riporto costituito da pezzette eterogenee ed eterogenee (pietra di tufo, frammenti di mattoni, resti di manufatti, ecc.), la parte basale è costituita da mattoni prevalentemente limo-argillosi marsoni -F
16	15.5	Via G. Sacco	4.2	7	Argille limose con sottili sabbie grigie, fitta laminazione crollata, da poco a mediamente plastiche, rara presenza di inclusi ghiaiosi -LA
17	15.5	Via G. Sacco	7	9.2	Argille limose grigio-marrose da mediamente plastiche a plastiche -LA
18	15.5	Via G. Sacco	9.2	11	Argille limose grigio-marrose mediamente compatte -LA
19	15.5	Via G. Sacco	11	17	Argille limose grigio-azzurre plastiche, con presenza di materiale sabbioso -AG
20	15.5	Via G. Sacco	17	24	Argille limose sabbie grigie plastiche, mediamente compatte, con frequenti livelli di limo argilloso, limo sabbioso e torso da poco a mediamente plastiche, presenza di alcuni livelli calcareo con sottili sabbie grigie, nei livelli torosi, frammenti di gusci di gastropodi -AG
21	15.5	Via G. Sacco	24	34	Argille limose sabbie grigie plastiche, a tratti variegata, da plastiche a mediamente compatte con livelli ricchi di legno, resti sabbiosi e gusci di gastropodi. Da 20 a 20.5 m argille limose sabbie grigie con livelli ricchi di legno in decomposizione, la parte basale si presenta torosa -AG
22	15.5	Via G. Sacco	32	47.5	Argille limose sabbie grigie plastiche a tratti plastiche, a 33.2, 34.5, 35.5 in senso presenti livelli dedometrici ricchi in legno -AG
23	15.5	Via G. Sacco	47.5	52.2	limo argilloso, argille limose e limo grigio toroso, da toroso a poco plastico, presenza di inclusi organici (legno) e di piccoli gastropodi, da 47.8 a 49.2 m livelli a faciliti con abbondanti porosità -AG
24	15.5	Via G. Sacco	52.2	55.8	Ghiaie e ciottoli variolati, sferziosi ed eterogenei, da poco a mediamente sabbiosi, prevalentemente di natura calcarea e calcareo, presenza di livelli calcareo di travertino -CA
25	15.5	Via G. Sacco	55.8	59.8	limo argilloso e limo marsoni, toroso, con sabbie, ghiaie e resti di piccoli coralli, di natura calcarea -CA
26	15.5	Via G. Sacco	59.8	66	Argille ed argille limose grigio-azzurre, fortemente compatte, molto compatte, con inclusi ghiaiosi di natura calcarea e resti di piccoli coralli, da 59.8 a 60 m livelli calcareo, a 62 m è presente un livello dedometrico di calcarenite -C

Figure 3.2. Visualization of the Excel file including boreholes properties

The map of the top of Monte Vaticano Unit visualized by the analysis of twelve boreholes in the study area and has been used as a guide whilst composing the top bedrock surface in GIS (Figure 3.3).



Figure 3.3. Depth of bedrock (m.asl) in the study area (Barberi et al, 2008)

The isopiezometric levels in general water table map of Rome, has provided us to take a view about the knowledge of flow direction in the city and were used in a future stage during the definition of flow to and within Holocene deposits of the study area (Figure 3.4).

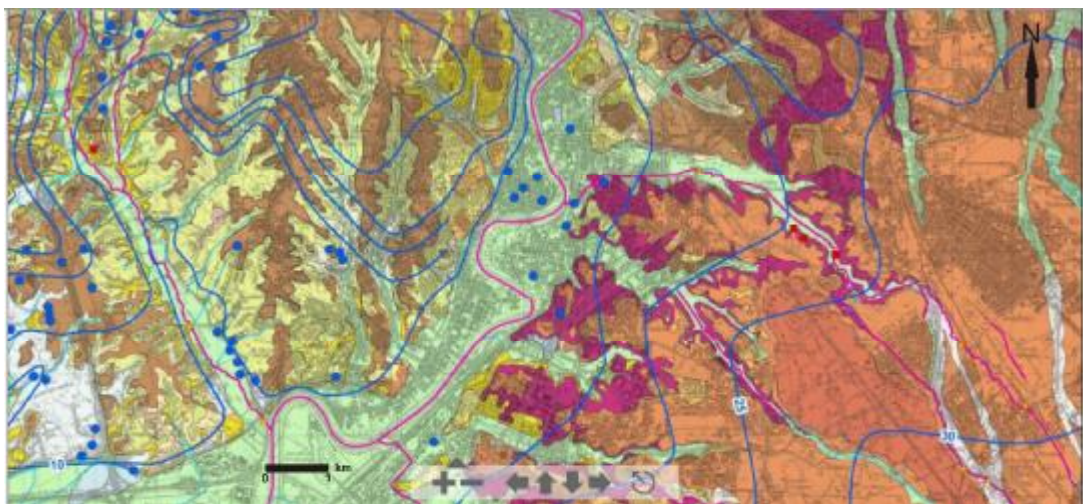


Figure 3.4. General water table of Rome (Capelli et al, 2008)

3.1.2. Groundwater monitoring instruments - dataloggers

Hydrogeological survey was started from depth and static level measurements of piezometers with the instruments which were taken from the Laboratory of Hydrogeology in Science Geology Department (Roma Tre University).

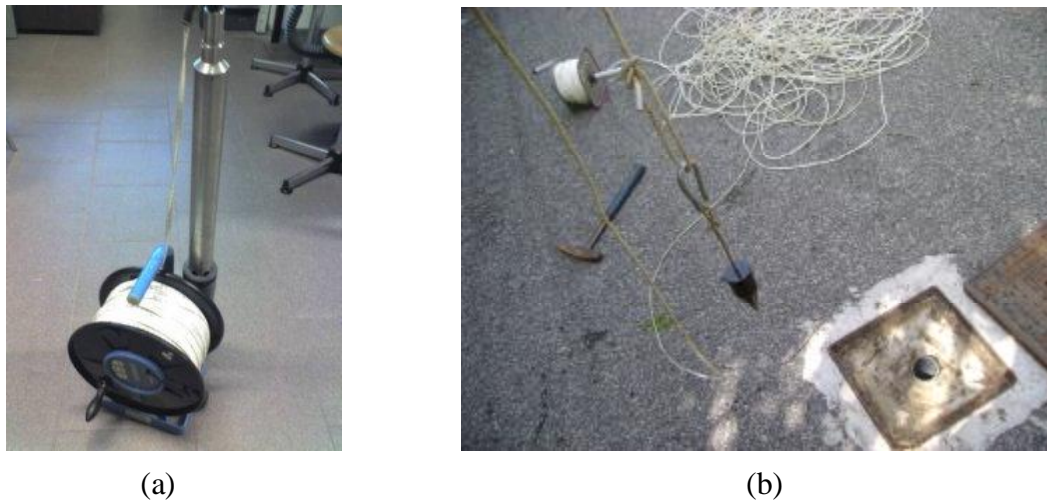


Figure 3.5. (a) Multiparametric instrument (with pH, Cond, T° probe) (b) Measuring the depth of piezometer manually with line

Portable Conductivity meter to immersion post-sampling for control the quality of the waters. It measures the electric conductivity and the temperature pH meter. (Figure 3.6)



Figure 3.6. Measurement from a piezometer in Science Geology Department

The monitoring of Tiber river and piezometers was performed using the automatic dataloggers during the period between 16 Sep 2009 and 5 Feb 2010. The CTD-diver measures water level, water temperature and conductivity. It consists of a pressure sensor for measuring the water level, a temperature sensor, a four-electrode conductivity cell, a non-volatile memory to store the measurements and a battery (Figure 3.7).

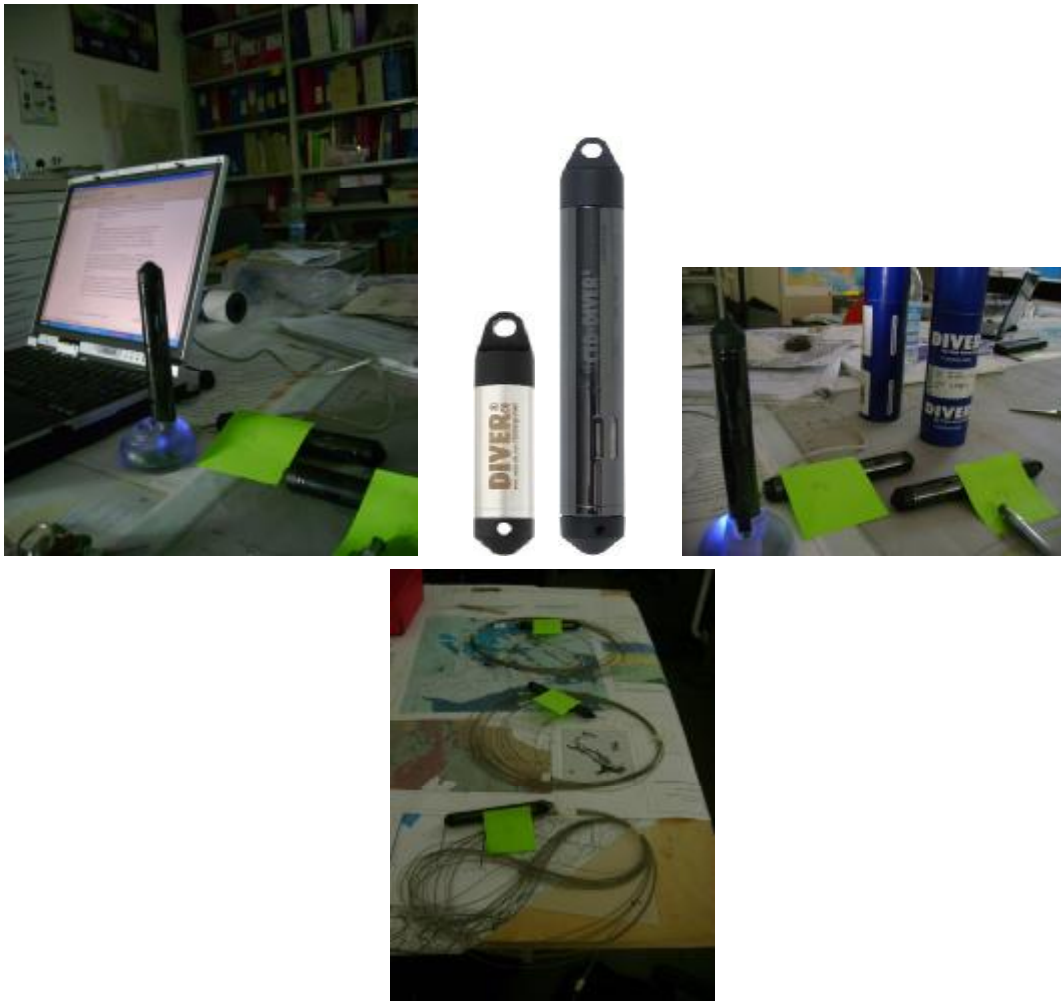


Figure 3.7. CTD-diver dataloggers used in the study

3.2. Methods

The procedure for applying a groundwater model includes these following steps :

- Define study objectives - Data collection
- Develop a conceptual model
- Select a computer code or algorithm
- Construct a groundwater flow model
- Calibrate model and perform sensitivity analysis
- Make predictive simulations

These steps are generally followed in this order, however, there is substantial overlap between steps, and previous steps are often revisited as new concepts are explored or as new data are obtained (ASTM International, 2004).

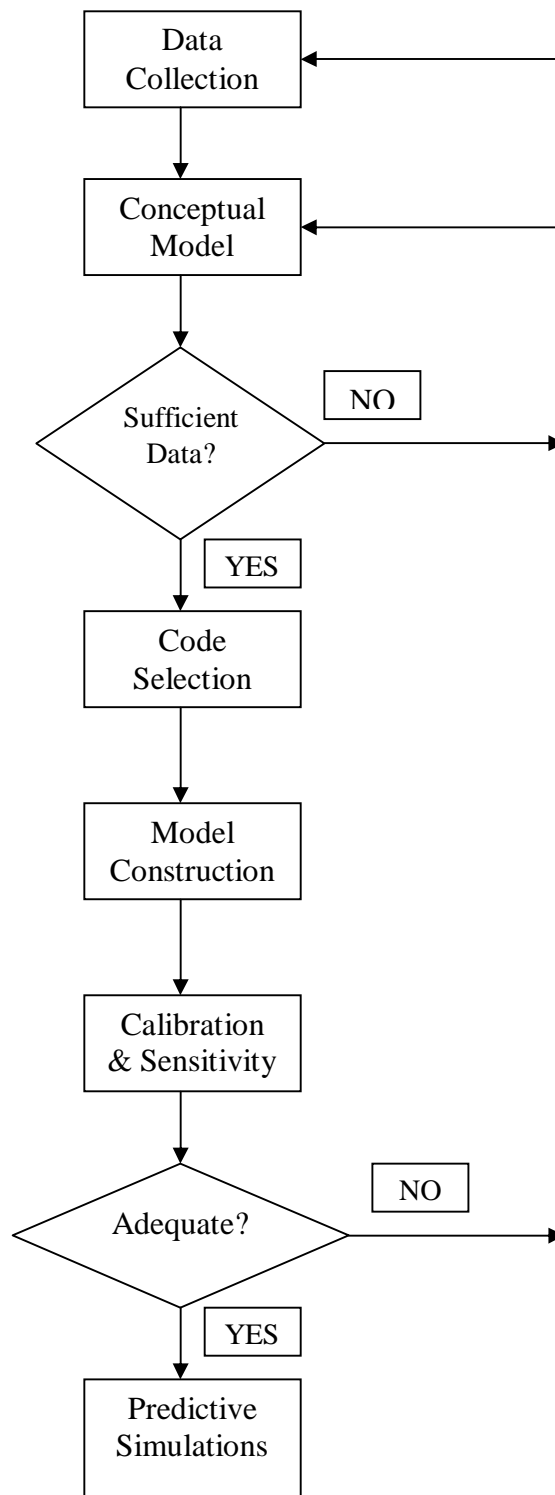


Figure 3.8. Flow chart of the modeling process (ASTM International, 2004)

3.2.1. Compilation of Data

ArcMap version 9.2 personal geodatabase managed by ArcGIS® (ESRI, Inc.) was used in every step of data collection.

Scanned maps do not normally contain spatial reference information (either embedded in the file or as a separate file). With aerial photography and satellite imagery, sometimes the locational information delivered with them is inadequate and the data does not align properly with other data which may had (from the User's Manual of ArcMap 9.2).

Thus, to use some raster datasets in conjunction with other spatial data, it may necessary to align, or georeference, to a map coordinate system. When a raster dataset is going to be georeferenced, its location using map coordinates should be defined to assign a coordinate system. Georeferencing raster data allows it to be viewed, queried, and analyzed with other geographic data (from the User's Manual of ArcMap 9.2).

The interpolation method selection is the important part of studies during the creation of surface maps in GIS. Dataset can be arranged for interpolation considering the depth of boreholes and features have selected in a layer or records in a table by bulding a query.

The Inverse Distance Weighted (IDW) and Spline methods which performs on a point dataset are referred to as deterministic interpolation methods because they assign values to locations based on the surrounding measured values and on specified mathematical formulas that determine the smoothness of the resulting surface. IDW assumes that the surface is being driven by local variation. It is best if sample points are evenly distributed throughout the area and if they are not clustered (from the User's Manual of ArcMap 9.2).

3.2.2. Conceptual model

A conceptual model is an idealization of the real world that summarizes the current understanding of site conditions and how the groundwater flow system works (Spitz and Moreno, 1996). It is an interpretation or working description of the characteristics and dynamics of the physical hydrogeologic system which can be evaluated quantitatively (ASTM International, 2004)

3.2.3. The Computer Code

A graphical user interface (GUI) has become a necessity which aids in the creation of input files for the model code to read and for visualising the model output. It is a type of user interface which allows people to interact with a computer and computer-controlled devices which employ graphical icons, visual indicators or special graphical elements called "widgets", to represent the information and actions available to a user. The GUIs are the future in integrated hydrogeological modelling using modelling geomatics and expert systems.

MODFLOW-2005 is a three-dimensional finite-difference groundwater model. It simulates steady and nonsteady flow in an irregularly shaped flow system in which aquifer layers can be confined, unconfined, or a combination of confined and unconfined. PHAST simulates multi-component, reactive solute transport in three-dimensional saturated groundwater flow systems.

ModelMuse (Winston, 2009) is a graphical user interface (GUI) for MODFLOW-2005 (Harbaugh, 2005) and PHAST (Parkhurst and others, 2004).

3.2.3.1. Groundwater flow equation

The three-dimensional movement of ground water of constant density through porous earth material may be described by the partial-differential equation ;

$$\frac{\partial}{\partial x} \left(K_{xx} \frac{\partial h}{\partial x} \right) + \frac{\partial}{\partial y} \left(K_{yy} \frac{\partial h}{\partial y} \right) + \frac{\partial}{\partial z} \left(K_{zz} \frac{\partial h}{\partial z} \right) + W = S_s \frac{\partial h}{\partial t} \quad (3.1)$$

Where

K_{xx} , K_{yy} , and K_{zz} are values of hydraulic conductivity along the x, y, and z coordinate axes, which are assumed to be parallel to the major axes of hydraulic conductivity (L/T);

h is the potentiometric head (L);

W is a volumetric flux per unit volume representing sources and/or sinks of water, with $W < 0.0$ for flow out of the ground-water system, and $W > 0.0$ for flow into the system (T^{-1}); S_s is the specific storage of the porous material (L^{-1}); and t is time (T). Equation 3.1 describes ground-water flow under nonequilibrium conditions in a heterogeneous and anisotropic medium, provided the principal axes of hydraulic conductivity are aligned with the coordinate directions. Equation 3.1., together with specification of flow and/or head conditions at the boundaries of an aquifer system and specification of initial-head conditions, constitutes a mathematical representation of a ground-water flow system.

3.2.3.2. Finite-difference approach for groundwater flow equation

Figure 3.9 shows a spatial discretization of an aquifer system with a grid of blocks called cells, the locations of which are described in terms of rows, columns, and layers. An i,j,k indexing system is used. Within each cell there is a point called a "node" at which head is to be calculated. Many schemes for locating nodes in cells could be used; however, the finite-difference equation uses the block-centered formulation in which the nodes are at the center of the cells.

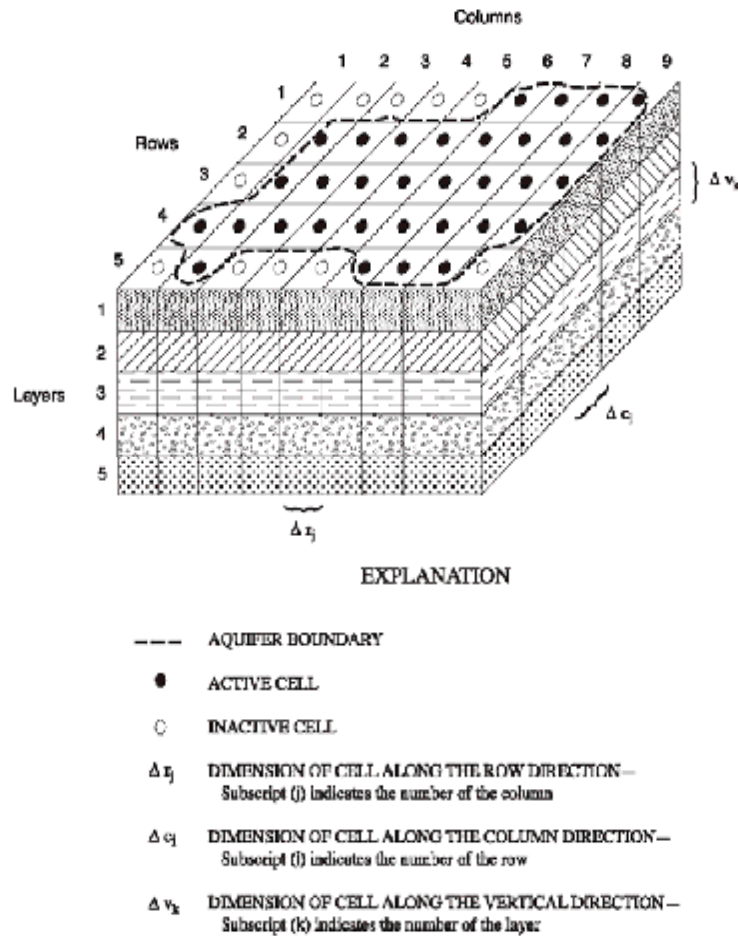


Figure 3.9. A discretized hypothetical aquifer system (Modified from McDonald and Harbaugh, 1988).

In equation 3.1. the head, h , is a function of time as well as space so that, in the finite difference formulation, discretization of the continuous time domain is also required. Time is broken into time steps, and head is calculated at each time step.

3.2.3.3. Derivation of Finite-difference Equation

Development of the ground-water flow equation in finite-difference form follows from the application of the continuity equation: the sum of all flows into and out of the cell must be equal to the rate of change in storage within the cell. Under

the assumption that the density of ground water is constant, the continuity equation expressing the balance of flow for a cell is

$$\sum Q_i = S_s \frac{\Delta h}{\Delta t} \Delta V \quad , \quad (3.2)$$

Where

Q_i is a flow rate into the cell (L^3T^{-1});

S_s has been introduced as the notation for specific storage in the finite-difference formulation; its definition is equivalent to that of S_s in equation 3.1., that is, S_s is the volume of water that can be injected per unit volume of aquifer material per unit change in head (L^{-1}); ΔV is the volume of the cell (L^3); and Δh is the change in head over a time interval of length Δt .

The term on the right-hand side is equivalent to the volume of water taken into storage over a time interval Δt given a change in head of Δh . Equation 3.2. is stated in terms of inflow and storage gain. Outflow and loss are represented by defining outflow as negative inflow and loss as negative gain.

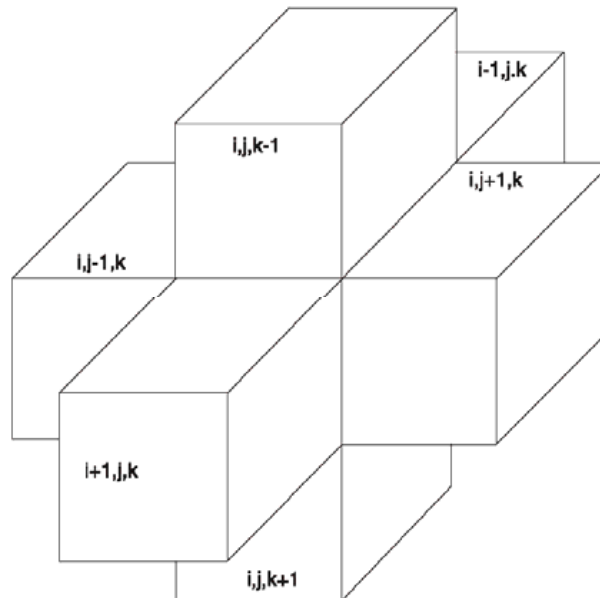


Figure 3.10. Indices for the six adjacent cells surrounding cell i,j,k (hidden). (Modified from McDonald and Harbaugh, 1988.)

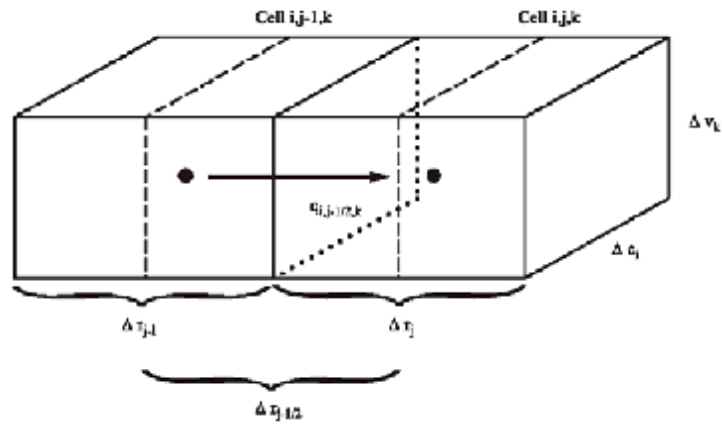


Figure 3.11. Flow into cell i,j,k from cell $i,j-1,k$. (Modified from McDonald and Harbaugh, 1988.)

Figure 3.10 depicts six aquifer cells adjacent to cell i,j,k — $i-1,j,k$; $i+1,j,k$; $i,j-1,k$; $i,j+1,k$; $i,j,k-1$; and $i,j,k+1$. To simplify the following development, flows are considered positive if they are entering cell i,j,k ; the negative sign usually incorporated in Darcy's law has been dropped from all terms. Following these conventions, flow into cell i,j,k in the row direction from cell $i,j-1,k$ (Figure 3.11), is given by Darcy's law as;

$$q_{i,j-1/2,k} = KR_{i,j-1/2,k} \Delta c_i \Delta v_k \frac{(h_{i,j-1,k} - h_{i,j,k})}{\Delta r_{j-1/2}}, \quad (3.3)$$

Where

$h_{i,j,k}$ is the head at node i,j,k , and $h_{i,j-1,k}$ is the head at node $i,j-1,k$;

$q_{i,j-1/2,k}$ is the volumetric flow rate through the face between cells i,j,k and $i,j-1,k$ (L^3T^{-1});

$KR_{i,j-1/2,k}$ is the hydraulic conductivity along the row between nodes i,j,k and $i,j-1,k$ (LT^{-1});

$\Delta c_i \Delta v_k$ is the area of the cell faces normal to the row direction; and

$\Delta r_{j-1/2}$ is the distance between nodes i,j,k and $i,j-1,k$ (L).

$$q_{i,j+1/2,k} = KR_{i,j+1/2,k} \Delta c_i \Delta v_k \frac{(h_{i,j+1,k} - h_{i,j,k})}{\Delta r_{j+1/2}}, \quad (3.4)$$

while for the column direction,

$$q_{i+1/2,j,k} = KC_{i+1/2,j,k} \Delta r_j \Delta v_k \frac{(h_{i+1,j,k} - h_{i,j,k})}{\Delta c_{i+1/2}} \quad (3.5)$$

$$q_{i-1/2,j,k} = KC_{i-1/2,j,k} \Delta r_j \Delta v_k \frac{(h_{i-1,j,k} - h_{i,j,k})}{\Delta c_{i-1/2}} \quad (3.6)$$

For the vertical direction,

$$q_{i,j,k+1/2} = KV_{i,j,k+1/2} \Delta r_j \Delta c_i \frac{(h_{i,j,k+1} - h_{i,j,k})}{\Delta v_{k+1/2}}, \quad (3.7)$$

$$q_{i,j,k-1/2} = KV_{i,j,k-1/2} \Delta r_j \Delta c_i \frac{(h_{i,j,k-1} - h_{i,j,k})}{\Delta v_{k-1/2}} \quad (3.8)$$

Each of equations 3.3 through 3.8 expresses inflow through a face of cell i,j,k in terms of heads, grid dimensions, and hydraulic conductivity.

3.2.3.4. River - Aquifer interaction

The notation can be simplified by combining grid dimensions and hydraulic conductivity into a single constant, the "hydraulic conductance" or, more simply, the "conductance." The Conductance is the factor that relates the difference in head to the rate of flow. In MODFLOW, the Conductance (CRIV) has units of L^2/t and is equal to KLW/M where,

K = the hydraulic conductivity of the sediment in the boundary condition such as a river or drain,

L = the length of the boundary condition in the cell,

W = the width of the boundary condition, and

M = the thickness of the sediment in the boundary condition.

3.2.3.5. Construct a steady-state groundwater flow model - Defining Boundary Conditions

A model boundary is the interface between the model calculation domain and the surrounding environment. Boundaries occur at the edges of the model domain and at other points where external influences are represented, such as rivers, wells or chemical spills and so forth (Spitz and Moreno, 1996).

In Modelmuse, the Time-Variant Specified-Head package is sometimes referred to as the Constant Head package. The abbreviation (CHD) for the Time-Variant Specified-Head package comes from this alternate name. "Constant Head" however does not accurately describe how the boundaries in the Time-Variant Specified-Head package actually work because the specified heads in the package can vary with time (Arlen Harbaugh, personal communication of R.B.Winston, 2007).

A steady-state problem requires only a single solution of simultaneous equations, rather than multiple solutions for multiple time steps. The length of the stress period and time step will not affect the head solution because the time derivative is not calculated in a steady-state problem. (Harbaugh, 2005).

3.2.4. Calibrating the Model and Perform a Sensitivity Analysis

Model calibration, is the process of varying uncertain model input data over likely ranges of values, as adjusting hydraulic parameters, boundary conditions and initial conditions within reasonable ranges, until a satisfactory match between

simulated and observed data is obtained (Spitz and Moreno, 1996). In practice, model calibration is frequently accomplished through trial-and-error adjustment of the model's input data to match field observations (ASTM International, 2004) which was applied to this model. The calibration is evaluated through analysis of residuals. A residual is the difference between the observed and simulated variable (ASTM International, 2004) (residual = observed head – simulated head).

Sensitivity analysis is performed during model calibration and during predictive analyses. Model sensitivity provides a means of determining the key parameters and boundary conditions to be adjusted during model calibration. Sensitivity analysis is used in conjunction with predictive simulations to assess the effect of parameter uncertainty on model results (ASTM International, 2004).

In model verification, the calibrated model is used to simulate a different set of aquifer stresses for which field measurements have been made. The model results are then compared to the field measurements to assess the degree of correspondence.

3.2.5. Make Predictive Simulations and Perform a Postaudit

Predictive simulations are the analyses of scenarios defined as part of the study objectives. In cases where the groundwater flow model has been used for predictive purposes, a postaudit may be performed to determine the accuracy of the predictions (ASTM International, 2004).

4. RESULTS AND DISCUSSION

Information from more than 280 wells within and around the study area, including continuous coring vertical boreholes and wells, together with detailed geological maps, measured stratigraphic logs were analysed, homogenized and archived in ArcMap version 9.2 personal geodatabase managed by ArcGIS® (ESRI, Inc.). Approximately 268 boreholes and stratigraphic logs were encoded and retrieved from the database in order to reconstruct the stratigraphic, structural, and depositional setting of the study area.

4.1. Geological interpretation

Geological interpretation was based on 268 borehole data which 12 of them were drilled in 2009 by private companies (Figure 4.2). First of all, these boreholes had been plotted on a 1:5000 scale topographic map of the area. Several maps (n°374140, n°374100 and n°374102) (with elevation modified)¹, which represent the study area have been used during the process of creating the database in software ESRI (ArcMap 9.2). All the raster datasets and vector feature classes have been geo-referenced with the coordinate system ED_1950_UTM_Zone_33N.

4.1.1. Sediment survey of Tiber valley in Valco San Paolo

In both the main alluvial valley and the Grotta Perfetta left-bank tributary, Holocene units bedded with approximately 1,5 km wide - 3 km long and 0,5 km wide - 0,8 km long, respectively.

(1) : the urbanization process in recent years give rise to a thundering change in terms of altitude

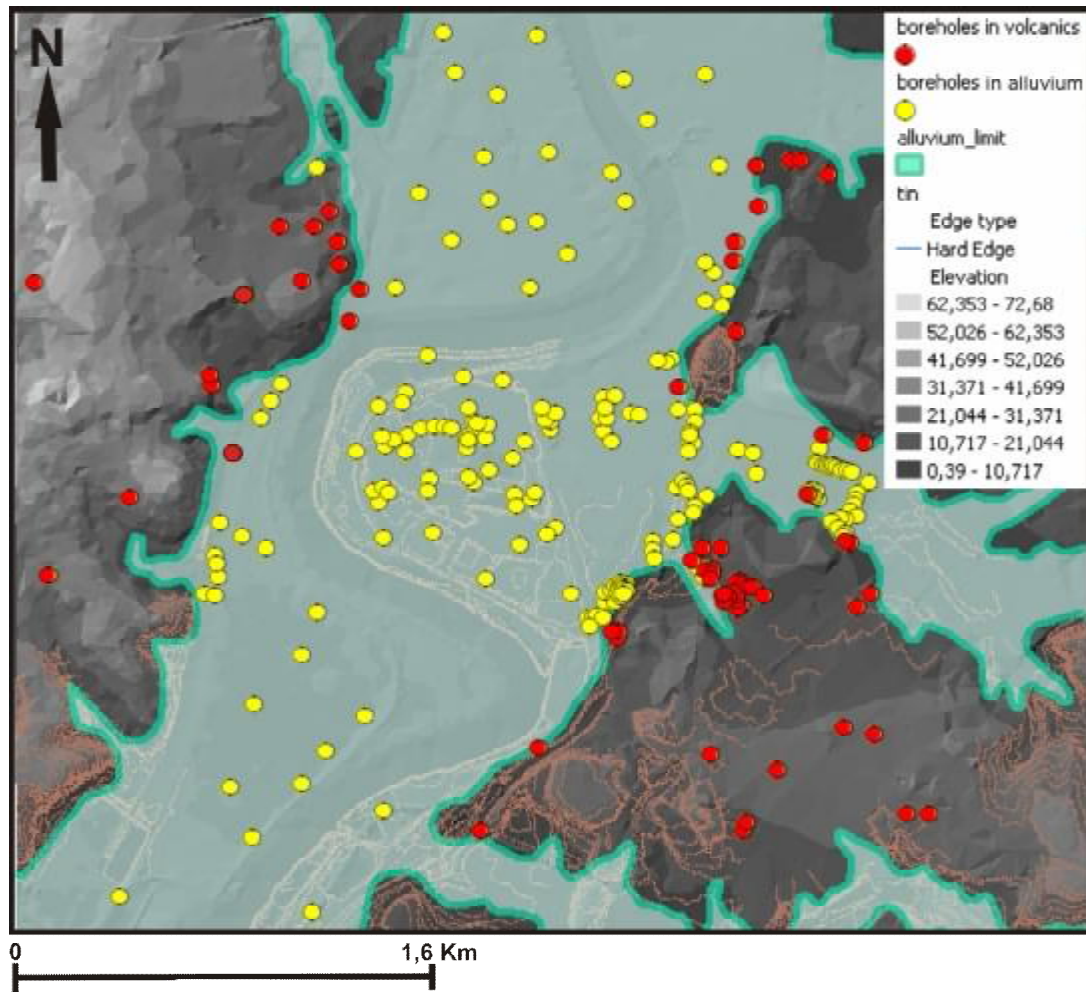
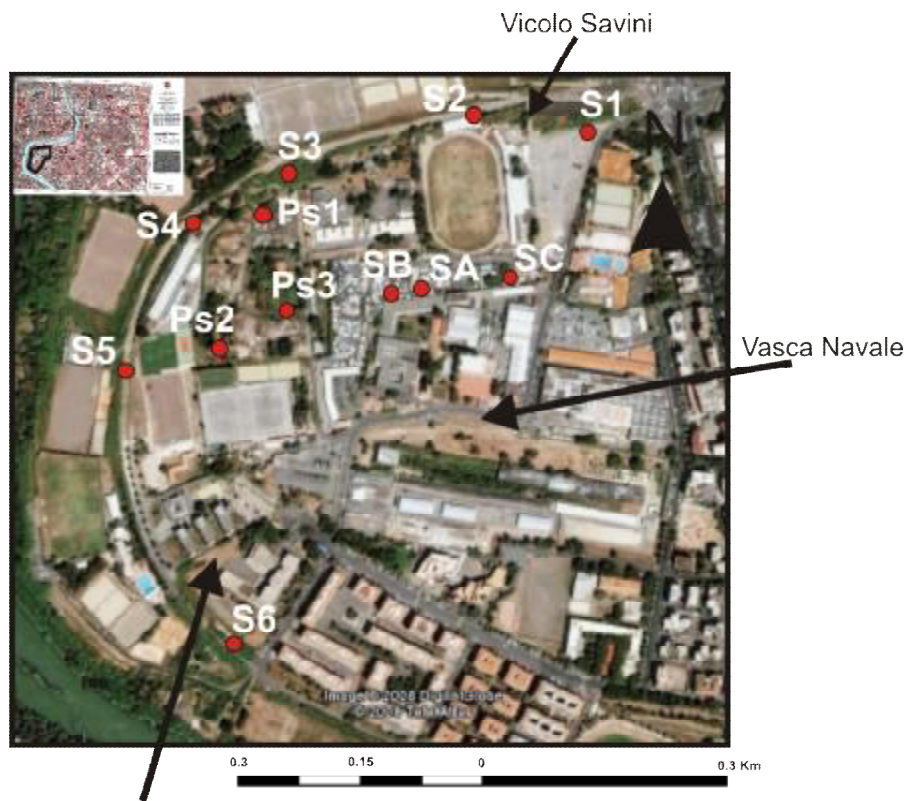


Figure 4.1. Holocene alluvium limit in the area with location of selected boreholes

220 boreholes exist in the alluvium, 48 borehole in volcanics which 33 of them cross the Paleotiber unit (fluvio-lacustrine sand and clay) have been used in geological interpretation of the 6,6 km² large study area (Figure 4.1).

The collected information was classified and filtered according to specific criteria before being archived in the geodatabase, i.e., selecting boreholes with a reliable location, and, possibly, a detailed lithologic description.



Department of Geological Sciences, RomaTRE

(a)



(b)

Figure 4.2. (a) Location of recent boreholes drilled by private companies
 (b) A view from drillings no° SA, SB, SC

By means of the correlation of borehole data, 7 cross-sections with several directions to compose the subsurface geology of the site had drawn, which is more detailed and realistic the more boreholes are close to each other (Figure 4.3).

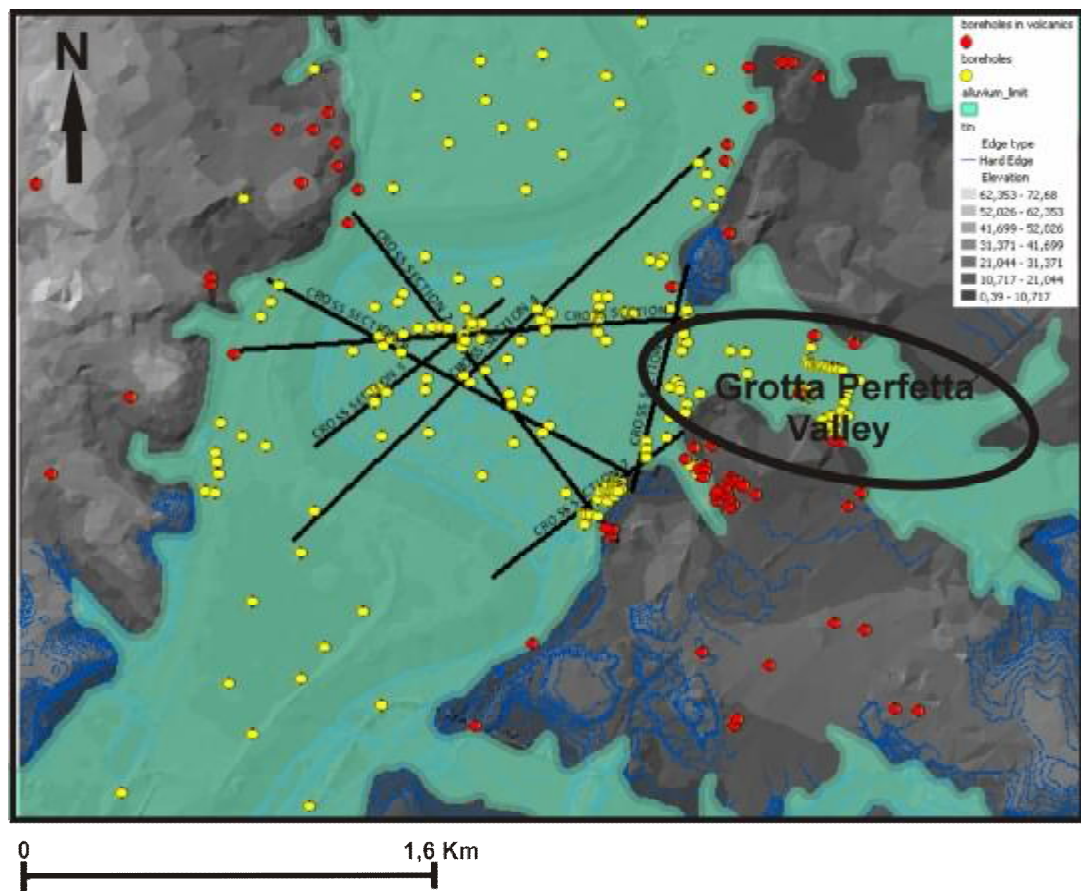


Figure 4.3. Location of the cross sections and the ancient Tiber River's left-bank tributary; Grotta Perfetta stream

Blue colored boreholes are exactly on the cross sections, the others are projected, but inside a buffered 50 meters area for each line.

In the cross section n°1, fifteen boreholes, (three of them exactly crossing the section) reaching 20 to 90 m of depth, have been correlated an approximately 1850 m long, geological section across the E-W length of the Tiber valley, has been drawn in Fig 4.4.

All five main sedimentary horizons (Lithotype R, A, B, C, G) can be identified within the alluvial body however concerning the Lithotype B, clay unit had observed directly below the loam in borehole no° S1S584 which has been drilled in correspondence of the joint of the main Tiber valley with the Grotta Perfetta tributary.

The bedrock erosional surface on which the alluvial sediments are deposited is almost horizontal and is found at an average elevation of around -50 m a.s.l., resulting in an overlying sediment thickness of about 65 m. Within the eroded valley basal gravel found above the Pliocene bedrock along 1400 m width basis. As illustrated in the Figure 4.4. that at the west valley wall; the erosional process interested not only the bedrock but the Pleistocene - Paleo Tiber Unit is also present with an average elevation of around -15 m a.s.l above the Monte Vaticano Unit (UMV). Lithotype C is deposited above the basal gravel and form the major part of the alluvial fill. Towards the interior of lithotype C, these lateral heteropic bodies consisting of alternating sandy-silty units (Lithotype D) which has observed in some certain circles until 25 m thick like within the borehole log no°S1S572. Lithotype C is also found along the section outside of the full eroded valley above the PaleoTiber.

The reconstruction consists of about a variable thickness from 0,5 m to 7 m man-made fill (Lithotype R), about 8 - 10 m of clay silt into weakly silty loam (Lithotype A), roughly 10 m of sand (Lithotype B) which is more thick in the west part and in connection with the river, approximately 30 m of silty clay with diffuse organic matter (Lithotype C); abundant organic matter is also present throughout the clay unit, either as diffuse fragments of vegetal remains, as well as mm-to-dm thick peat levels, about 10 m of prevalently calcareous-marly gravel (Lithotype G).

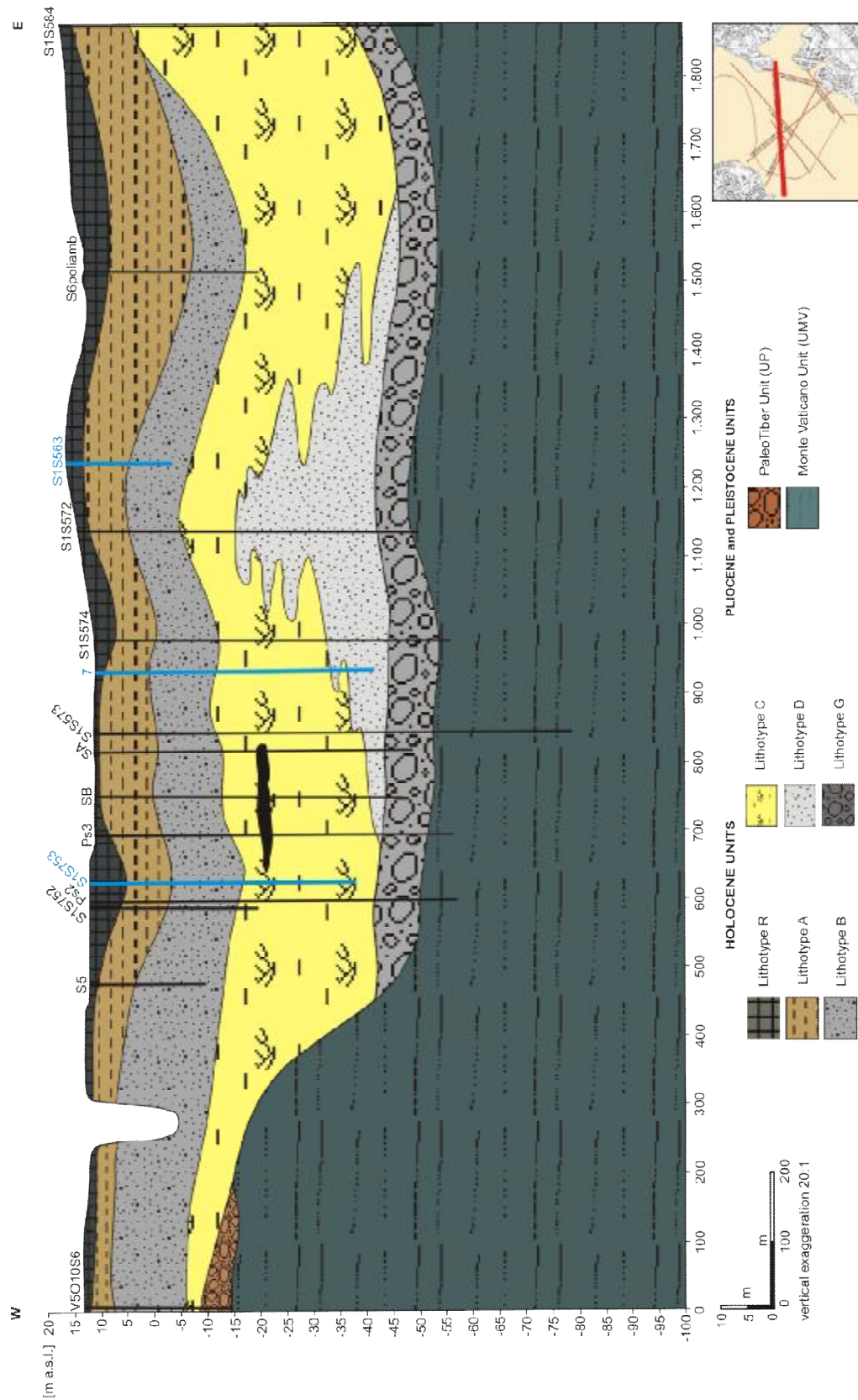


Figure 4.4. Cross section No 1

In the cross section n°2, fifteen boreholes, (four of them exactly crossing the section), reaching 12 to 90 m of depth, have been correlated an approximately 1650 m long, geological section across the NW - SE length of the Tiber valley, has been drawn in Fig 4.5.

The bottom of valley width; where has covered with Lithotype G is 1400 m. Bedrock within the valley is found at an average elevation of around -53 m a.s.l. resulting in an overlying sediment thickness of about 70 m however, in the west and east hills of the valley, bedrock is found at around - 20 m a.s.l. and - 40 m a.s.l., respectively.

The lithotype B overlie lithotype C along sharp, undulating contacts. Their geometry is generally lenticular in transversal section but becomes tabular near the southern slope of the valley. Lithotype B strongly characterises the northern part of this section near the present Tiber riverbed and reach up to 20 m in thickness, although thins in the center and continues straightly towards the border of the valley.

The two difference between west and east borders is the thickness of the PaleoTiber and Volcanic unit above which has both geologically and most probably hydrogeologically connection with lithotype A and B. Even though the amount of PaleoTiber deposits is less than the east border, the relation with sand unit in the west is largely than the connection in the east side.

The upper surface of lithotype A is being weakly undulating and a homogenized thickness; less than 2 m of man-made fill continued in the center until the urbanized southeastern part as a result of a unit at about 8,2 m thickness of lithotype R had observed.

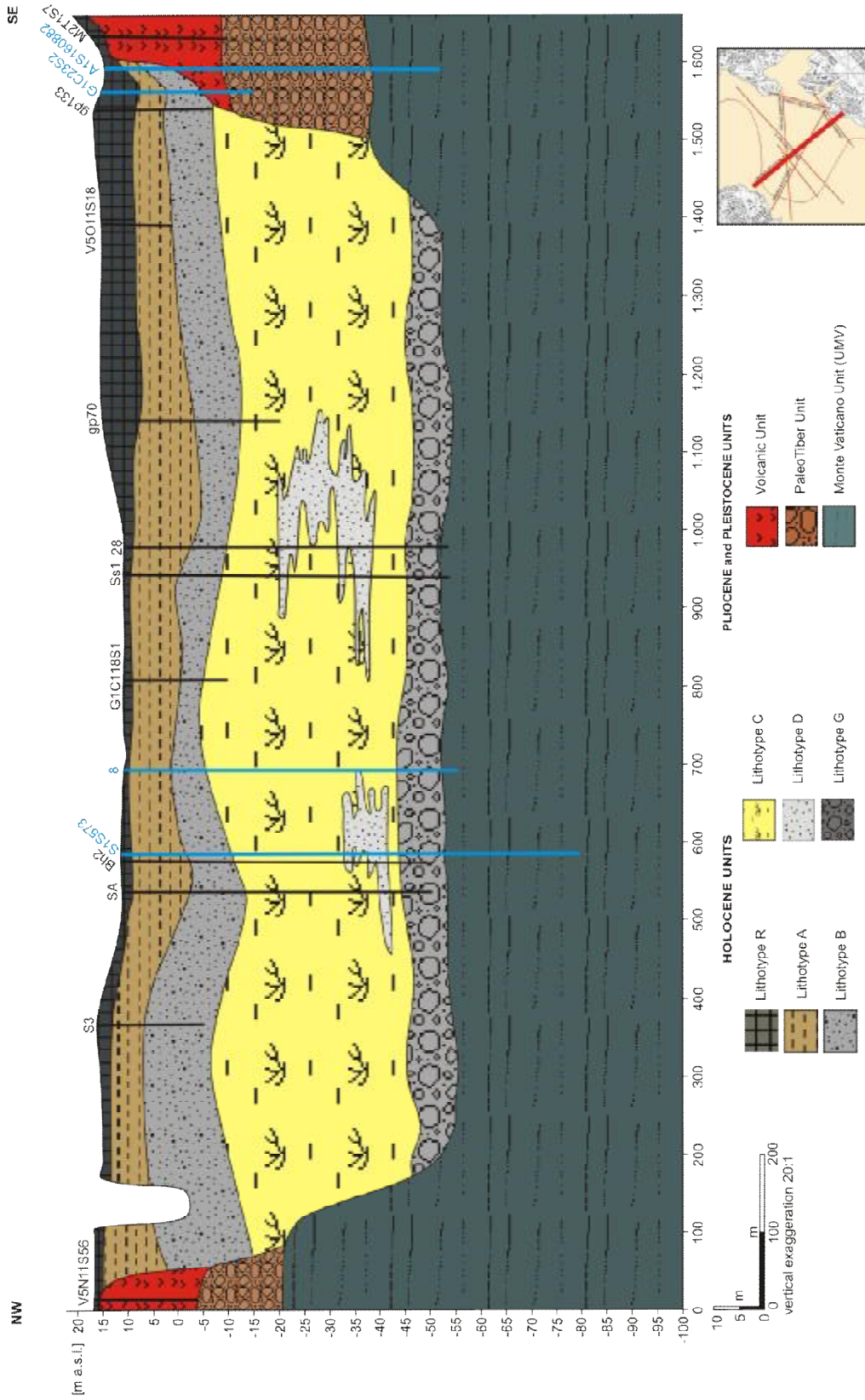


Figure 4.5. Cross section No 2

In the cross section n°3, five boreholes, (one of them exactly crossing the section), reaching 42 to 66 m of depth, have been correlated an approximately 575 m long, geological section across the N - S length of the Grottaperfetta tributary, has been drawn in Fig 4.6.

Locally pedogenized and/or peaty horizons where pieces of vegetation can be observed. The sandy unit of the main valley (Lithotype B) disappears in this sector while, stratigraphic data of boreholes n°11 and n°G1C11S1 show that volcanic origin basal gravel of the tributary mixed with the limestone origin basal gravel of Tiber valley.

According to the borehole log of n°11, the basal gravel deposit is characterized by variable-colored gravel and pebbles, heterogenic and heterometric, from little to on average thickened approximately 7 m thickness, mainly of calcareous and volcanic nature; presence of levels centimeter of travertine. This observation indicates a lateral relationship between these gravels in the mouth of Grottaperfetta tributary.

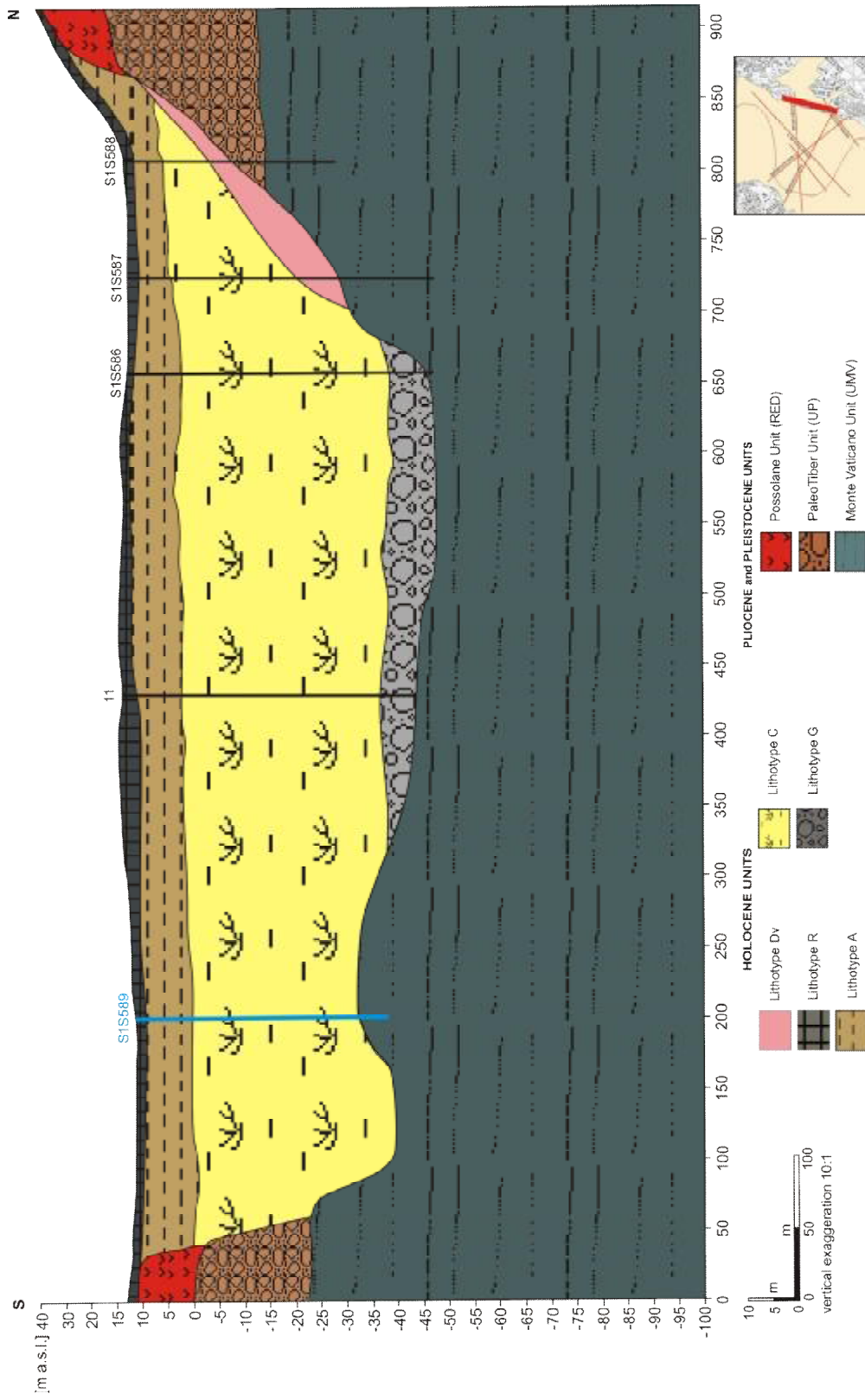


Figure 4.6. Cross section No 3

In the cross section no^o4, seven boreholes, (two of them exactly crossing the section), reaching 15 to 65 m of depth, have been correlated and an approximately 2200 m long, geological section across the NE-SW length of the Tiber valley, has been drawn (Figure 4.7).

Basal gravel was found uniformly above the erosional surface, with an undulating upper surface. Clay is deposited directly above this basal gravel and form the major part of the alluvial fill. Toward the middle of the valley, loam unit is getting thicker whilst sand unit undulated below the river, and ended through the east hills.

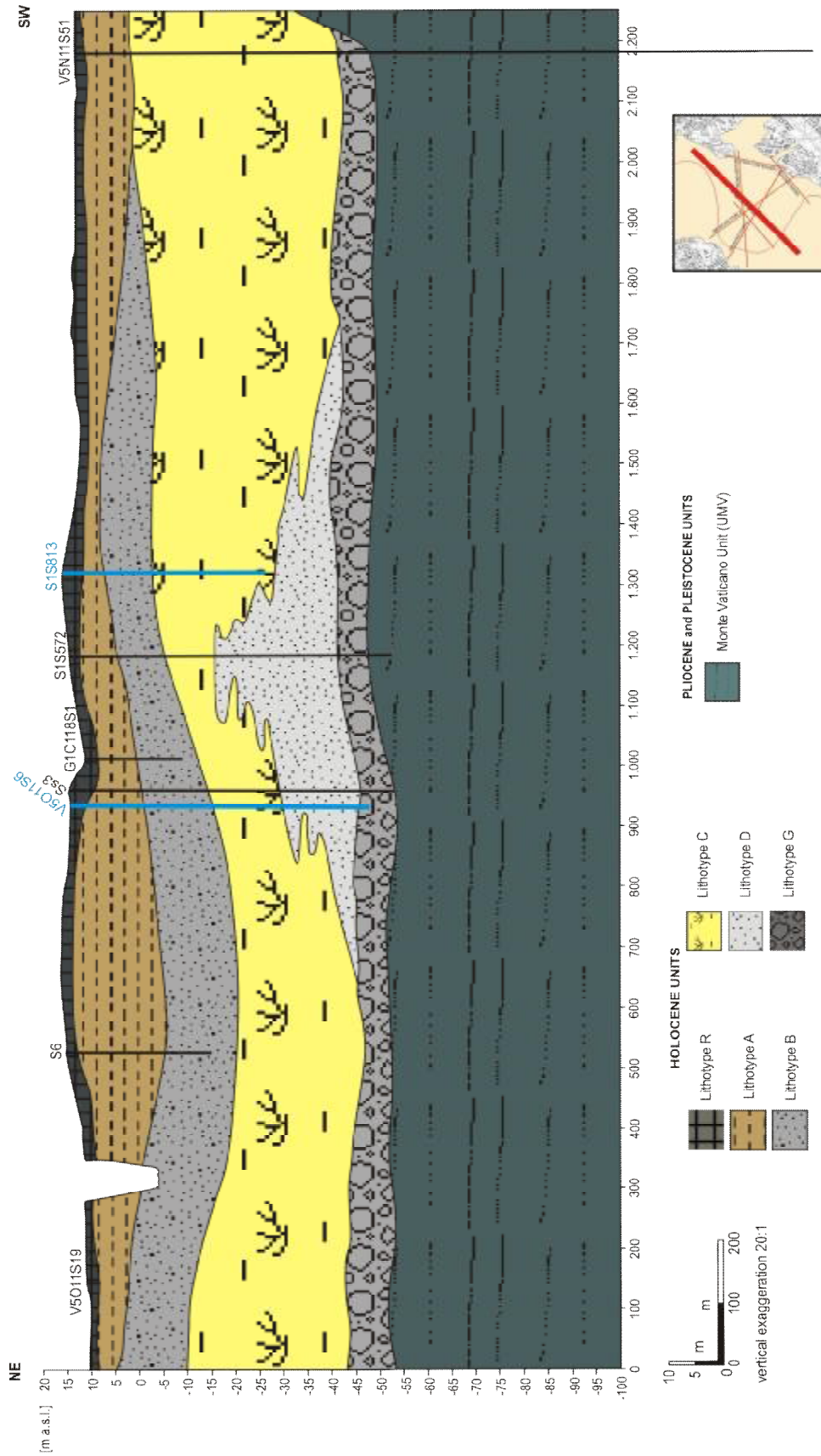


Figure 4.7. Cross section No 4

In the cross section no^o 5, eight boreholes (one of them exactly crossing the section), reaching 15 to 65 m depth, have been correlated and an approximately 950 m long, geological section across the SW-NE length of the Tiber valley, has been drawn (Fig. 4.8)

The irregular basal contact of silty sand and medium-fine grained sand within Lithotype B and the related geometry of these bodies, imply erosional activity with the partial reincision of the alluvial body and successive filling of valleys. The irregular setting of the alluvial deposits above the B–C contact characterises the zone below and near the present Tiber River channel.

Lithotype B consists a larger grain size inside, it is likely that currents along the principal channel had a higher energy than those in the tributaries.

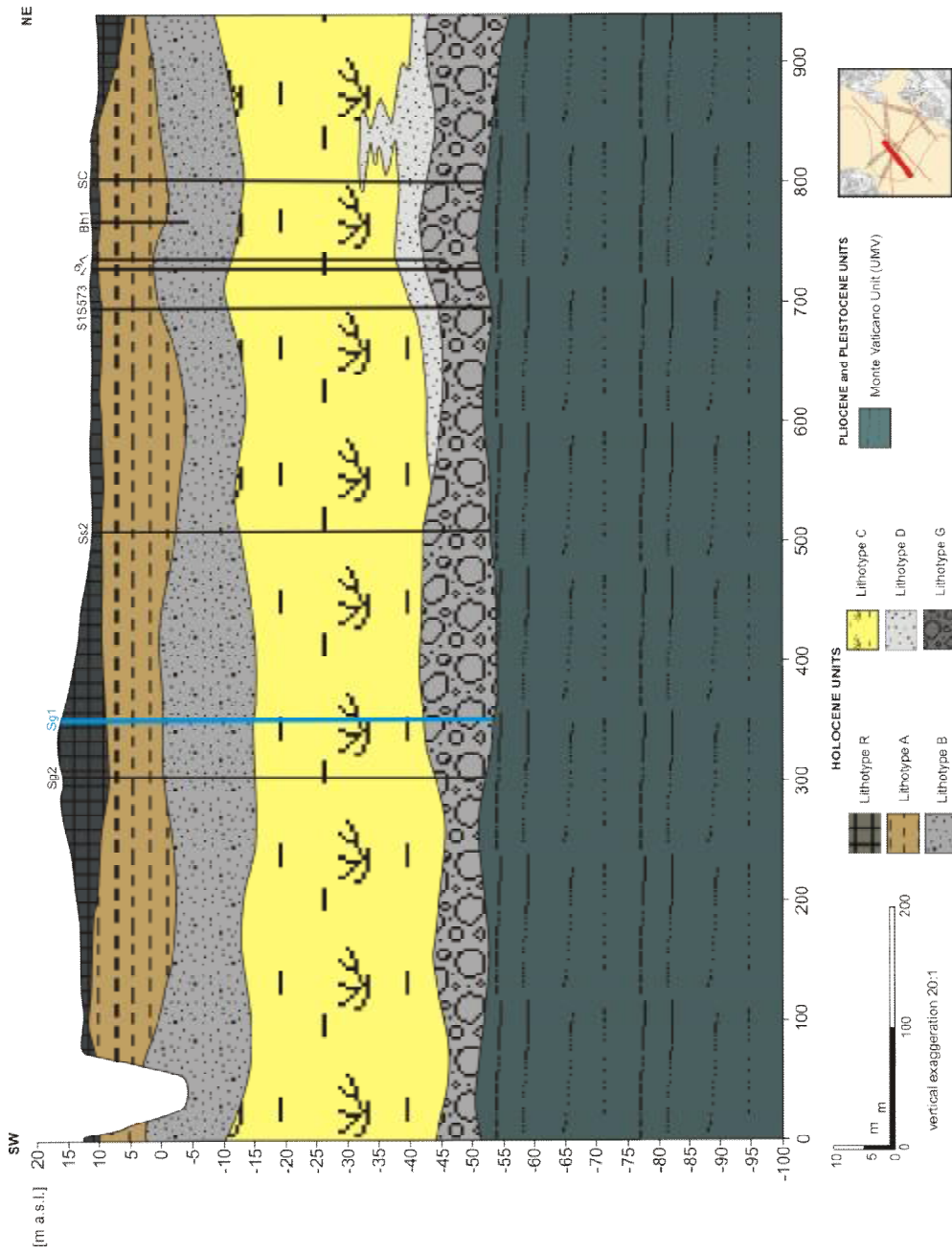


Figure 4.8. Cross section No 5

In the cross section n°6, eight boreholes (two of them exactly crossing the section), reaching 30 to 75 m of depth, have been correlated and an approximately 1600 m long geological section across the NW-SE length of the Tiber valley, has been drawn. These bodies occur as lenses (Fig 4.9) where the section is transverse to the Tiber River valley.

The geometry is irregular and difficult to resolve on the basis of the available borehole data; a unit consisting of slope deposits, lithotype D_v, has been inferred on the basis of data from one borehole drilled along west valley walls and from literature. The geometry and extent of this unit (D_v) is clearly somewhat simplified due to the limited amount of data available.

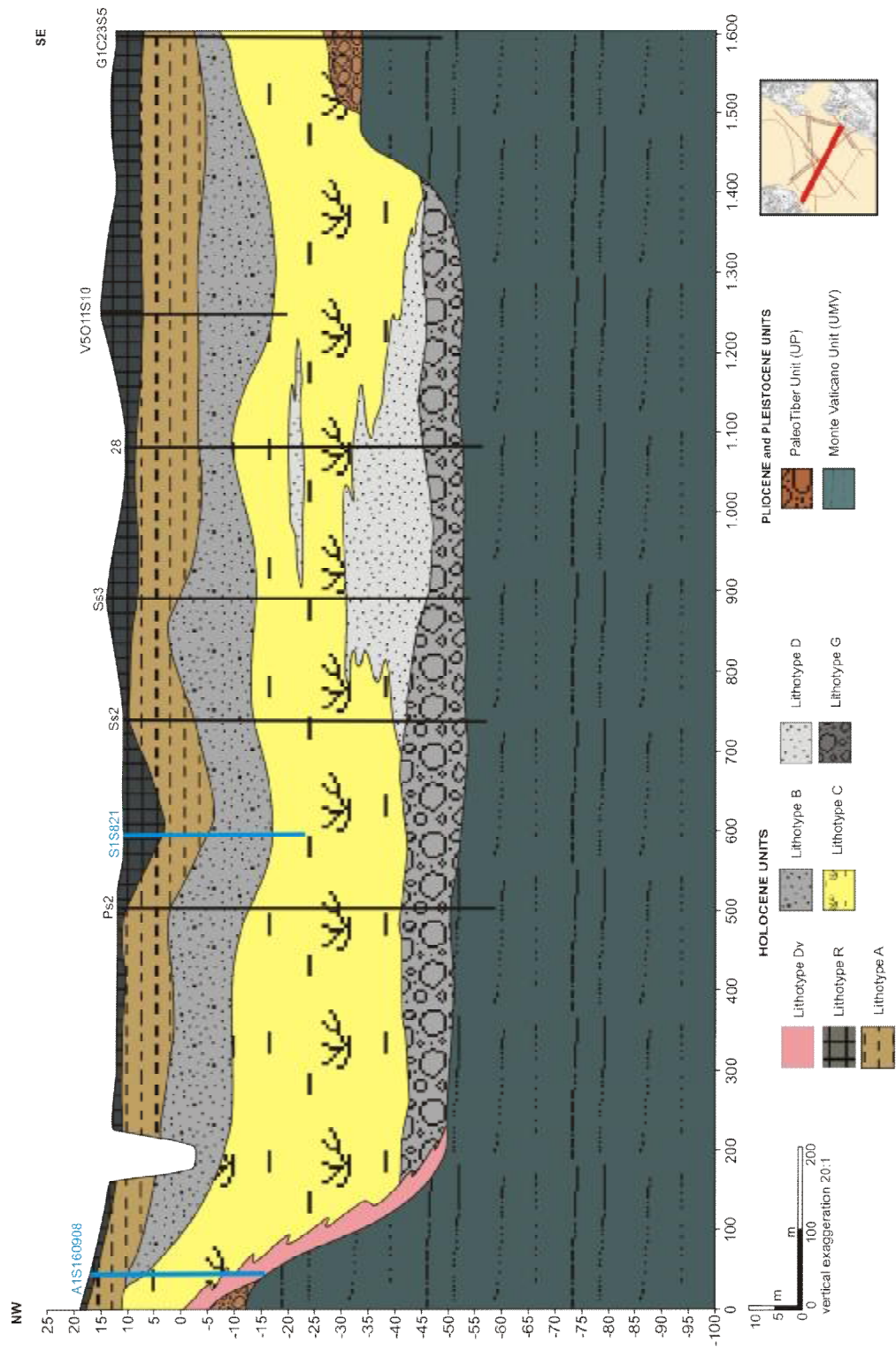


Figure 4.9. Cross section No 6

In the cross section n^o7, six boreholes reaching 10 to 60 m of depth, have been correlated and an approximately 950 m long, geological section across the SW-NE length of the Tiber valley, has been drawn (Fig 4.10).

The variations in thickness of lithotype A and R on the right and the left banks of the Tiber River almost compensate each other if their summed total thickness is considered. In other words, it appears that the deposition of alluvial sediments on the right bank was contemporaneous with that of the anthropic detritus on the left – an interpretation that is supported by what is known regarding the urbanisation of the area.

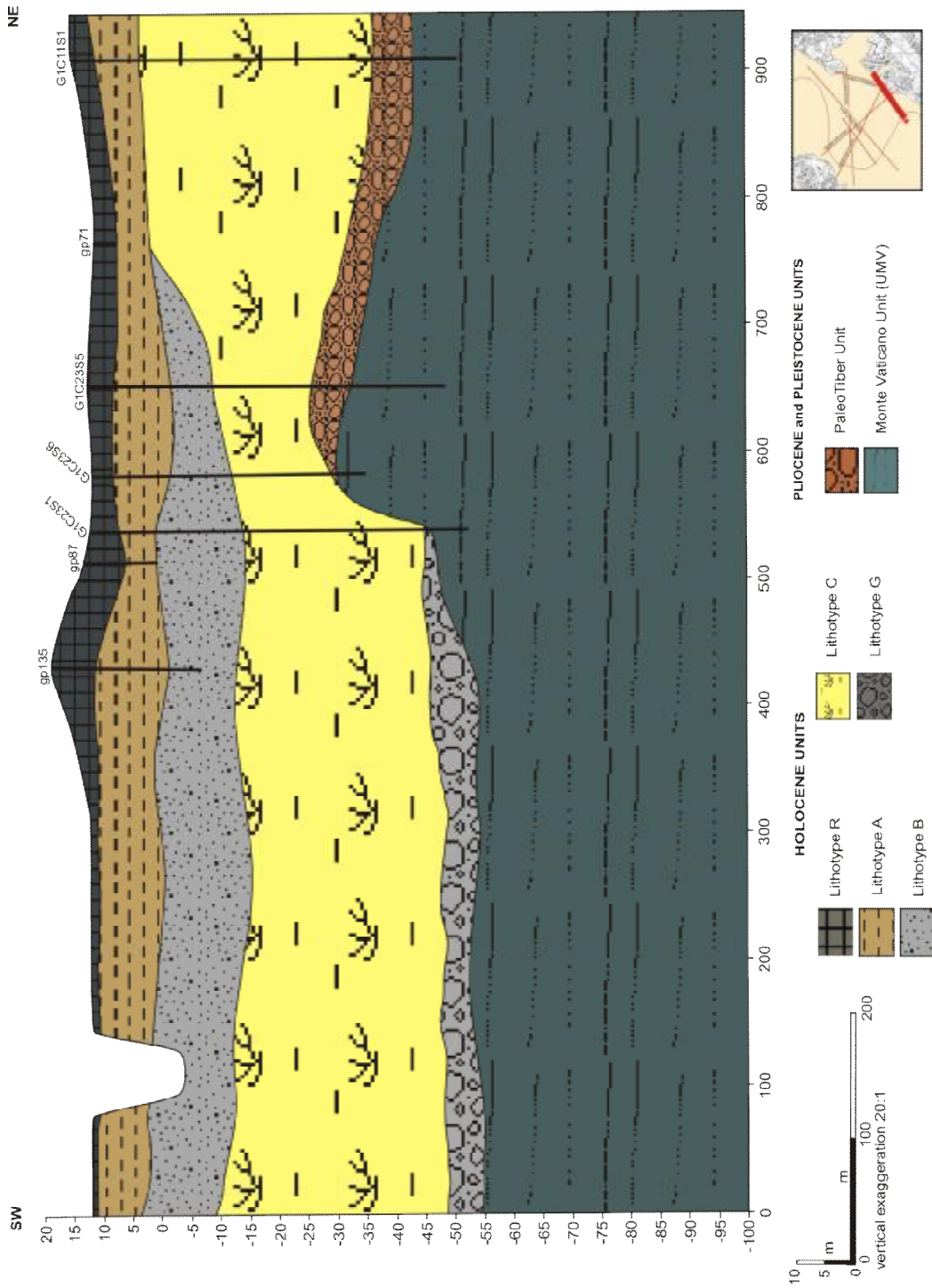


Figure 4.10. Cross section No 7

Holocene ;



Lithotype R : anthropogenic fill material characterised by abundant, variously sized brick fragments and blocks of tuff embedded in a brown-green silty-sandy matrix. This horizon also contains ceramic and mortar fragments. More or less dense and/or consistent; very variable permeability.



Lithotype A : silty and sandy deposits with brick fragments

- green-grey silty sand and silty loam, poorly dense and/or consistent, averagely permeable
- hazel-coloured clay and clayey silty bands which contain organic matter and black-brown pyroclastics, averagely consistent, averagely poorly permeable.



Lithotype B : predominantly yellow-brown, medium- to fine-grained sand and sandy loam; loose or moderately aggregated with pieces of wood or plant material, averagely dense, permeable.



Lithotype C : grey clay and silty clay with a variable organic content that gives a local black colour. Occasional up to 100 mm thick peat levels and rare sandy silt layers with gravel are also present. Poorly to averagely consistent with low to very low permeability.



Lithotype D : alternating silty-sandy, sandy-silty, clayey-silty and clayey levels. Viewed together, this unit is grey in colour, from averagely to poorly dense, averagely permeable.



Lithotype G : predominantly limestone gravel in a grey, sandy-silty matrix, very dense and very permeable.



Lithotype D_v : slope detritus located near the scarp of the Tiber paleovalley. It consists of brown and grey, coarse-grained sand has been found (at the foot of the

paleoscarp) to overlie a 5 m thick block of lithoid tuff which is probably related to a paleo-landslide body.

Middle Pleistocene ;



Volcanic : Characterised by good permeability ignimbrite, made of a massive and chaotic, scoria and ash



PaleoTiber : Highly permeable fluvial conglomerate sand and clay

Pliocene ;



UMV: Deep marine clay, characteristic with its very low permeability and considered as Aquiclude under all aquifer formation.

In the layer definition respect, the point that noticed during the composition of cross sections is the two neighbor unit which represent different base lithologies can have similar facies inside hence lithological descriptions on cm base can not be deemed as inconsiderable.

4.1.2. Creating surfaces with ArcMap 9.2

After the comparison of analysed boreholes, calculated altitudes of layers had been arranged within the database of boreholes; an attribute table that composed of several fields about top elevation values (a.s.l.) for each layer has been developed with ArcMap 9.2. (Table 4.1)

Table 4.1. Attributes of boreholes

ID	SHAPE	COO_POZZO	OMOTADIMSL	Bot Eiport	TOP LIMB	TOP SAID	TOP CLAY	TOP GRAVEL	Top Grd 2	Top Grd 3	TOP IMAV	Top of MV2	Top MV 3	Top Volume	Top Paleot
1	Point	31	16	12	12	999	999	999	999	999	999	999	999	999	999
2	Point	33	16	12	12	999	999	999	999	999	999	999	999	999	999
3	Point	32	16	15	15	999	999	999	999	999	999	999	999	999	999
4	Point	26	13,5	12	12	999	999	999	999	999	999	999	999	999	999
5	Point	30	13,2	11	11	0	999	999	999	999	999	999	999	999	999
6	Point	24	10,5	15	15	999	999	999	999	999	999	999	999	999	999
7	Point	17	9	2	2	-35	-35	-35	-35	-35	-43	-43	-43	-43	-43
8	Point	19	11	10	10	1	-11	-11	-11	-11	999	999	999	999	999
9	Point	8	11	10	10	2	-10	-10	-10	-10	-51	-51	-51	-51	-51
10	Point	15	13	6	6	999	0	999	999	999	999	999	999	999	999
11	Point	14	13,5	6	6	999	0	999	999	999	999	999	999	999	999
12	Point	13	13	6	6	999	0	999	999	999	999	999	999	999	999
13	Point	12	13	6	6	999	-1	-40	-40	-40	-45	-45	-45	-45	-45
14	Point	11	15,5	11	11	999	4	-37	-37	-37	-43	-43	-43	-43	-43
15	Point	51	17,6	5	5	999	999	999	999	999	999	999	999	999	999
16	Point	52	16,7	4	999	999	4	999	999	999	999	999	999	999	999
17	Point	53	16,1	14	14	7	999	999	999	999	999	999	999	999	999
18	Point	54	15,6	10	10	2	999	999	999	999	999	999	999	999	999
19	Point	55	15,2	14	14	8	999	999	999	999	999	999	999	999	999
20	Point	56	15,2	14	14	-5	999	999	999	999	999	999	999	999	999
21	Point	51	11,6	11	11	2	-15	-42	-42	-42	-50	-50	-50	-50	-50
22	Point	53	11,43	9	9	-1	-13	-42	-42	-42	-51	-51	-51	-51	-51
23	Point	52	11,21	11	11	2	-13	-41	-41	-41	-50	-50	-50	-50	-50
24	Point	52	16	9	9	0	-15	-44	-44	-44	-52	-52	-52	-52	-52
25	Point	523	16	12	12	0	-14	-45	-44	-44	-52	-52	-52	-52	-52
26	Point	534	16	9	9	0	-15	-44	-44	-44	-52	-52	-52	-52	-52
27	Point	501	16	9	9	0	-15	-43	-43	-43	-53	-53	-53	-53	-53
28	Point	531	11	10	10	1	-9	-45	-45	-45	-52	-52	-52	-52	-52
29	Point	553	14,5	9	9	0	-14	-46	-46	-46	-52	-52	-52	-52	-52
30	Point	552	11	10	10	-2	-13	-42	-42	-42	-53	-53	-53	-53	-53
31	Point	56	11,43	10	10	0	-13	-44	-44	-44	-53	-53	-53	-53	-53
32	Point	5A	11,2	10	10	-3	-13	-44	-44	-44	-53	-53	-53	-53	-53
33	Point	5C	11,79	10	10	-1	-14	-43	-43	-43	-53	-53	-53	-53	-53
34	Point	5H2	11,62	10	10	-3	-11	-44	-44	-44	-53	-53	-53	-53	-53
35	Point	5H1	11,62	10	10	-1	999	999	999	999	999	999	999	999	999
36	Point	56	12	10	10	-1	-6	-50	-50	-50	-59	-59	-59	-59	-59
37	Point	V5010511	16	15	15	2	999	999	999	999	999	999	999	999	999
38	Point	V5010529	16	12	12	-1	999	999	999	999	999	999	999	999	999
39	Point	V5010530	11	10	10	999	999	999	999	999	999	999	999	999	999
40	Point	V5011519	10	9	9	999	999	999	999	999	999	999	999	999	999
41	Point	V5011520	10	9	9	999	999	999	999	999	999	999	999	999	999
42	Point	V5011522	10	9	9	999	999	999	999	999	999	999	999	999	999
43	Point	V5011521	10	9	9	999	999	999	999	999	999	999	999	999	999
44	Point	V5011524	9	8	8	999	999	999	999	999	999	999	999	999	999
45	Point	V5011525	9	8	8	999	999	999	999	999	999	999	999	999	999
46	Point	V5011526	9	8	8	999	999	999	999	999	999	999	999	999	999
47	Point	V5011527	9	8	8	999	999	999	999	999	999	999	999	999	999
48	Point	V5011528	9	8	8	999	999	999	999	999	999	999	999	999	999
49	Point	V5011529	9	8	8	999	999	999	999	999	999	999	999	999	999
50	Point	V5011530	9	8	8	999	999	999	999	999	999	999	999	999	999
51	Point	V5011531	9	8	8	999	999	999	999	999	999	999	999	999	999
52	Point	V5011532	9	8	8	999	999	999	999	999	999	999	999	999	999
53	Point	V5011533	9	8	8	999	999	999	999	999	999	999	999	999	999
54	Point	V5011534	9	8	8	999	999	999	999	999	999	999	999	999	999
55	Point	V5011535	9	8	8	999	999	999	999	999	999	999	999	999	999
56	Point	V5011536	9	8	8	999	999	999	999	999	999	999	999	999	999
57	Point	V5011537	9	8	8	999	999	999	999	999	999	999	999	999	999
58	Point	V5011538	9	8	8	999	999	999	999	999	999	999	999	999	999
59	Point	V5011539	9	8	8	999	999	999	999	999	999	999	999	999	999
60	Point	V5011540	9	8	8	999	999	999	999	999	999	999	999	999	999
61	Point	V5011541	9	8	8	999	999	999	999	999	999	999	999	999	999
62	Point	V5011542	9	8	8	999	999	999	999	999	999	999	999	999	999
63	Point	V5011543	9	8	8	999	999	999	999	999	999	999	999	999	999
64	Point	V5011544	9	8	8	999	999	999	999	999	999	999	999	999	999
65	Point	V5011545	9	8	8	999	999	999	999	999	999	999	999	999	999
66	Point	V5011546	9	8	8	999	999	999	999	999	999	999	999	999	999
67	Point	V5011547	9	8	8	999	999	999	999	999	999	999	999	999	999
68	Point	V5011548	9	8	8	999	999	999	999	999	999	999	999	999	999
69	Point	V5011549	9	8	8	999	999	999	999	999	999	999	999	999	999
70	Point	V5011550	9	8	8	999	999	999	999	999	999	999	999	999	999
71	Point	V5011551	9	8	8	999	999	999	999	999	999	999	999	999	999
72	Point	V5011552	9	8	8	999	999	999	999	999	999	999	999	999	999
73	Point	V5011553	9	8	8	999	999	999	999	999	999	999	999	999	999
74	Point	V5011554	9	8	8	999	999	999	999	999	999	999	999	999	999
75	Point	V5011555	9	8	8	999	999	999	999	999	999	999	999	999	999
76	Point	V5011556	9	8	8	999	999	999	999	999	999	999	999	999	999
77	Point	V5011557	9	8	8	999	999	999	999	999	999	999	999	999	999
78	Point	V5011558	9	8	8	999	999	999	999	999	999	999	999	999	999
79	Point	V5011559	9	8	8	999	999	999	999	999	999	999	999	999	999
80	Point	V5011560	9	8	8	999	999	999	999	999	999	999	999	999	999
81	Point	V5011561	9	8	8	999	999	999	999	999	999	999	999	999	999
82	Point	V5011562	9	8	8	999	999	999	999	999	999	999	999	999	999
83	Point	V5011563	9	8	8	999	999	999	999	999	999	999	999	999	999
84	Point	V5011564	9	8	8	999	999	999	999	999	999	999	999	999	999
85	Point	V5011565	9	8	8	999	999	999	999	999	999	999	999	999	999
86	Point	V5011566	9	8	8	999	999	999	999	999	999	999	999	999	999
87	Point	V5011567	9	8	8	999	999	999	999	999	999	999	999	999	999
88	Point	V5011568	9	8	8	999	999	999	999	999	999	999	999	999	999
89	Point	V5011569	9	8	8	999	999	999	999	999	999	999	999	999	999
90	Point	V5011570	9	8	8	999	999	999	999	999	999	999	999	999	999
91	Point	V5011571	9	8	8	999	999	999	999	999	999	999	999	999	999
92	Point	V5011572	9	8	8	999	999	999	999	999	999	999	999	999	999
93	Point	V5011573	9	8	8	999	999	999	999	999	999	999	999	999	999
94	Point	V5011574	9	8	8	999	999	999	999	999	999	999	999	999	999
95	Point	V5011575	9	8	8	999	999	999	999	999	999	999	999	999	999
96	Point	V5011576	9	8	8	999	999	999	999	999	999	999	999	999	999
97	Point	V5011577	9												

The following names correspond to the field of the borehole database :

Cod_Pozzo: name of the borehole

Quotadtmsl: altitude of ground (slm). Ground elevation values of numerical flow simulation which will be composed the model top

Bot_Riport: bottom elevation of Lithotype R. In alluvium; equal to *top_limo*, out of alluvium; equal to *top_volcnc*

Top_Loam: top elevation value of Lithotype A. 999 means no Lithotype A or as a result of inadequate depth of drilling.

Top_Sand: top elevation value of Lithotype B. 999 means no Lithotype B or as a result of inadequate depth of drilling.

Top_Clay: top elevation value of Lithotype C. 999 means no Lithotype C or as a result of inadequate depth of drilling.

Top_Gravel: top elevation value of Lithotype G. 999 means no Lithotype G or as a result of inadequate depth of drilling.

Top_Grvl_2: appraised assigned values by considering the average thickness of neighbouring boreholes including as a result of inadequate depth of drilling. This field consist *top_gravel* values

Top_MV: top elevation values of MV unit (bedrock). 999 means as a result of inadequate depth of drilling.

Top_MV_2: appraised assigned values by considering the average thickness of gravel from neighbouring boreholes including as a result of lack info or inadequate depth of drilling. This field consist *top_MV* values and the active domain limit of numerical flow simulation composed by these values

Top_Volcnc: top elevation value of volcanic unit; 999 means no volcanic layer or as a result of inadequate depth of drilling.

Top_PaleoT: top elevation value of PaleoTiber unit. 999 means no PaleoTiber layer or as a result of inadequate depth of drilling.

Concerning of having lack information about elevations; some additional borehole points have plotted to help the interpolator according to the average elevation of each surface from original borehole datas and bibliographic informations about average thickness of units. The density of additional boreholes is different for each layer and had been continued until attaining the most eligible surface map.

Both selected original and additional boreholes had been extracted in new shape files for each layer in order to constitute the surface elevation map of every unit through executing raster interpolation. Generally, the inverse distance weighted (IDW) technique utilized to interpolate surfaces from points.

Terrain Elevation (Top of model); Triangulated irregular networks (tin) are a digital means to represent surface morphology such as terrain elevation. A tin map of the area which elevation datum derives from the 1:5000 topographic map in order to compose one of the leading objects of modelling such as top of model has been used. The topography is smooth at around 10 - 12 m a.s.l. within the alluvium, ~14 m a.s.l. in Grottaperfetta valley and rising to 38 - 56 m a.s.l. at the hills (Fig 4.11).

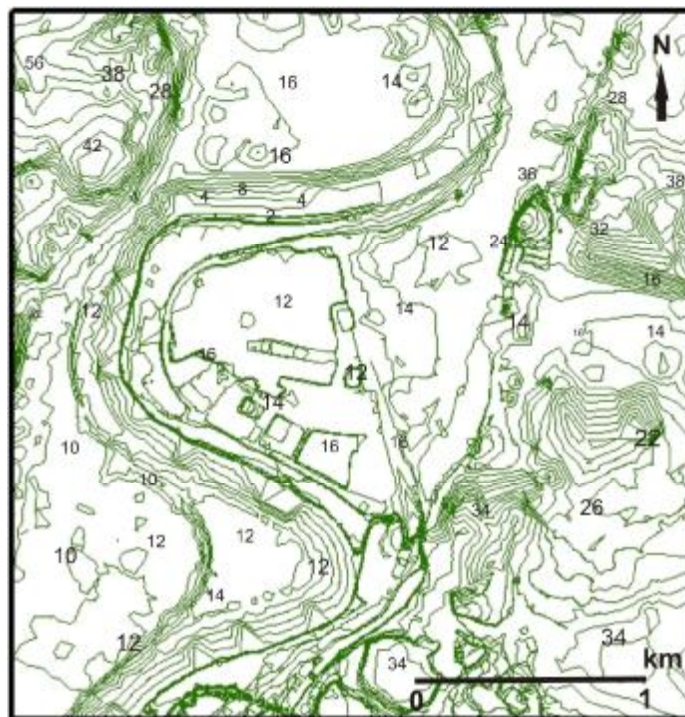


Figure 4.11. Terrain elevation contour map

The following figures show the interpolation results for every surface:

Bottom of Lithotype R; the only unit that represents the whole area on account of being an urbanized place. Constituted by means of combining the *top_loam* values in alluvial valley and *top_vlcnc* values at the hillsides. In the North, top elevation of Lithotype A is around 4 m a.s.l. near the bank of Tiber river and spreading until 13 m a.s.l. to the sides of alluvium and finally ended with 30 m a.s.l. as Volcanics at the hills .

It continues with 10 m a.s.l. in the center of the study area however the altitude of lithotype A is lowering about 7 m a.s.l. within the tributary as it is expected to supersede a part of lithotype B which does not exist in the Grottaperfetta valley (Figure 4.12). In the south of the study area, the altitude is around 8 m a.s.l.

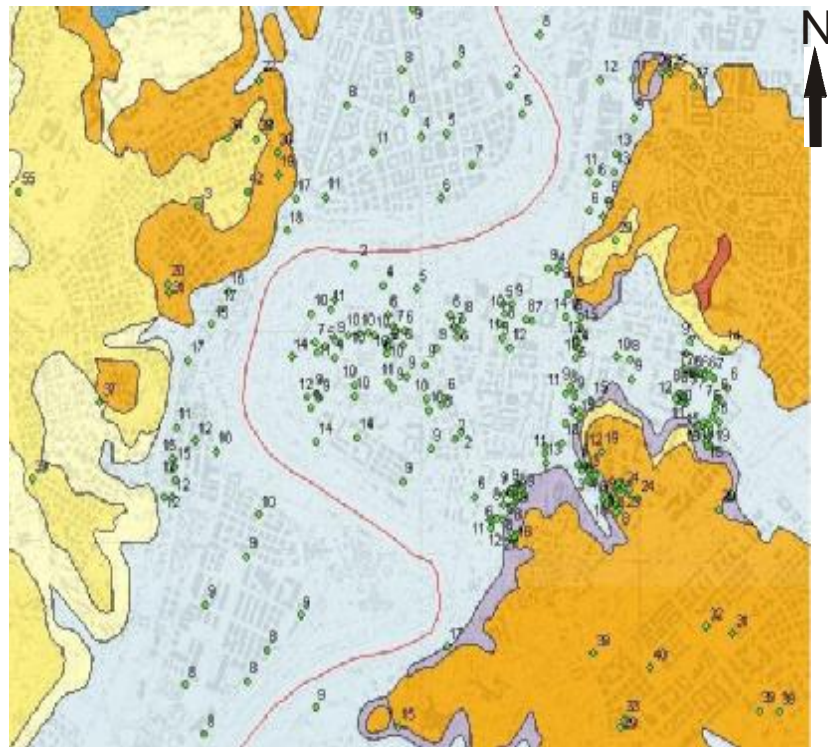


Figure 4.12. Boreholes displayed with bottom elevation values (m.a.s.l.) of lithotype R

The surface has formed with the values presented, support of additional boreholes did not consider through the lack informations in literature for lithotype R that can quote a case about thickness (Figure 4.13).

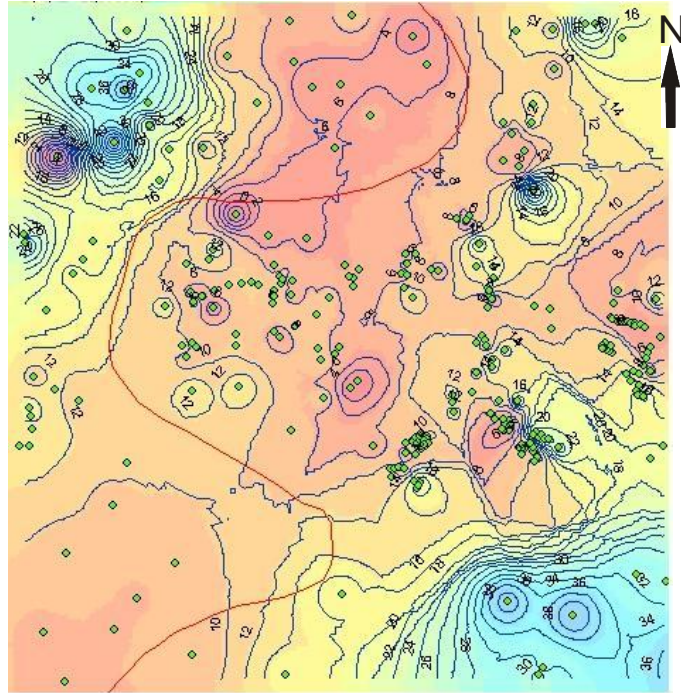


Figure 4.13. Contoured IDW map (m.a.s.l.) of bottom of lithotype R

Top of Lithotype B; the original top elevation database of Lithotype B has formed by 90 boreholes which disperse unevenly and have majority on some local places in the study area. The average altitude variable within the center is about -2 m a.s.l. however the altitude decreases until -8 m a.s.l. where the mouth of the crossing area between main valley and tributary then continues with -1 m a.s.l. in the south (Figure 4.14).

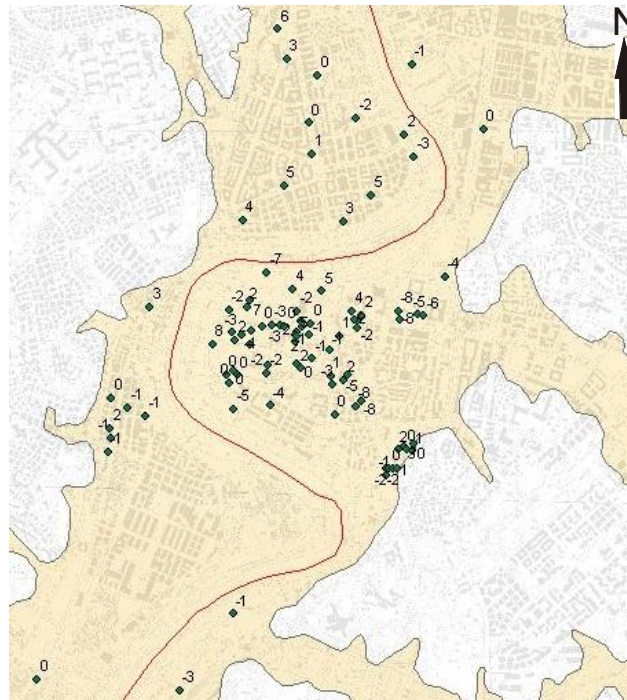


Figure 4.14. Boreholes displayed with top elevation values of lithotype B

129 additional boreholes have been used which decided mainly according to the average values between boreholes, limit of sand unit in the main valley considering the relations in cross sections (Figure 4.15)

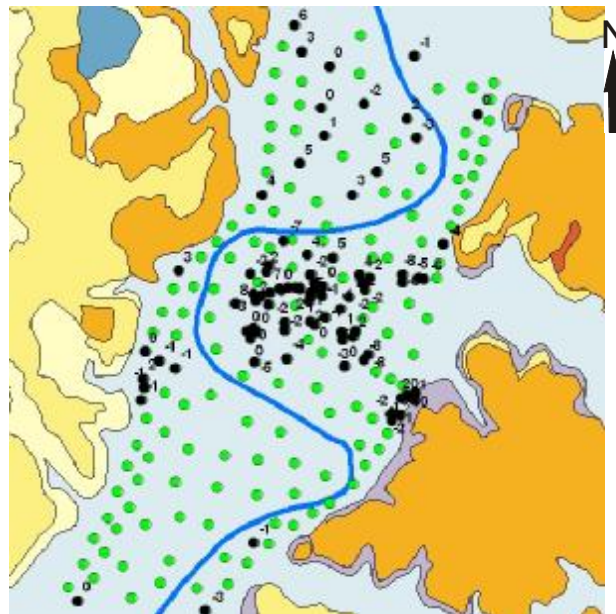


Figure 4.15. Additional boreholes with original boreholes for lithotype B

Additional boreholes has started from the alluvium limit and the density has been controlled under the supply of data for interpolation as much as the interpolator needs (Figure 4.16).



Figure 4.16. Contoured IDW top elevation map of lithotype B

Top of Lithotype C; as is understood from the cross sections, the clay unit consists the most thick layer in the study area. 109 boreholes which were exceeded in numbers in the center and in the secondary valley, have formed the basis of the surface of lithotype C.

The average altitude is starting at -13 m a.s.l. to -6 m a.s.l. with undulating respectively from the north to the south-west. From the center of the valley to the tributary there is a great top altitude change of lithotype C from -18 m a.s.l. to -2 m a.s.l. as presented in the cross sections. The lack of lithotype B unit in Grottaperfetta valley resulted with the rising of lithotype C top altitude (Figure 4.17).

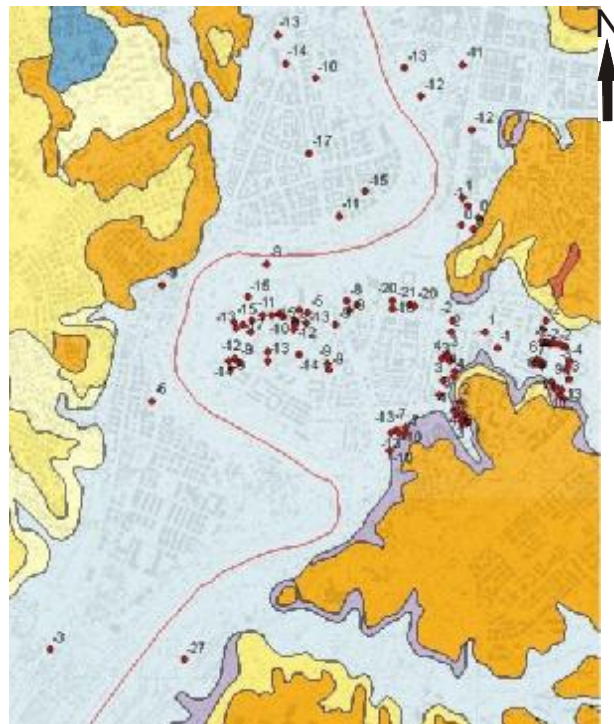


Figure 4.17. Boreholes displayed with top elevation values of lithotype C

These 109 boreholes were supported by 137 additional ones which had started to plot from the border of the alluvium. The distribution of the additional boreholes is homogenized within the areas where the original boreholes rarely scattered (Figure 4.18).

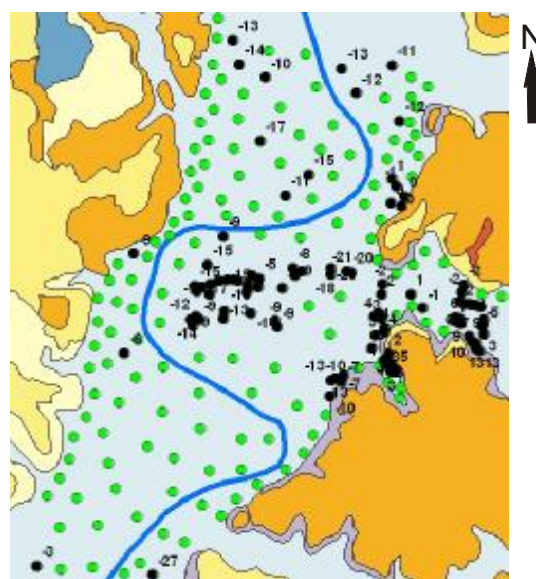


Figure 4.18. Additional boreholes with original boreholes for lithotype C

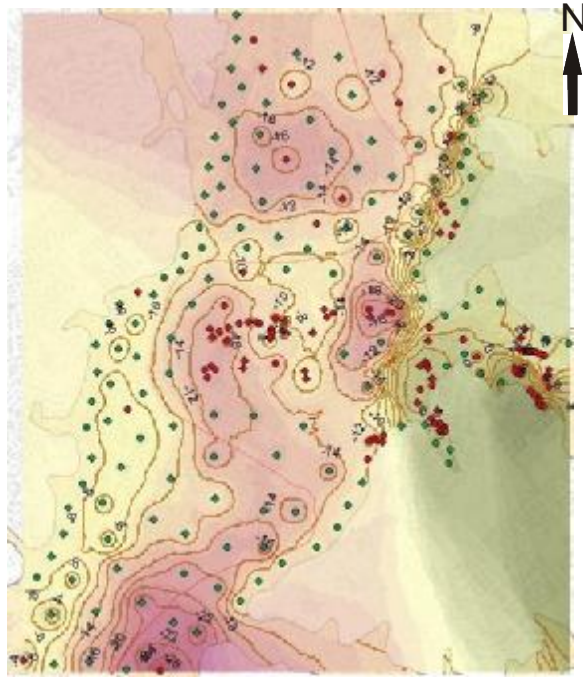


Figure 4.19. Contoured IDW top elevation map of lithotype C

Top of Lithotype G; 58 original boreholes were used during the construction of the top surface of basal gravel. Out of the average thickness estimation, a few boreholes enclosed herein were perpetuated which had fall short of distance to arrive the bedrock. Lengthwise the Grottaperfetta together with the main valley, the altitude of top surface had been encountered about -36 m a.s.l. and -44 m a.s.l., respectively (Figure 4.20).

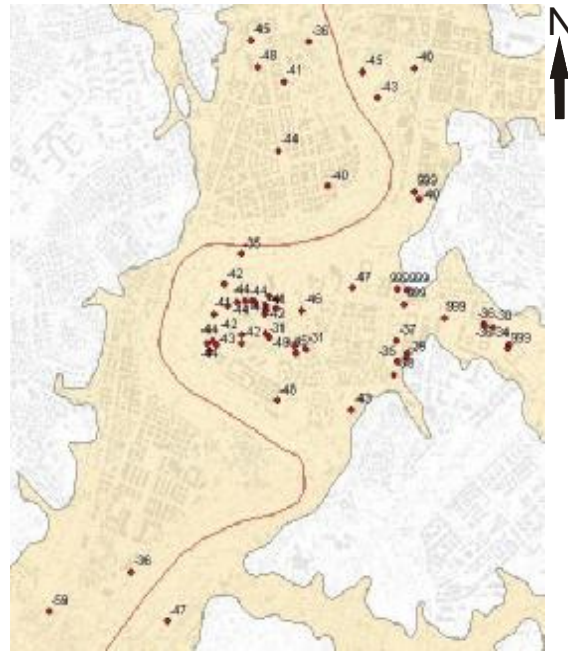


Figure 4.20. Boreholes displayed with top elevation values of lithotype G (999 means no value)

In addition to original datas, 93 additional boreholes were used in order to get the optimum result for top surface of gravel. Exploited from the cross sections for continuity and distance relation with alluvium border to determine the locations of invented boreholes (Figure 4.21).

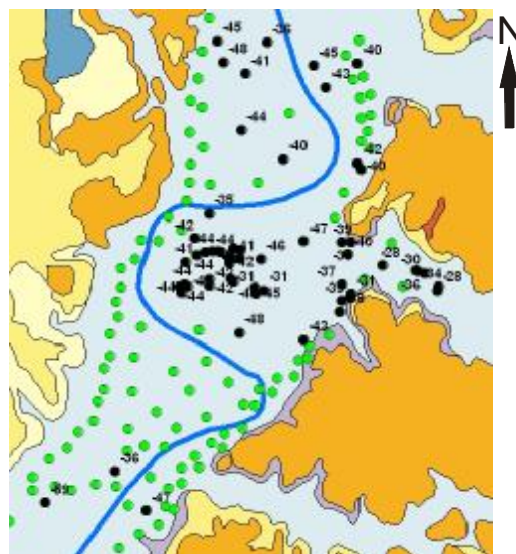


Figure 4.21. Additional boreholes with original boreholes for lithotype G

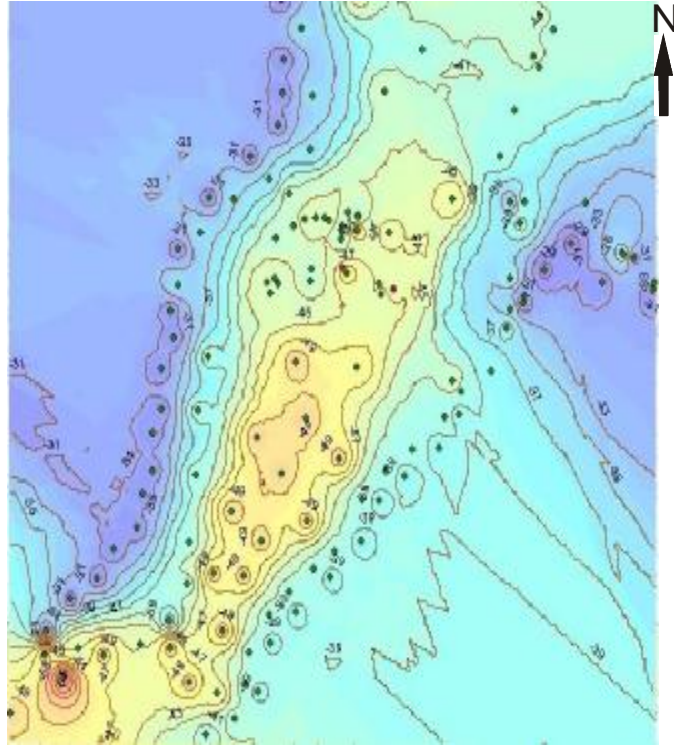


Figure 4.22. Contoured with IDW method top elevation map of lithotype G

Top_MV, top of Monte Vaticano was the surface which had been focused on upwards the others during the interpolation phase. The Monte Vaticano unit, in other words bedrock, constitutes the basis both for whole alluvium and Pleistocene units furthermore underlies the active domain limit of the groundwater flow model in the next stage. Insufficiently boreholes distributed in the south and out of the valley gave inadequate information concerning the surface morphology of the bedrock. The average altitude had been -53 m a.s.l. within the valley although risen up to -10 m a.s.l. out of the valley (Figure 4.23).

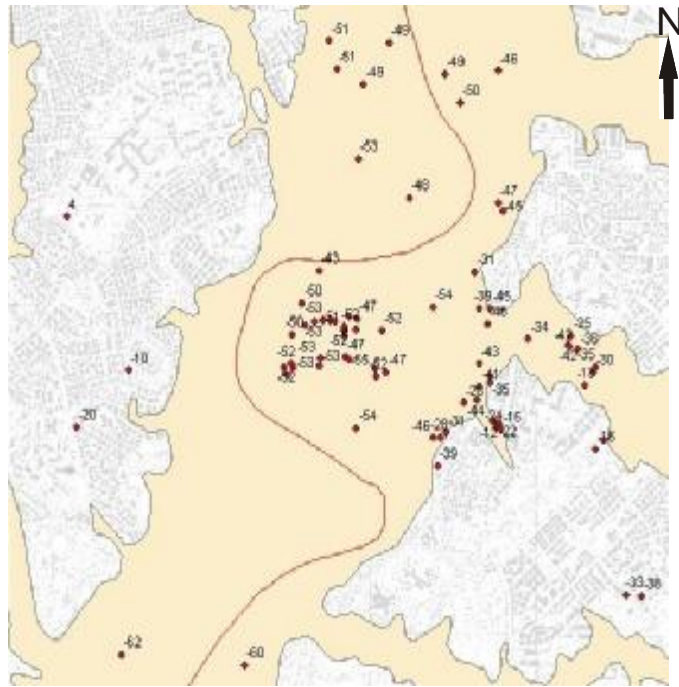


Figure 4.23. Boreholes displayed with top elevation values of Monte Vaticano Unit

The distribution of 155 additional, determined by 75 original boreholes with the analysis of both geological and geomorphological map of the bedrock in the literature (Figure 4.24).

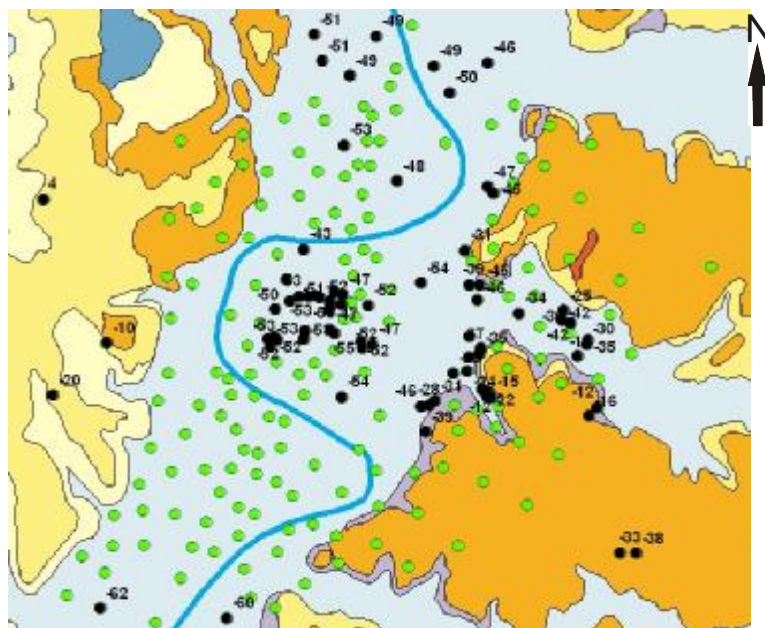


Figure 4.24. Additional boreholes with original boreholes for Monte Vaticano Unit

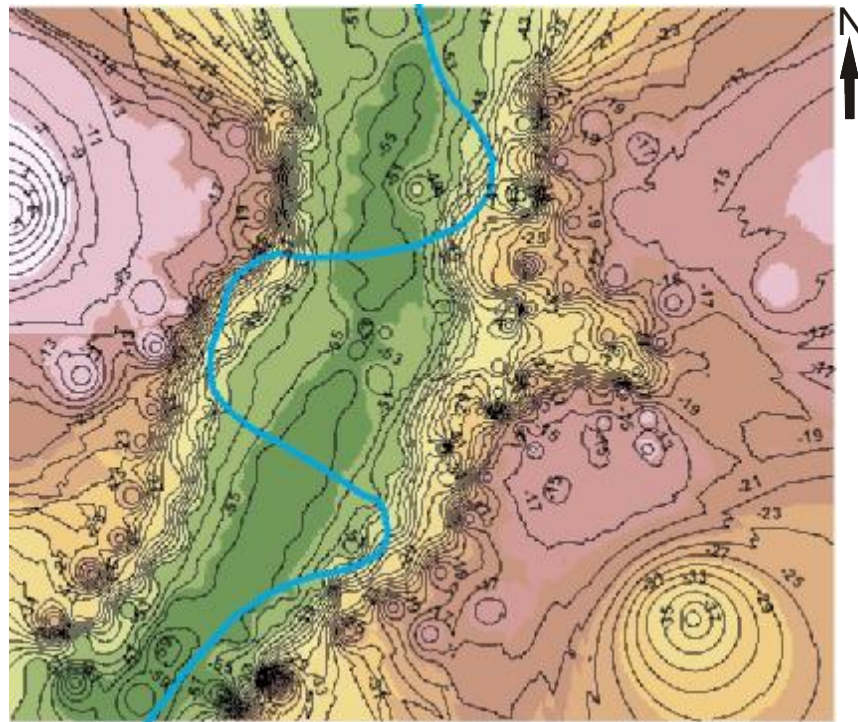


Figure 4.25. Contoured with IDW method top elevation map of Monte Vaticano Unit

4.2. Hydrological and hydrogeological survey

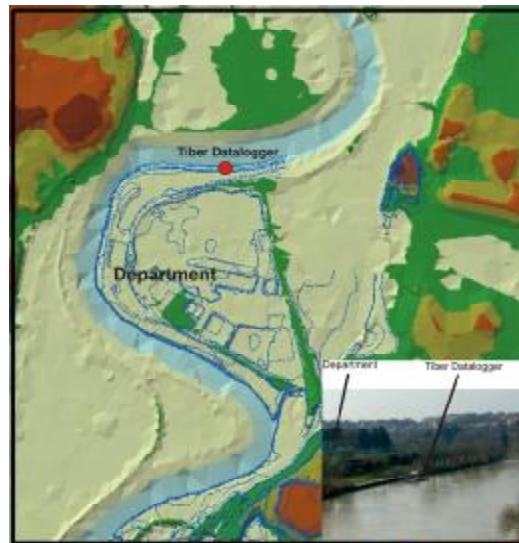
The hydrogeological analysis was based on an interpretation of water-level data obtained from 16 open tube piezometers and one Casagrande piezometer installed in some boreholes drilled in the area along the section together with permeability data for the different lithotypes from background literature information.

4.2.1. Monitoring results in Valco San Paolo

Water level, temperature and electric conductivity properties of two principal aquifer were monitored by two wells in gravel aquifer (lithotype G) and two in sand (lithotype B) during the period between 16 Sep 2009 and 5 Feb 2010. In addition to these wells, six well in gravel with five in sand had measured eleven times in the study period. Only one measuring point for monitoring the river had located in the center course of Tiber (Figure 4.26.a.,b.).



(a)



(b)

Figure 4.26. Location of (a) piezometers (b) Tiber datalogger

The station has approximately 800 m distance from the department where the datalogger had installed for monitoring the river. It has chosen for its easement of access however after the flood event in december 2009, at the time of a visit for installing data, realised that it was standing under a thick amount of mud and the line had broken loose and finally lodged while taking the datalogger from the river.

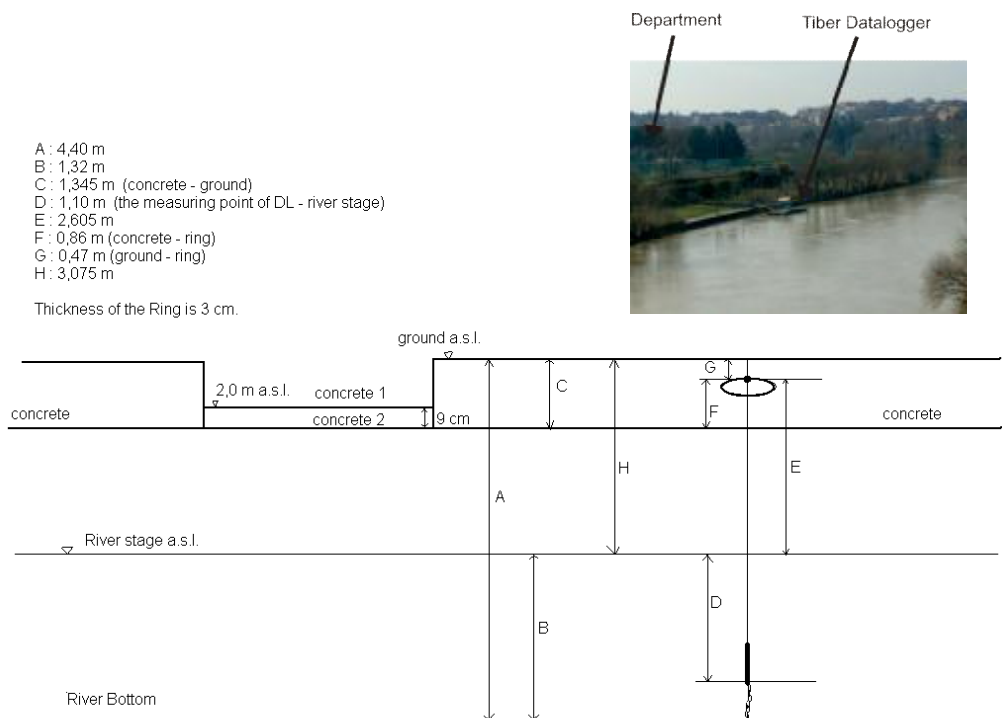


Figure 4.27. Installing datalogger in Tiber River (No scale)



Figure 4.28. Monitoring wells

4.2.2. Physical Analysis of groundwater

The graphs were constituted at a result of four months monitoring period.

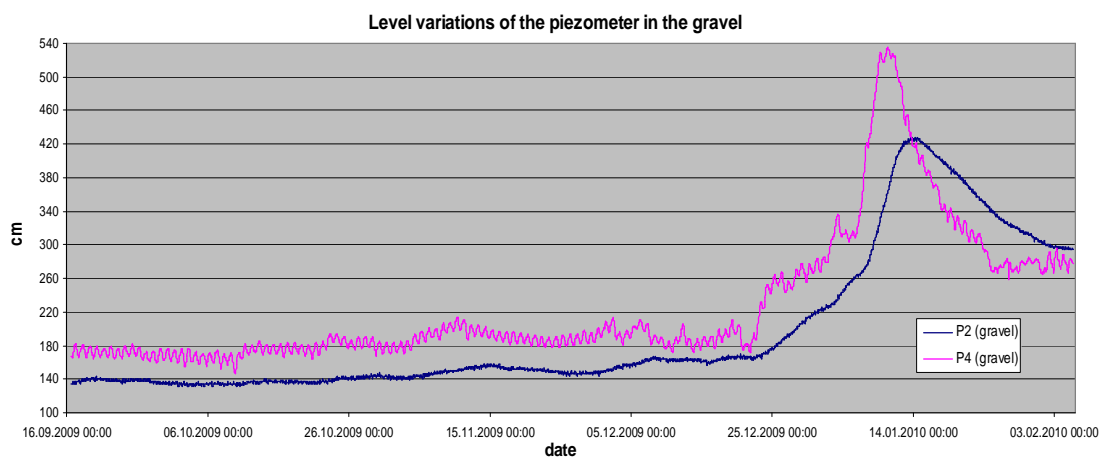


Figure 4.29. Hourly groundwater level variation in gravel

In both piezometers P2 and P4; water level trend is similar along 3 months, the average values are around 1,46 m s.l.m. and 1,82 m s.l.m, respectively until the unaccountable water level rising at the end of December 2009.

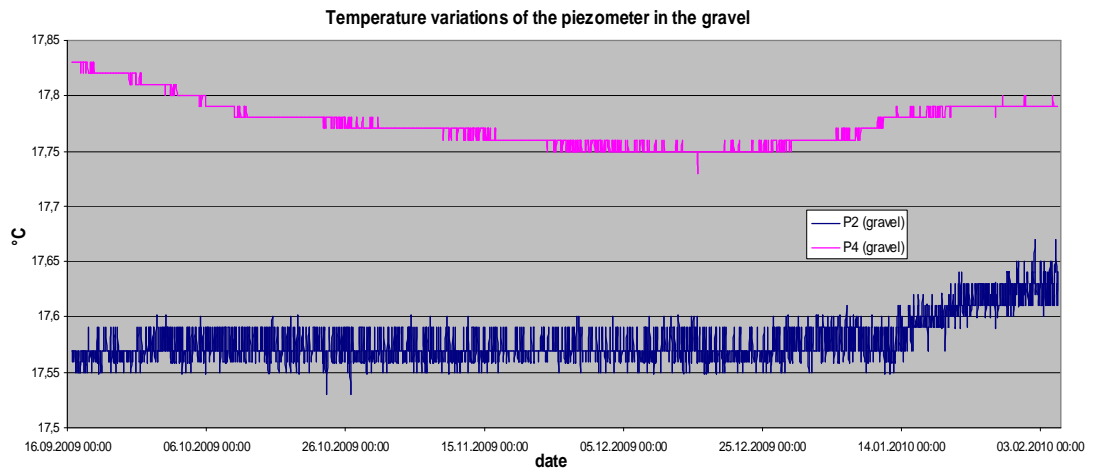


Figure 4.30. Hourly water temperature variation in gravel

Temperature in gravel aquifer varying around 17,78 °C - 17,58 °C. Except the initial days of monitoring with the end of January, a walloping change in temperature was not observed.

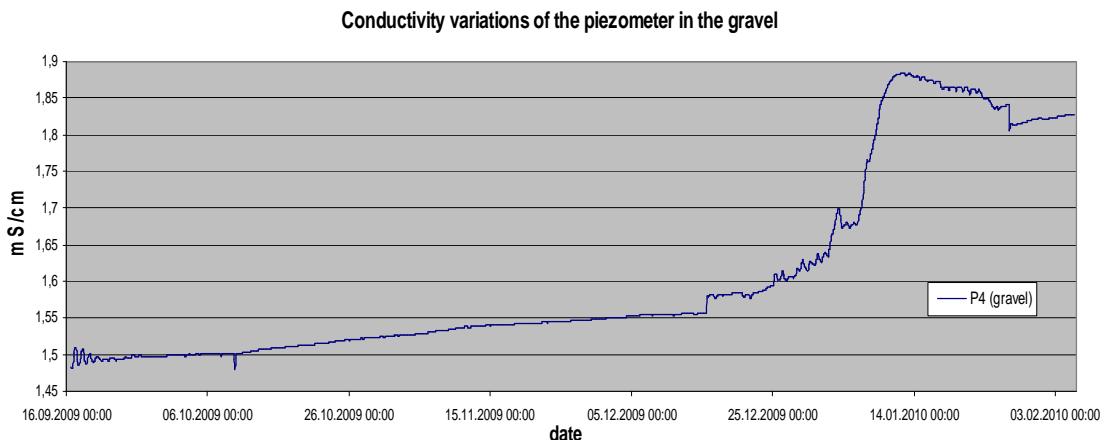
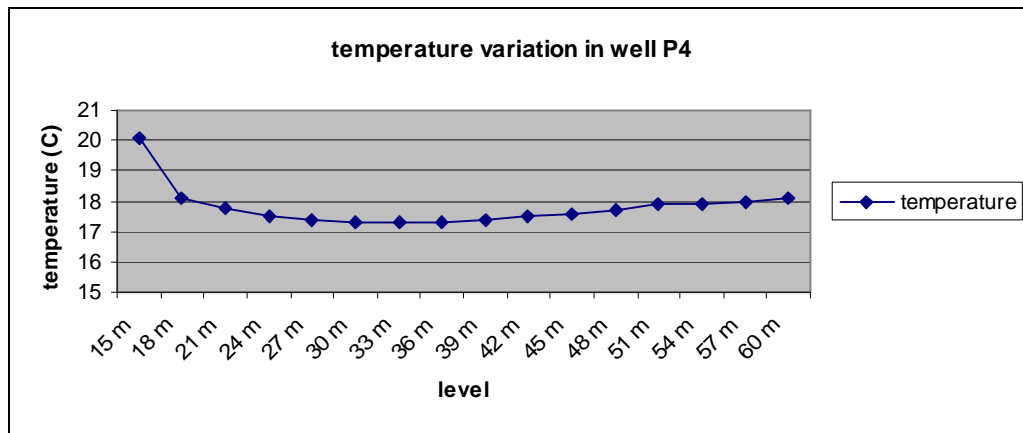


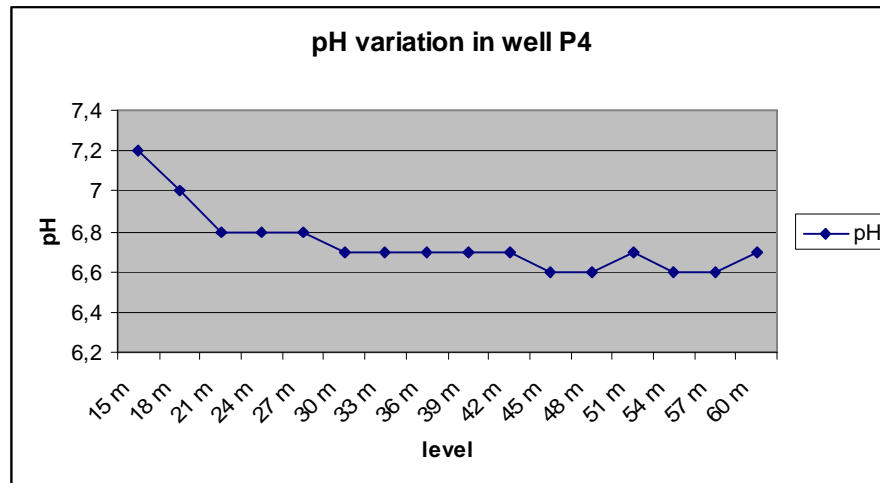
Figure 4.31. Hourly conductivity variations of the piezometer in gravel

Electrical conductivity is locally rather high with values slightly exceeding 1,5 mS/cm and increasing until 1,885 mS/cm whereas the pH is mostly neutral and slightly acid (6,6 - 6,7) in some zones.

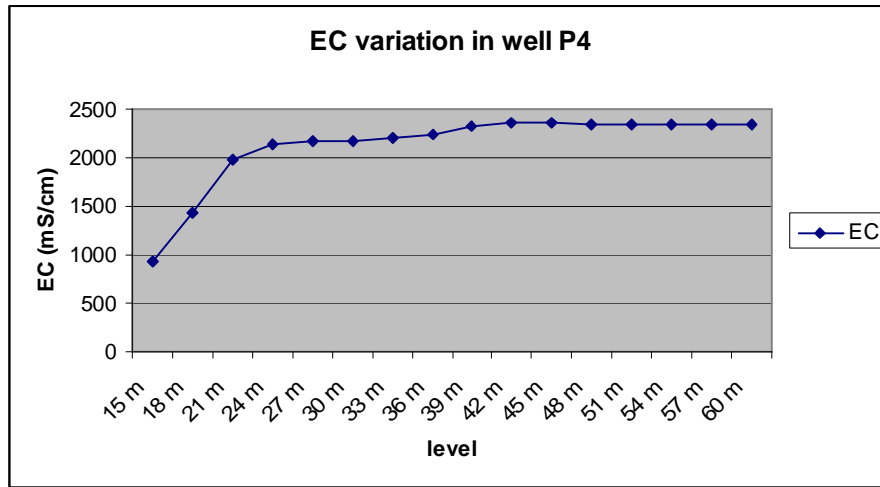
Variations due to the exact position of sonda in gravel showed the temperature and also electrical conductivity rises because the multiparameter sonda meets the real aquifer water in the last 10 meters.



(a)



(b)



(c)

Figure 4.32. Log profile of well P4; a. T(°C), b. pH and c. EC(mS/cm) measurement (Department of Geological Sciences, RomaTRE University 16/07/2009)

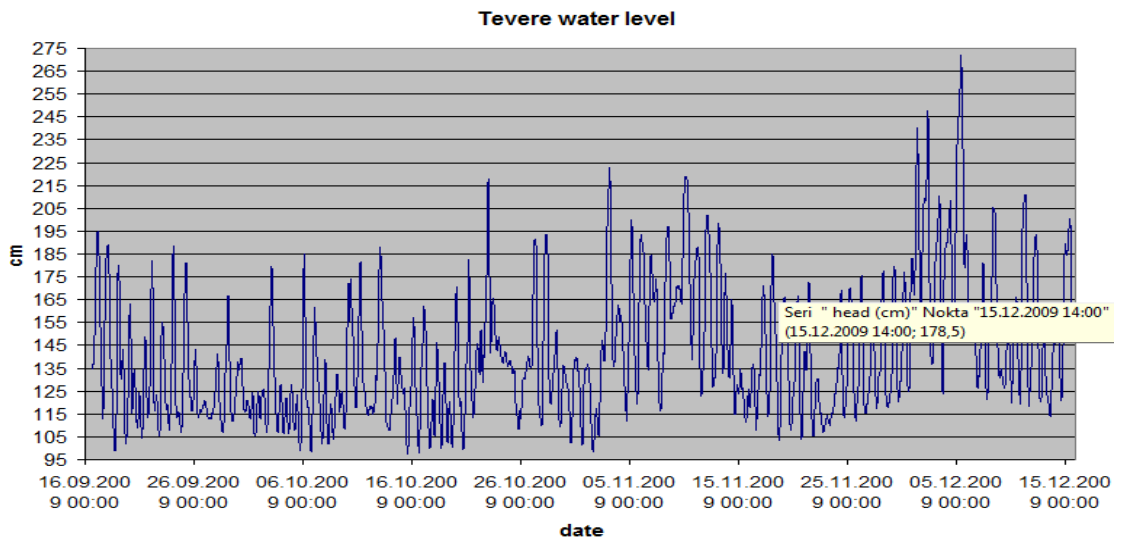


Figure 4.33. Hourly Tiber river level variation

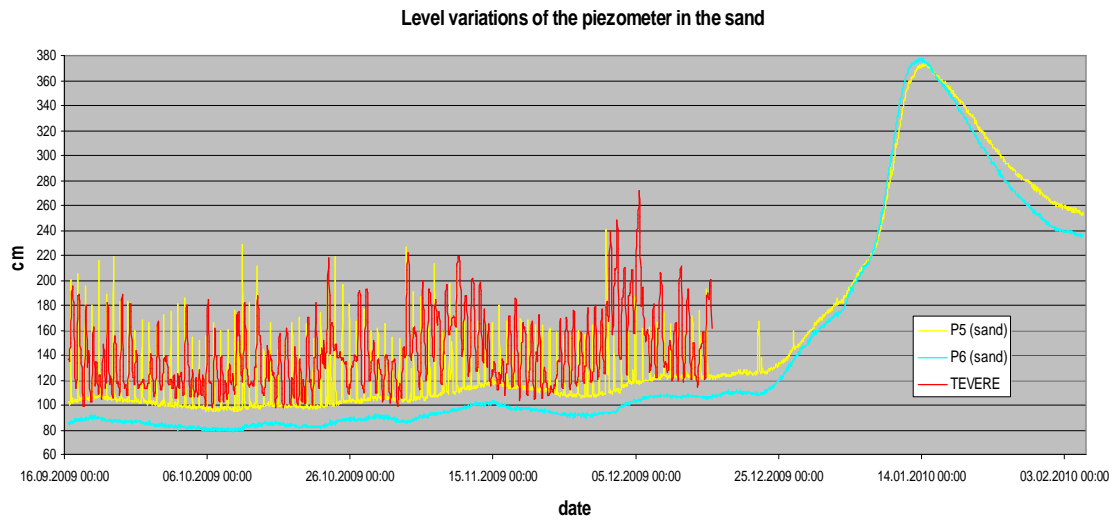


Figure 4.34. Hourly level variations of the piezometers in sand compared with Tiber river variations

Tiber river could not be observed after 15 December 2009 by reason of flood affair.

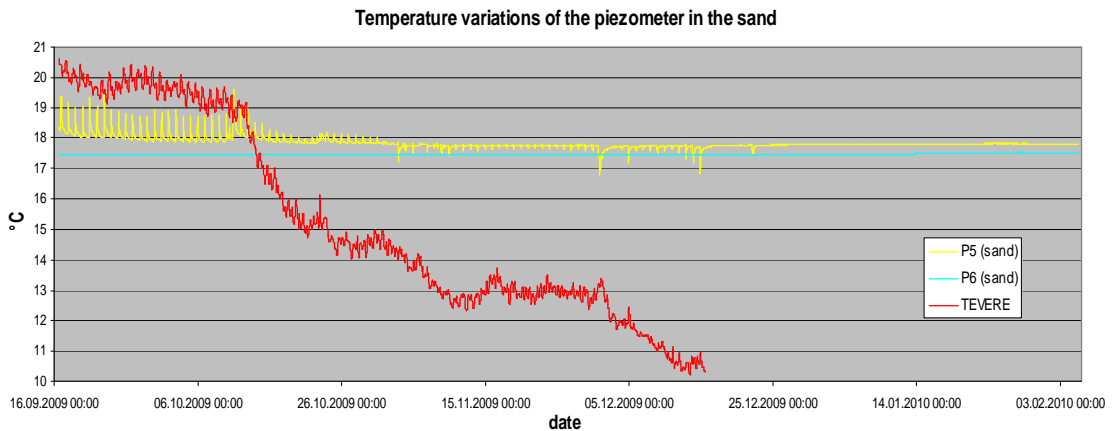


Figure 4.35. Hourly temperature variations of the piezometers in sand compared with Tiber variations

The variation of temperature in sand aquifer is highly similar in both piezometers (between 17,45-17,85 °C). If comparison is needed the temperature of sandy aquifer is 0,35°C lower than in gravel aquifer.

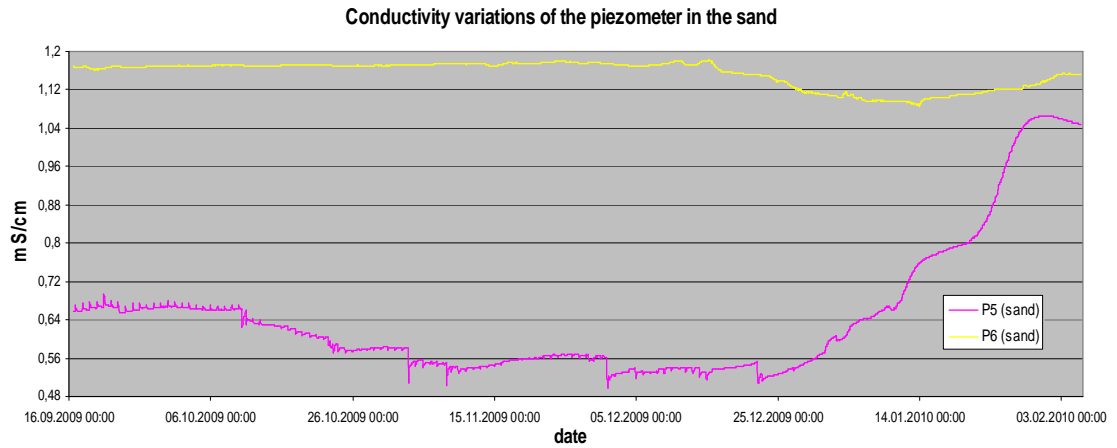


Figure 4.36. Hourly electrical conductivity variations of the piezometers in sand

Conductivity varies homogenically at around 1,17 mS/cm within the sand aquifer, in another well EC is increasing after a few time. Nonetheless, the increasing of gravel and sand aquifer is more or less compatible (25/12/2009).

Table 4.1. Static level measurements of wells in sand aquifer

Well no:	P5	P1	P6	Vicolo Savini SC	Vicolo Savini SB	Pian-2-Torri	Vivaio
Quota (m)	16,03	15,92	15,98	12	11,84	10,34	14,09
Depth (m)	29,5	24	24,5	15	15	33,90	25
Measuring date (1)	27.01.2010	27.01.2010	28.01.2010	29.01.2010	29.01.2010		
Static L. (slm)	2,69	2,69	2,56	3,05	2,89		
Measuring date (2)				16.03.2010	16.03.2010		
Static L. (slm)				4,04	4,03		
Measuring date (3)	23.03.2010		23.03.2010	23.03.2010	23.03.2010		23.03.2010
Static L. (slm)	3,25		3,07	3,60	3,43		4,16
Measuring date (4)	09.04.2010			09.04.2010	09.04.2010		
Static L. (slm)	2,38			2,97	2,82		
Measuring date (5)	16.04.2010			16.04.2010	16.04.2010		
Static L. (slm)	2,33			2,84	2,64		
Measuring date (6)	26.04.2010			26.04.2010	26.04.2010	26.04.2010	
Static L. (slm)	2,09			2,67	2,51	3,38	
Measuring date (7)	29.04.2010			29.04.2010	29.04.2010		
Static L. (slm)	2,05			2,62	2,48		
Measuring date (8)	07.05.2010			07.05.2010	07.05.2010		
Static L. (slm)	1,92			2,63	2,44		
Measuring date (9)				18.05.2010	18.05.2010		
Static L. (slm)				3,69	3,55		
Measuring date (10)	28.05.2010			28.05.2010	28.05.2010		
Static L. (slm)	2,71			3,08	2,94		
Measuring date (11)	11.06.2010	11.06.2010	11.06.2010	11.06.2010	11.06.2010	11.06.2010	11.06.2010
Static L. (slm)	1,91	1,89	1,8	2,57	2,45	2,96	3,15

Table 4.2. Static level measurements of wells in gravel aquifer

Well no:	Eucalipti	P4	P2	Vasca Navale S3	Vicolo Savini SA	Vicolo Savini SBC	Vigli	Esso
Quota (m)	10,86	16,11	15,97	10,23	11,87	11,76	10,44	10,62
Depth (m)	62	64	65		60	60	58,36	60
Measuring date		16.07.2009	16.07.2009					
Static L. (slm)		1,34	1,12					
Measuring date (1)	15.12.2009	27.01.2010	27.01.2010	28.01.2010	29.01.2010	29.01.2010	02.02.2010	
Static L. (slm)	1,67	2,73	2,64	2,23	3,11	3,08	2,69	
Measuring date (2)	16.03.2010				16.03.2010	16.03.2010	16.03.2010	
Static L. (slm)	3,74				4,29	4,24	3,56	
Measuring date (3)	23.03.2010	23.03.2010			23.03.2010	23.03.2010	23.03.2010	
Static L. (slm)	3,21	3,35			3,67	3,63	3,02	
Measuring date (4)	09.04.2010	09.04.2010			09.04.2010	09.04.2010	09.04.2010	
Static L. (slm)	2,17	2,95			3,29	3,18	2,68	
Measuring date (5)	16.04.2010	16.04.2010	16.04.2010		16.04.2010	16.04.2010	16.04.2010	
Static L. (slm)	2,82	2,90	2,65		3,19	3,16	2,64	
Measuring date (6)	26.04.2010	26.04.2010			26.04.2010	26.04.2010	26.04.2010	
Static L. (slm)	2,62	1,92			2,93	3,02	2,43	
Measuring date (7)	29.04.2010	29.04.2010	29.04.2010		29.04.2010	29.04.2010	29.04.2010	
Static L. (slm)	2,65	2,35	2,01		3,28	3,06	2,51	
Measuring date (8)	07.05.2010	07.05.2010			07.05.2010	07.05.2010	07.05.2010	
Static L. (slm)	2,60	2,60			2,91	2,93	2,55	
Measuring date (9)	18.05.2010	18.05.2010	18.05.2010		18.05.2010	18.05.2010	18.05.2010	
Static L. (slm)	3,94	4,02	3,01		4,46	4,43	3,87	3,78
Measuring date (10)	28.05.2010	28.05.2010	28.05.2010	28.05.2010	28.05.2010	28.05.2010	28.05.2010	28.05.2010
Static L. (slm)	2,91	2,97	2,68	2,81	3,31	3,32	2,88	2,91
Measuring date (11)	11.06.2010	11.06.2010	11.06.2010	11.06.2010	11.06.2010	11.06.2010	11.06.2010	11.06.2010
Static L. (slm)	2,34	2,26	2,19	2,40	2,67	2,70	2,24	3,15

The water level of Tiber river had been measured in 11.06.2010 at two location which were selected according to the rivers' most measurable part from the up-stream and down-stream. These values are 1,31 m a.s.l. and 0,8 m a.s.l. located in the north and sufficiently south of Valco San Paolo, respectively. The course of the river has been reflected to the hydraulic gradient calculation. The 3500 meters between the two measured point have been divided into seven parts which conserved a 0,0728 m difference per 500 m in terms of water level. At the south part where the river had strongly curved, the 500 m distance had decreased to 250 m in order to represent the intensive curve, following this; the values plotted in ArcMap 9.2.

As showed in Figure 4.37., different points of water level values exist on a line object would be deficient to explain the river flow direction in a computer based media, consequently; to create the contour lines, several supporting points which the same value with each measuring points had plotted astride own measuring point on a perpendicular line to the river. The values are valid just in the river course.

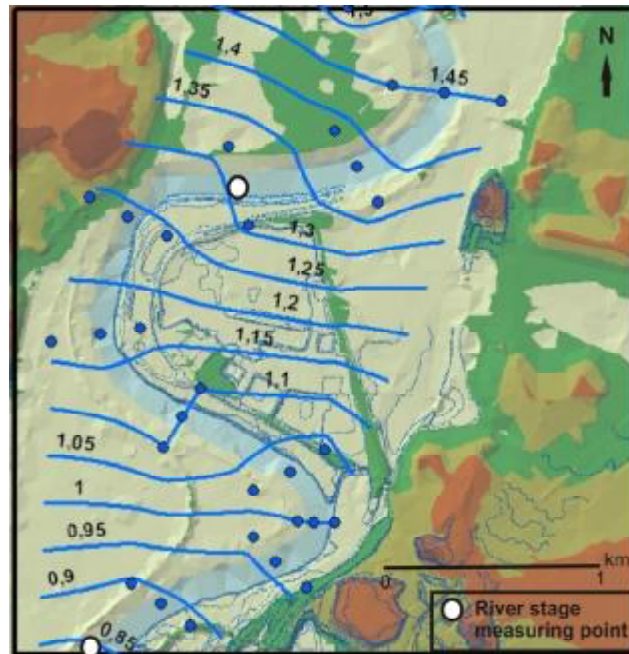


Figure 4.37. River stage gradient along the Tiber River (contour interval : 0,05 m)

The sand unit has embodied the principal aquifer in the study area nonetheless have a hydraulic relation with the Tiber river. According to the piezometer and river stage measurements of 11.06.2010, a water table map has been drawn (Figure 4.38).

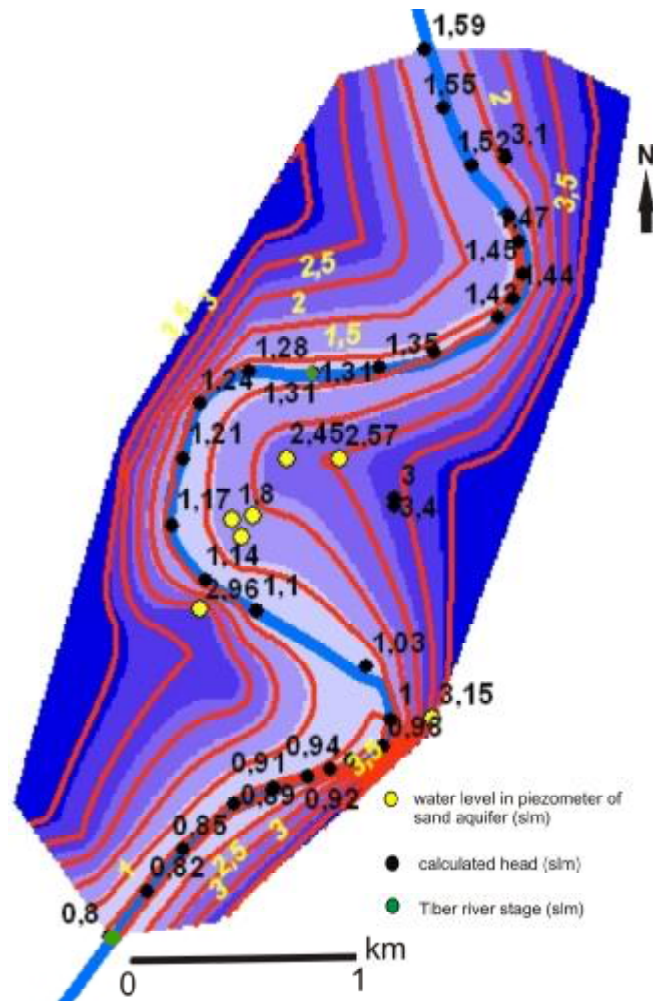


Figure 4.38. Water table map of sand aquifer (contour interval : 0,5 m)

It is observed that, there is a significant amount of groundwater influx to the river, when the flow directions encountered nearby the river. The intervals of water table contours of sand became frequent where the sand aquifer is geologically in strong relation with Paleotiber and volcanic units.

The other important aquifer of the area is within the basal gravel. Due by the geology showed in the cross sections and by the levels measured in its piezometers the aquifer can be considered confined. Seven piezometers were measured in

11.06.2010 with 2,7 m a.s.l. from the north to 2,1 m a.s.l. to the south. As is the case in sand aquifer, about 19 estimated points plotted in order to facilitate the interpolator taking into account the hydraulic gradient.

Finally appeared that the study area head change varies approximately between 4 - 2 m a.s.l. (Figure 4.39).

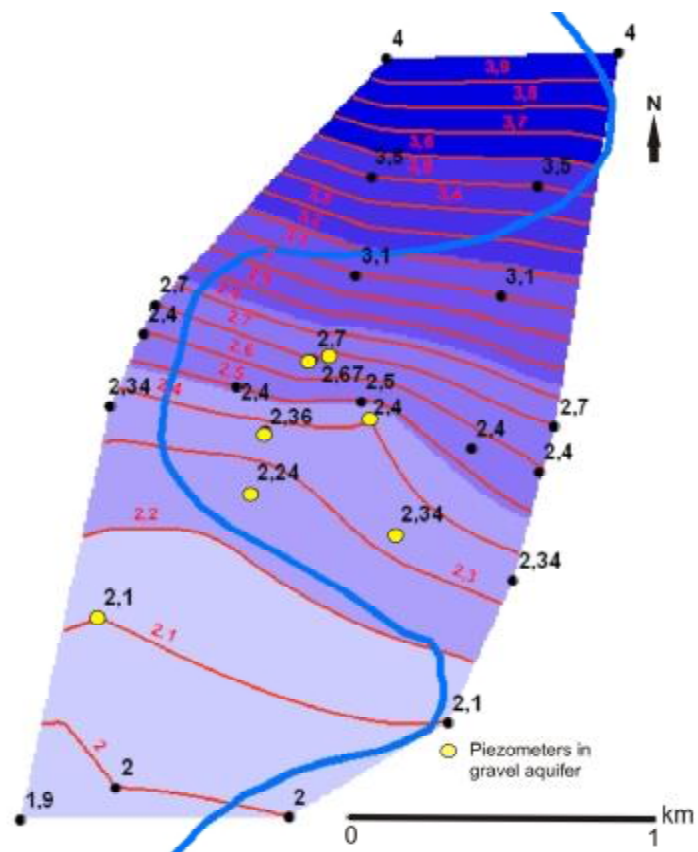


Figure 4.39. Potentiometric level map of gravel aquifer (contour interval : 0,1 m)

4.3. Hydrogeological Conceptual Model

It is possible to develop a ground water conceptual model comparing all results of the study (Fig 4.40). The Valco San Paolo area is characterized by eight main hydrostratigraphic units;

The considerably thick (more than 800 m) deep marine clay with sand intercalations (Monte Vaticano unit) considered as aquiclude, constitute the bedrock. Very low permeability ($k = 10^{-10}$ m/s).

The basal gravel aquifer (lithotype G) ($k=10^{-3}$ m/s) which hosts mineralized water (on average EC 1,540 mS/cm, T 17,67°C) is confined downward by the Monte Vaticano aquiclude and upward by impermeable clay deposits (lithotype C).

The Grottaperfetta basal gravel ($k=10^{-5}$ m/s) differentiated as standing on a -47 m a.s.l. high bedrock with 5 m thickness.

The clay with rich organic material (lithotype C) ($k=10^{-8}$) represents a low permeability unit; in the center of the area, middle permeable sandy lenses which represented as local aquifers exist (lithotype D) ($k=10^{-7}$).

The medium to fine grained sand unit (lithotype B) ($k=10^{-6}$) is hydrogeologically in connection mainly with Tiber river within the plain and with Pleistocene fluvial deposits within the nearby hills which provides recharge for this semi-confined aquifer (on average EC 0,870 mS/cm, T 17,6°C).

The low permeability silty loam unit (lithotype A) ($k=10^{-8}$) is deemed as unconfined superficial aquifer; acquires the surface flow cycle within the plain and involved with the middle-lower permeable volcanic ash deposits that bound the valley.

The Paleotiber unit ($k=10^{-4}$) has been supposed to be in strong relation with sand unit through the NW-SE direction. In the northwest hills these units has a few relation whereby the geological interpretation.

The volcanic unit ($k=10^{-6}$) has more relation with silty loam however in the southwest has a serious contact with sand aquifer.

The anthropogenic fill sediments (lithotype R) ($k=10^{-7}$) indicate an unconfined aquifer bounded by a low permeability base formed of silty loam (lithotype A) in the alluvium and volcanic deposits in the nearby hills.

It is possible to identify two main circulations in the Valco San Paolo area; the first one is in the sandy aquifer which has feeding from the Pleistocene units hillsides through the alluvial valley and it varies according to the regime of Tiber, the second one is in the confined basal gravel aquifer that hydraulic gradient in the study area is not so high, the flow pass through from north to south.

They are locally not in relation by the analysed boreholes of the area, notwithstanding the level variation graphs of the gravel and sand aquifers show a very similar trend after the Tiber flood event of December 2009. The hydraulic communication probably occurs upstream to the study area.

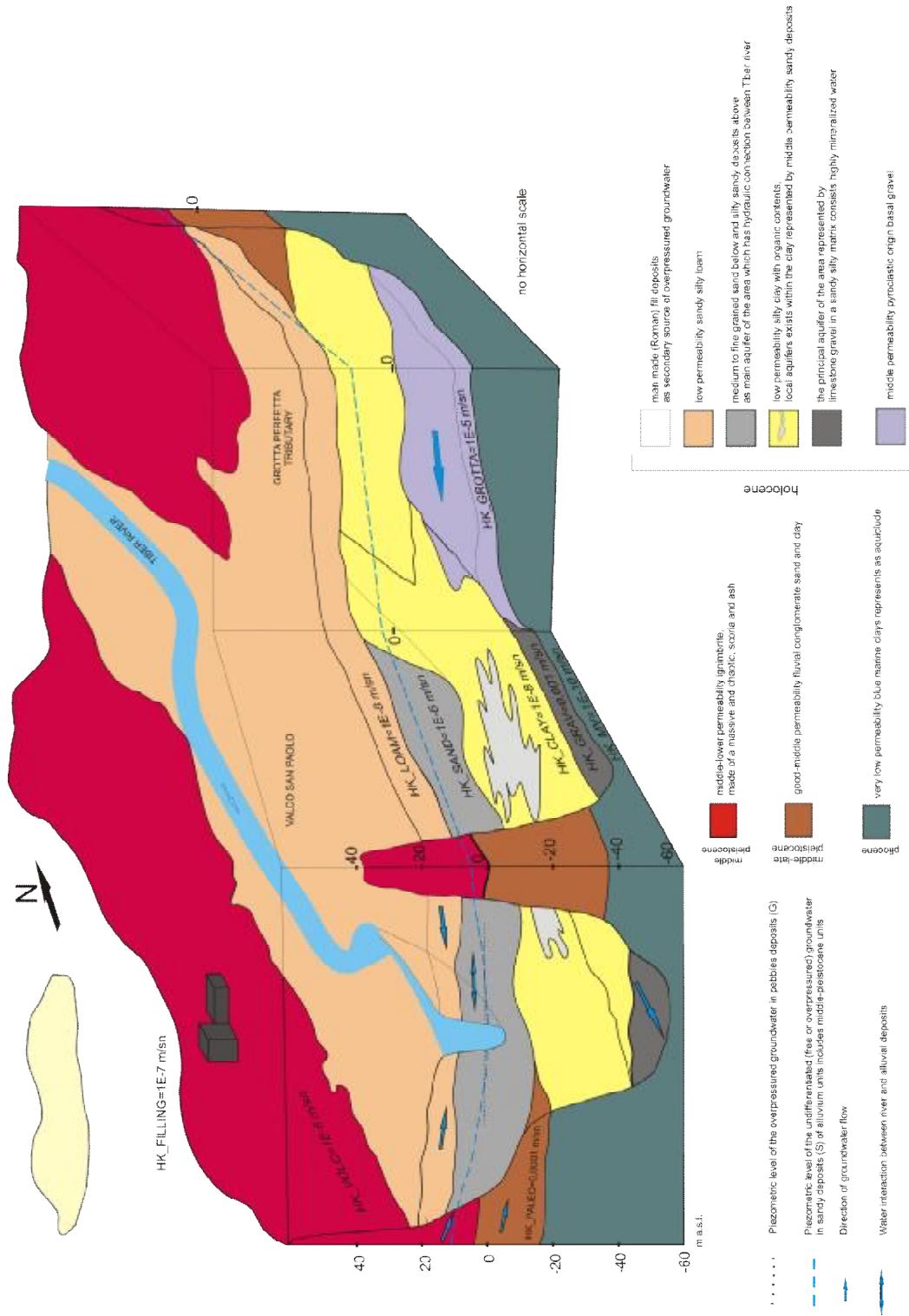


Figure 4.39. The hydrogeological conceptual model

4.4. Numerical Model

4.4.1. Grid construction and layer discretization

The study area which is 6,6 km², was discretized with a finite-difference grid that was composed of 26 rows and 25 columns with uniform cell dimensions of 100 m by 100 m. There are 2575 active cells in all model domain. The model domain was divided into five layers corresponding to the main geological surfaces with 562 active cells in the first four layer besides, 327 active cells in the fifth layer. The whole sixth layer was represented inactive.

Contour maps which values of them are set by interpolation for each layer with digital topography map prepared with ArcMap 9.2 were used to determine the cell elevations.

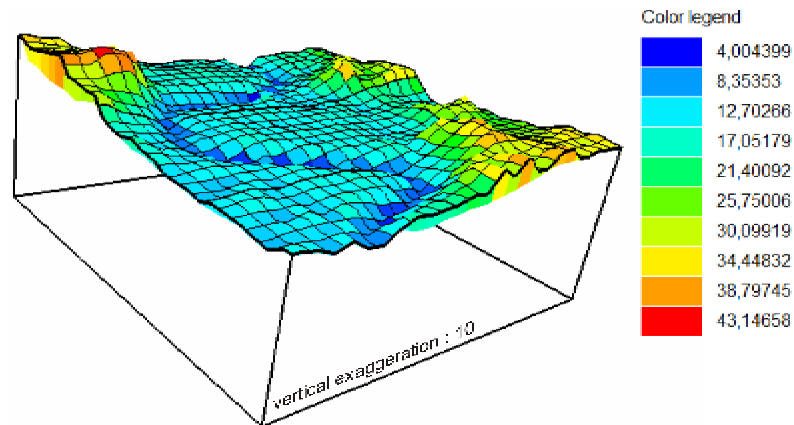


Figure 4.41. 3D visualization of top model topography

Within the simulation, elevation of model top and the bottom topography of the active domain limit range from 2 to 44 m and 11 to - 55 m a.s.l., respectively. All the layers were mainly constructed to represent different properties of Holocene alluvium however, on the east and west hillsides; the third layer represents the paleofluvial unit and second layer is shared by volcanic ash besides loam.

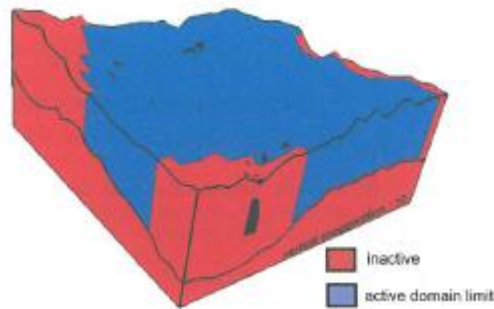


Figure 4.42. Displayed active domain limit of the model

In Modelmuse, Formulas are also used to define the geometry of 3-D objects. When a Formula is applied to a data set or boundary condition with a line, point or a polygon, the formula will only be used for those nodes or elements that the object affects. During the layer discretization, objects with formulas were used in several places in order to prevent the crossing aspects between two surface.

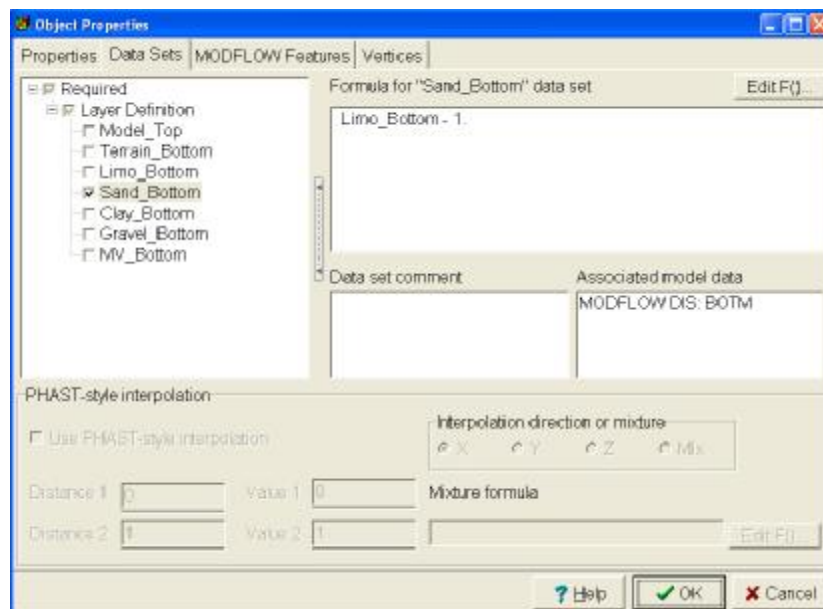


Figure 4.43. Formula for “Sand_Bottom” data set

Layer 1 represents low permeability backfill deposits (filling). In the areas where backfill unit did not observed in the borehole logs; the bottom surface

contours of filling were crossing with the topographic contours of model thus polygons were defined with formula [bottom of terrain = model top - 1].

Layer 2 represents the low permeable silty loam units in correspondence of the valley and the volcanic units at the borders.

Layer 3 represents the middle permeable sand unit in correspondence of the valley and the fluvial Paleotiber unit at the borders.

Layer 4 represents the very low permeable clay unit. Out of the alluvial valley where the gravel is discontinuous, the continuity of the clay bottom contours can not be also ignored. Thus, the contours of clay bottom and gravel bottom are colliding in three notable places. Therefore, in order to bring away these crossing layer boundaries; polygons were seated in these places with formula [clay bottom=gravel bottom+1]

Layer 5 represents the high permeable basal gravel aquifer in the area which meet with the basal gravel of the left-bank tributary in the same layer.

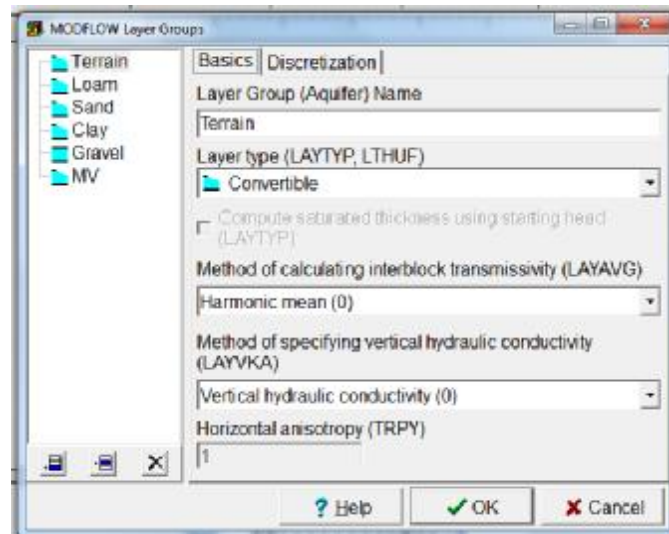


Figure 4.44. Modflow layer groups tab

The first four layer together with bedrock were modeled as confined-unconfined type. At the beginning, layer 6 was defined as convertible type owing to have sand intercalations within clay however it has considered inactive in order to simplify the model, subsequently. The fifth layer simulated as confined.

Layer Property Flow (LPF) Package was used to simulate flow in the saturated zone. The initial HK (horizontal hydraulic conductivity) parameters for the first execute were based on literature information. Nine HK parameters in the LPF package were defined by means of polygon objects to represent each lithology (Fig. 4.45).

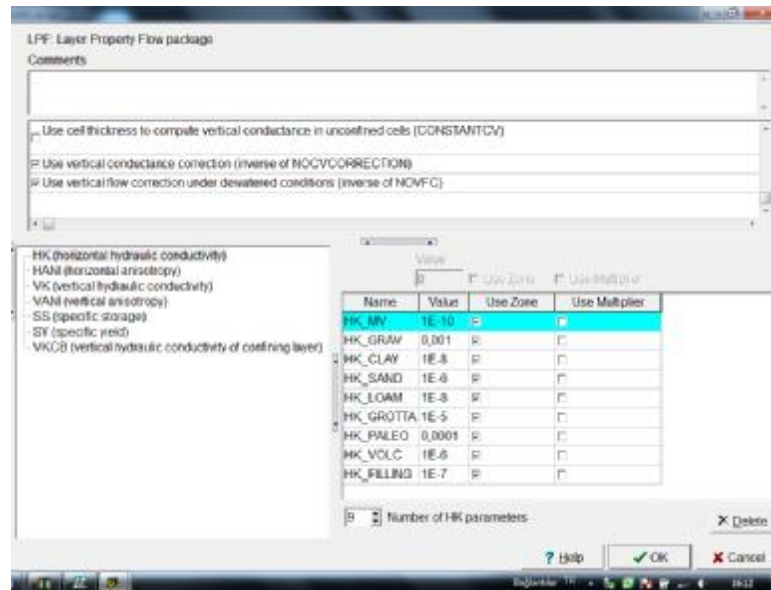
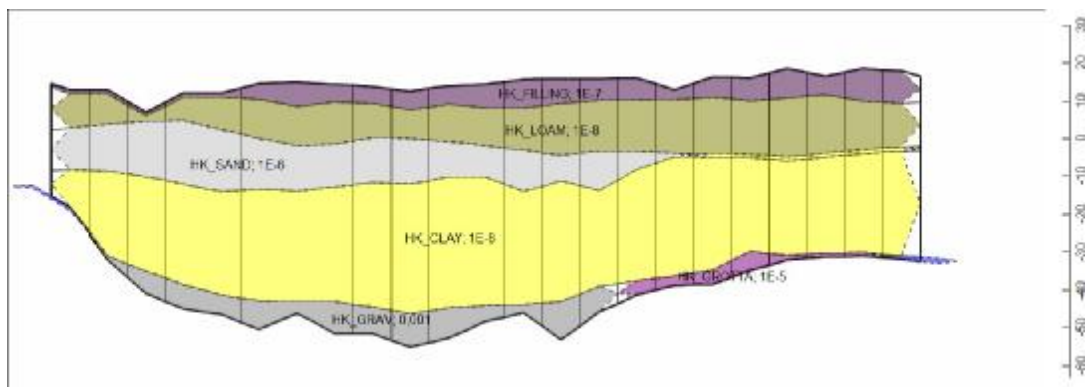
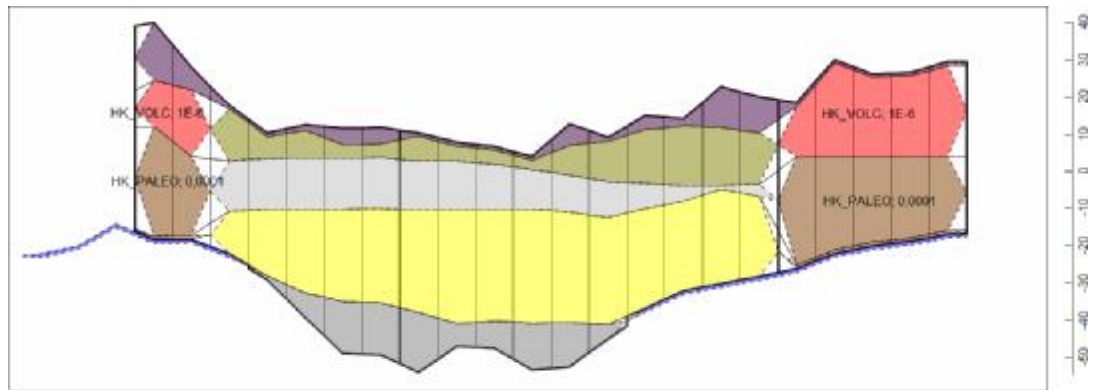


Figure 4.45. The values shown above were defined as HK parameters under LPF package in MODFLOW.



(a)



(b)

Figure 4.46. (a) Schematic view of vertical grid discretization
 (b) initial general hydraulic conductivity values of the starting simple Valco S.Paolo model

4.4.2. Boundary conditions

Direct “Recharge” was not considered because urban areas are usually very impermeable and the rainflow goes to sewers, and then, the river effect is so high that the recharge rate can be considered irrelevant at this scale.

The specified-head boundaries are constituted at the outline of two category; for the first four layer, the 10 m isopiezometer contour value of the general water table of Rome (Fig.4.47) was defined as “Constant Head” boundary at the east and west side of the active model domain. This boundary condition is available from the layer 1 to layer 4.

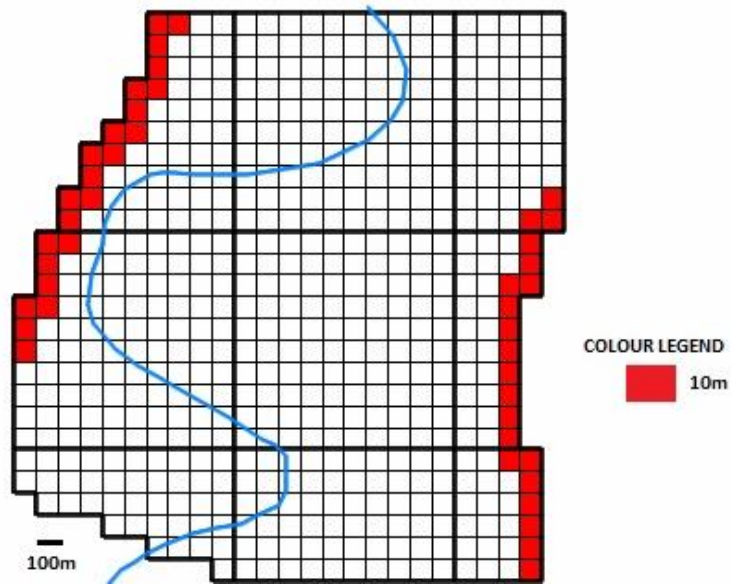


Figure 4.47. Constant head boundaries of convertible aquifers from Layer 1 to 4

In addition to the eastern specified head boundary, estimated values according to the potentiometric water table of the confined aquifer, 4 m a.s.l. in the north and 2 m a.s.l. in the south together with 10 m a.s.l. in the east Grotta Perfetta basal gravel zone in layer five, assigned to the northern, southern and eastern specified heads.

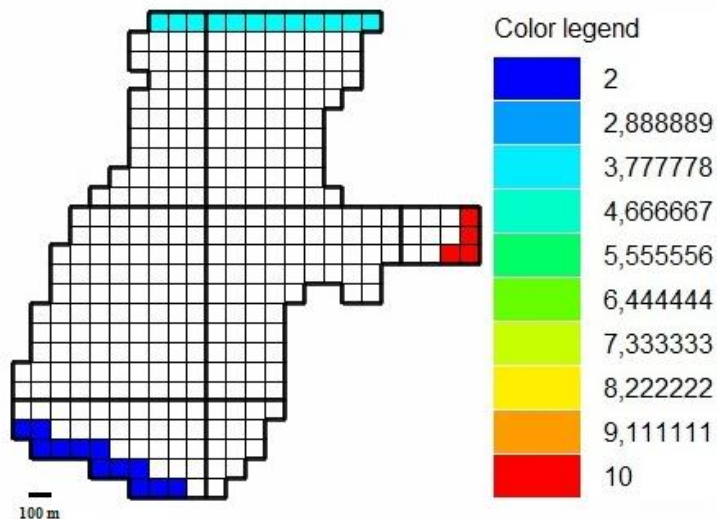


Figure 4.48. Constant head boundary of confined basal gravel aquifer

The Tiber river is represented by “River” boundary conditions (simulated by means of the River package). River bottom was assigned -6m. The measurements in 11.06.2010 were assigned to specify the Head Observation Package (HOB) (Table 4.4, 4.5).

Table 4.4. Head observations of the piezometers in sand

Piezometer in Sand	Level (m)
P5	1,91
P1	1,89
P6	1,8
VicSavini_SC	2,57
VicSavini_SB	2,45
Vivaio	3,15

Table 4.5. Head observations of the piezometers in gravel

Piezometer in Gravel	Level (m)
Eucalipti	2,34
P4	2,26
P2	2,19
Vasca Navale	2,40
VicSavini_SA	2,67
VicSavini_SBG	2,70
Vigili	2,24
Esso	3,15

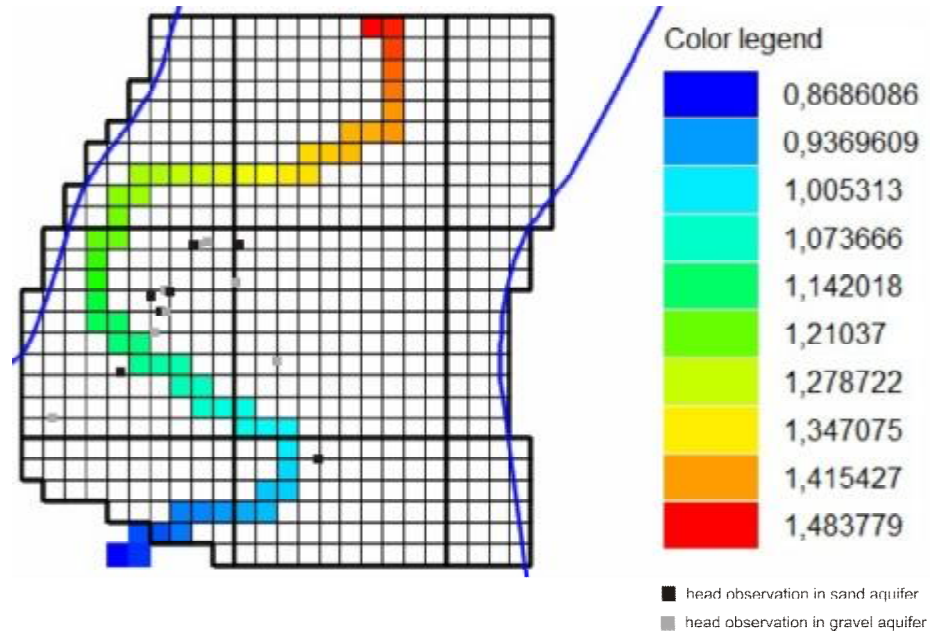


Figure 4.49. Head observation locations with Tiber river head change

As specified flux boundary conditions; the average pumping rates had calculated for five observed wells pumping along 4 hour per day for each of them (simulated by means of the Well Package) (Table 4.6).

Table 4.6. Pumping rates of wells

Well no:	Pumping rate (l/s)	Average pumping rate (m ³ /day)
Eucalipti	2,5	0,0004167
Vigili	2,2	0,0003667
Esso	0,5	0,0000833
Pian2Torri	0,5	0,0000833
Vivaio	1	0,0001667

4.4.3. Steady-state model calibration

Temporal dimensionality has chosen as steady-state to coordinate with data availability, a steady-state model without pumping is developed first and used to produce a preliminary overlook before pumping is applied. At steady-state without pumping, outflow occurs only as discharge to the river with about $1,91 \times 10^{-7} \text{ L}^3/\text{T}$ (Figure 4.50). In the first execute of this version (without pumping), percent discrepancy in the water budget was % 2,58 even though % 1 would be high. In order to fix the discrepancy to %0, HCLOSE and RCLOSE had set to $1\text{E}-6$ from Preconditioned Conjugate Gradient Package (PCG) (Richard B.Winston, from personal communication, 2010) (Figure 4.51)

```

DRAWDOWN WILL BE SAVED ON UNIT 38 AT END OF TIME STEP 1, STRESS PERIOD 1
VOLUMETRIC BUDGET FOR ENTIRE MODEL AT END OF TIME STEP 1 IN STRESS PERIOD 1
-----
CUMULATIVE VOLUMES      L**3      RATES FOR THIS TIME STEP      L**3/T
-----
IN:
---
STORAGE = 0.0000
CONSTANT HEAD = 8.9639E-03
RIVER LEAKAGE = 0.0000
TOTAL IN = 8.9639E-03
OUT:
----
STORAGE = 0.0000
CONSTANT HEAD = 6.3281E-03
RIVER LEAKAGE = 2.6359E-03
TOTAL OUT = 8.9641E-03
IN - OUT = -1.9185E-07
PERCENT DISCREPANCY = 0.00
IN:
---
STORAGE = 0.0000
CONSTANT HEAD = 8.9639E-03
RIVER LEAKAGE = 0.0000
TOTAL IN = 8.9639E-03
OUT:
----
STORAGE = 0.0000
CONSTANT HEAD = 6.3281E-03
RIVER LEAKAGE = 2.6359E-03
TOTAL OUT = 8.9641E-03
IN - OUT = -1.9185E-07
PERCENT DISCREPANCY = 0.00

```

Figure 4.50. Water budget of the steady-state model without pumping

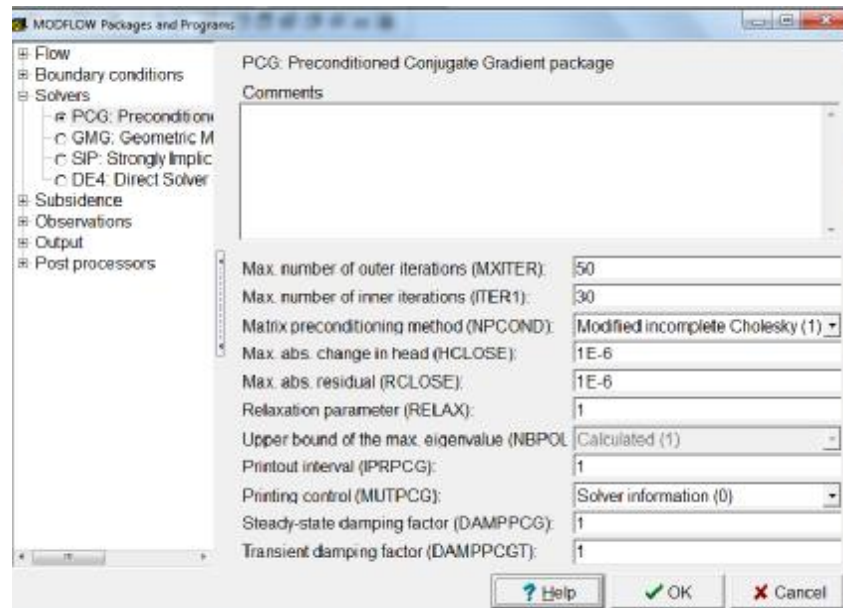


Figure 4.51. PCG Pane dialog box

In the model with plotted pumping ratio, as expected from a steady-state model, the volume of in-out is equal to zero (Figure 4.52).

VOLUMETRIC BUDGET FOR ENTIRE MODEL AT END OF TIME STEP 1 IN STRESS PERIOD 1

CUMULATIVE VOLUMES	L**3	RATES FOR THIS TIME STEP	L**3/T
IN:		IN:	
---		---	
STORAGE =	0.0000	STORAGE =	0.0000
CONSTANT HEAD =	5.3416E-03	CONSTANT HEAD =	5.3416E-03
WELLS =	0.0000	WELLS =	0.0000
RIVER LEAKAGE =	0.0000	RIVER LEAKAGE =	0.0000
TOTAL IN =	5.3416E-03	TOTAL IN =	5.3416E-03
OUT:		OUT:	
----		----	
STORAGE =	0.0000	STORAGE =	0.0000
CONSTANT HEAD =	5.1584E-04	CONSTANT HEAD =	5.1584E-04
WELLS =	1.1167E-03	WELLS =	1.1167E-03
RIVER LEAKAGE =	3.7090E-03	RIVER LEAKAGE =	3.7090E-03
TOTAL OUT =	5.3416E-03	TOTAL OUT =	5.3416E-03
IN - OUT =	0.0000	IN - OUT =	0.0000
PERCENT DISCREPANCY =	0.00	PERCENT DISCREPANCY =	0.00

Figure 4.52. Water budget of the steady-state model with pumping

Initial hydraulic conductivity values were assigned starting from bibliography (Bozzano, 2000) and intervals used in modified model based on literature (Spitz and Moreno, 1996) (Table 4.7).

Table 4.7. Calibration parameters used in model and intervals

Parameter	Calibration interval	Starting value	Calibrated value
Hydraulic conductivity (m/s)			
K _{xy} -1 (Gravel)	0,001 - 0,0001	1E-3	2E-4
K _{xy} -2 (Sand)	0,000001 - 0,0000007	1E-6	6E-7
K _{xy} -3 (Grotta)	0,00001 - 0,00006	1E-5	5E-5
K _{xy} -4 (Clay)	0,00000001 - 0,0000002	1E-8	1E-7
K _{xy} -5 (Paleo)	0,0001 - 0,00001	1E-4	1E-5
K _{xy} -6 (Loam)	0,00000001 - 0,0001	1E-8	1E-5
K _{xy} -8 (Filling)	0,0000001 - 0,00001	1E-7	1E-6
Constant Head (m)			
CH of Gravel North	4,1 - 3,5	4	3,5
CH of Gravel South	2,1 - 1,95	2	1,95

The parameters to calibrate were initially chosen as horizontal hydraulic conductivities and secondly, supported with the constant heads of confined gravel. A decreasing occurred in the southwest part of the valley when the HK of gravel was set to a low value.

During the initial stages of calibration, it was observed that the major deviations between the observed and simulated heads exist in the southwestern and eastern part of the flow domain in layer 3. The well named Vivaio, which located near the southeast hills was decreasing and became similar to observed value whilst the HK parameter of Paleotiber had set to 1E-5. A remarkable point is while the HK of clay had been increased, the head values of gravel in the center of the study area was effecting from this. The average of residuals are 0,6 m (Figure 4.53).

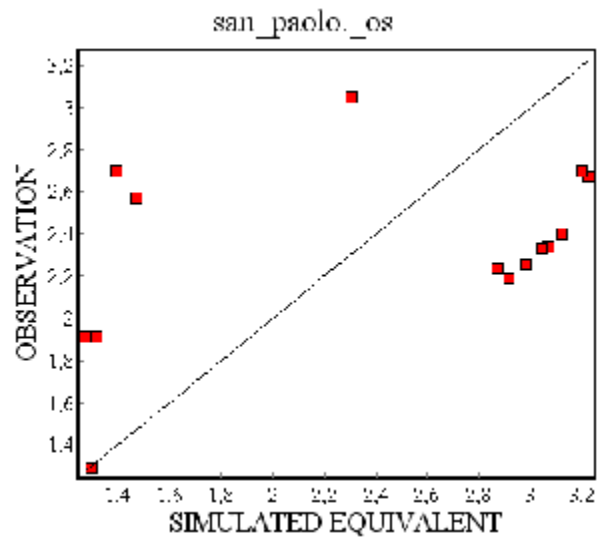


Figure 4.53. Comparison between observed and simulated heads of first model execute before calibration with pumping rates

At the end of calibration, the fit between observed - simulated values had arrived the optimum proximity to the equity line (1:1) shown in the scattered diagram (Figure 4.54). The average of residuals are 0,15 m (Figure 4.55).

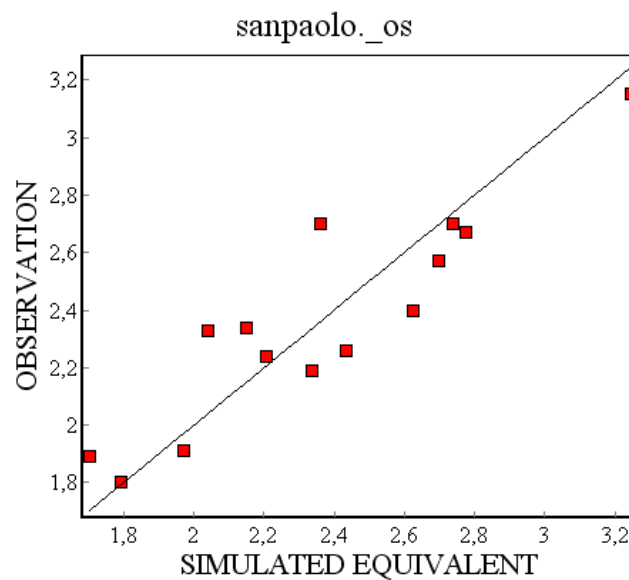


Figure 4.54. Calibrated Valco S.Paolo model fitting

HEAD AND DRAWDOWN OBSERVATIONS			
OBSERVATION NAME	OBSERVED VALUE	SIMULATED VALUE	DIFFERENCE
Eucalipti	2.3399999142	2.1510238647	0.18897604942
P4	2.2599999905	2.4353590012	-0.17535901070
P5	1.9099999666	1.9712331295	-6.12331628799E-02
P1	1.8899999857	1.7031369209	0.18686306477
P2	2.1900000572	2.3360228539	-0.14602279663
P6	1.7999999523	1.7939327955	6.06715679169E-03
Vasca_Navale	2.4000000954	2.6246757507	-0.22467565536
VicSavini_SC	2.5699999332	2.6972467899	-0.12724685669
VicSavini_SA	2.6700000763	2.7768032551	-0.10680317879
VicSav_SBG	2.7000000477	2.7397227287	-3.97226810455E-02
VicSavini_SB	2.7000000477	2.3593285084	0.34067153931
Vigili	2.2400000095	2.2047600746	3.52399349213E-02
Esso	2.3299999237	2.0419468880	0.28805303574
Vivaio	3.1500000954	3.2456862926	-9.56861972809E-02
SUM OF SQUARED DIFFERENCE:		4.15575E-01	

Figure 4.55. Calibrated observed-simulated values and residuals

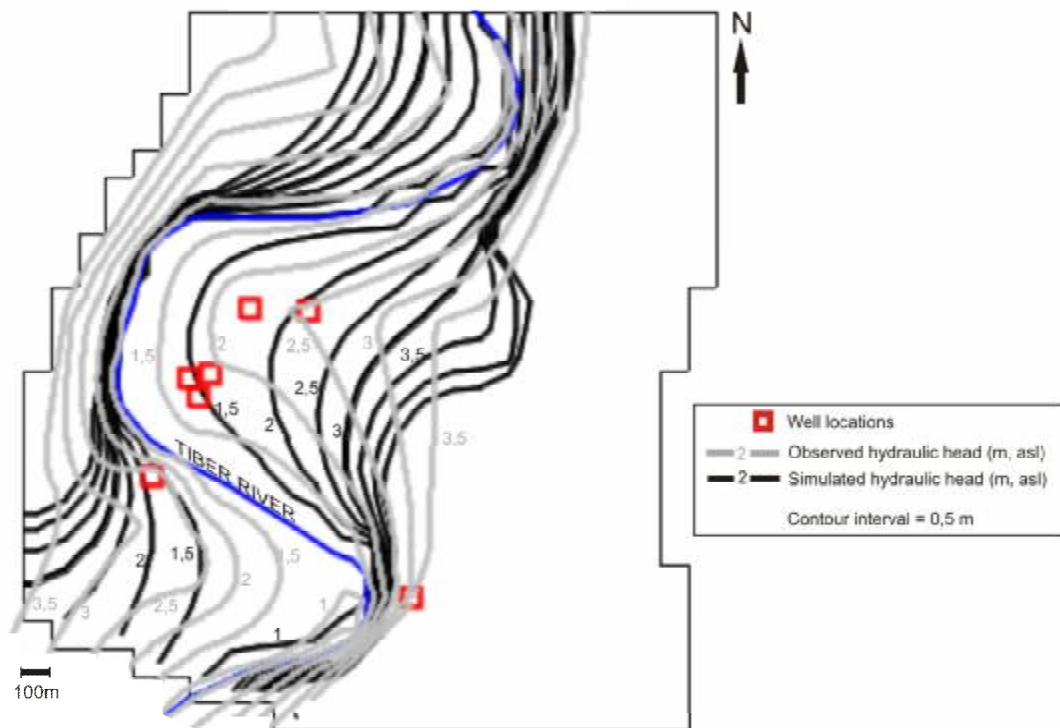


Figure 4.56. Observed and simulated hydraulic heads distribution of sand aquifer

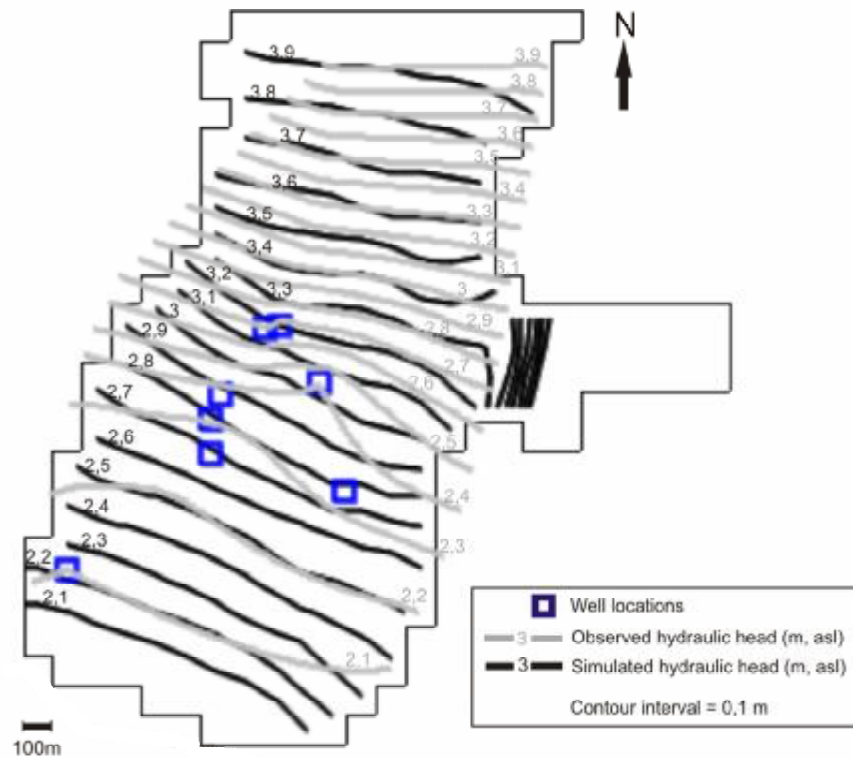


Figure 4.57. Observed and simulated hydraulic heads distribution of gravel aquifer

The difference between observed and simulated values has been considered acceptable considering the dimension of cells and the scale of the study.

Next stage was analysing the steady-state model verification. The simulation had executed one more time with another day head measuings to verify whether the quality of the calibration is similar. To do this, boundary conditions of sand have changed by modifying the river stage and the sand level observations according to the measuring data of a previous day (28.05.2010). The river stage values had considered with varied from the north 2,13 m a.s.l. to the south 1,67 m a.s.l. The average of residuals are 0,18 m a.s.l. (Figure 4.58).

HEAD AND DRAWDOWN OBSERVATIONS			
OBSERVATION NAME	OBSERVED VALUE	SIMULATED VALUE	DIFFERENCE
Eucalipti	2.3399999142	2.2413468361	9.86530780792E-02
P4	2.2599999905	2.5246317387	-0.26463174820
P5	2.7100000381	2.3699488640	0.34005117416
P2	2.1900000572	2.4244165421	-0.23441648483
Vasca_Navale	2.4000000954	2.7082657814	-0.30826568604
VicSavini_SC	3.0799999237	2.9577507973	0.12224912643
VicSavini_SA	2.6700000763	2.8569350243	-0.18693494797
VicSav_SBG	2.7000000477	2.8219680786	-0.12196803093
VicSavini_SB	2.9400000572	2.6574530602	0.28254699707
Vigili	2.2400000095	2.2901549339	-5.01549243927E-02
Esso	2.3299999237	2.0768260956	0.25317382812

Figure 4.58. Observed-simulated head values and residuals with measurings of date 28.05.2010 to verify the model

5. CONCLUSION

Key elements of the conceptual model were defining the model boundaries, simplifying the aquifer system, and determining the required model dimension to produce meaningful conclusions. Selecting model boundaries; in the center, Tiber river forms a natural boundary separated the model area as a head-dependent flux which has connection mainly with sand unit of the Holocene alluvium. Ten meter general water table of Rome has chosen as the constant head and surrounded the study area on the east and west sides encloses the all superficial aquifers in addition to volcanic origin basal gravel of Grotta Perfetta tributary. Although very limited borehole had evidence of a geologically interrelationship between the Tiber and Grotta perfetta basal gravels, a walloping hydrogeologic relation did not thought of among them.

Tiber river and deep aquifer systems in the investigated area are, separated by thick (~30m) layer of low permeability clay unit which contains organic peat levels. In the model, should be focused on data of pumping rates in depth and having at least one well in each layer in order to have a satisfactory result.

A more detailed representation of the shallow aquifer system seemed unnecessary due to the lack of data. Moreover, there are several difficulties to work in an urbanized area; construction of private buildings can avert to measure all the wells around, hard to comprise in an account the real pumping rates and estimate drawdown and another problem of Valco San Paolo in terms of urbanizing is founded near the boundaries of Tiber river water courses which has the flood risk especially in December-January of winter period.

The observed heads in the deep aquifer system do not correspond to the water table in the river, however which the interesting thing is the incredible water level rising in the gravel besides sand during the flood event of San Paolo in December 2009. At the time this modeling effort was undertaken, the hydrogeologic flow fundamentals of the alluvium was generally well understood. Some further development of our research are still in evaluation to understand where is the exact local sand units within the clay unit and seek for a connection by them

between the basal gravels and the sands. Therefore, this uncertain interconnection would be the answer of the water level rising in gravel aquifer observed by monitoring wells.

Results, in fact, show clearly the importance of applying not only trial-and-error or inverse distance automatic estimation methods for calibration but also to be prepared to change own conceptual model starting from collecting new hydrogeologic data to better understand the system (La Vigna, 2009). The proposed model is deemed to be a valid tool for predicting the evolution of hydraulic heads.

The most important thing should be considered that the proposed conceptual model is “local” it is just valid for Valco S.Paolo area. The mentioned connection within clay unit is out of the study area and out of the conceptual model.

Currently, the results of this model can help the projects including the geothermal investigations and new urban development plans of Valco San Paolo in terms of a strategic place in Rome. In fact, even if Modflow doesn't simulate heat transport, the local conceptual model and the current simulated groundwater flow process can help the further studies giving a base to start.

The flow model of the deep aquifer suggests a starting point for the purposes of its detailed geologic, geomorphologic and hydrogeological features. Further development of this study will be the automatic estimation methods for calibration and perform a sensitivity analysis. Successful verification of the groundwater flow model results in a higher degree of confidence in model predictions. A calibrated but unverified model may still be used to perform predictive simulations when coupled with a careful sensitivity analysis.

Another possible development of the research activity on Valco San Paolo could focus on considering transient data and transient simulations with changing the value of the constant head in gravels with time.

REFERENCES

- ALBANI, R., LOMBARDI, L., & VICINANZA, P., 1972. Idrogeologia della Città di Roma. *Ingegneria sanitaria*, 20 (3), Roma.
- AMBROSETTI, P., BONADONNA, FP.; 1967. Revisione dei dati del Plio-Pleistocene di Roma. *Atti Acc G Sci Nat Catania* 18: 33–70.
- ASTM International, 2004. Standard Guide for Application of a Ground-Water Flow Model to a Site-Specific Problem.
- ASTM International, 2006. Standard Guide for Documenting a Ground-Water Flow Model Application.
- BARBERI, F., CARAPEZZA, M.L., GIORDANO, G., PENSA, A., RANALDI, M.; 2008. L'acquifero nelle ghiaie di base del Tevere: una risorsa geotermica per la città di Roma (The geothermal resources of the city of Rome: the case study of the confined aquifer within the basal conglomerate of the Tiber river alluvial deposits. *La Geologia di Roma dal Centro Storico alla Periferia, Parte Prima. SELCA- Firenze*, 443p, 407-420.
- BELLOTTI, P., CHIOCCHINI, U., CASTORINA, F., TOLOMEO, L., 1994. Le unità clastiche plio-pleistoceniche tra Monte Mario (città di Roma) e la costa tirrenica presso Focene: alcune osservazioni sulla stratigrafia sequenziale. *Boll Serv Geol Ital CXIII*:3–24.
- BIGI, G., COSENTINO, D., PAROTTO, M., SARTORI, R., SCANDONE, P., 1990. Structural Model of Italy 1:500.000. C.N.R.-P.F.G., *Quaderni della Ricerca Scientifica* 114.
- BONI, C., BONO, P. & CAPELLI, G., 1986. Schema idrogeologico dell'Italia centrale. *Mem. Soc. Geol. It.*, 35, Roma.
- BONINI, M., 1997. Chronology of deformation and analogue modelling of the Plio-Pleistocene "Tiber Basin" implications for the evolution of the Northern Apennines (Italy).
- BOZZANO, F., FUNICIELLO, R., GAETA, M., MARRA, F., ROSA, C., VALENTINI, G; 1997. Recent alluvial deposit in Rome (Italy): morpho-stratigrafic,

- mineralogical and geomechanical characterisation. Proc. Int. Symp. Engineering geology and Environment, Publ 1, 1193-1198.
- BOZZANO, F., ANDREUCCI, A., GAETA, M., SALUCCI, R.; 2000. A geological model of the buried Tiber River valley beneath the historical centre of Rome. Bull. Eng. Geol. Env., 59, 1-21.
- BOZZANO, F., CASERTA, A., GOVONI, A., MARRA, F., and MARTINO, S.; 2008. Static and dynamic characterization of alluvial deposits in the Tiber River Valley: New data for assessing potential ground motion in the City of Rome. Journal of Geophysical Research, vol. 113, B01303, 1-21.
- CALVO, B., SAVÌ, F., NAPOLITANO, G., SEE, L.M., IRVINE, B. AND HEPPENSTALL, A.J. 2008. A conceptual and neural network model for real-time flood forecasting of the Tiber River in Rome. Capri, 13-15 Oct 2008.
- CAMPOLUNGI, M.P., CAPELLI, G., FUNICIELLO, R., LANZINI, M.; 2007. Geotechnical studies for foundation settlement in Holocenic alluvial deposits in the City of Rome (Italy). Elsevier B.V. Engineering Geology 89 (2007) 9–35.
- CAPELLI, G., MAZZA, R., GIORDANO, G., CECILI, A., DE RITA, D., SALVATI, R., 2000. The Colli Albani Volcano (Rome, Italy): equilibrium breakdown of a hydrogeological unit as a result of unplanned and uncontrolled over-exploitation. Hydrogéologie, 4, 63-70.
- CAPELLI, G., MAZZA, R., 2005. Schema idrogeologico della Città di Roma- Gestione della risorse idrica e del rischio idrogeologico. In: Atti del convegno “la IV Dimensione- Lo spazio sotterraneo di Roma” Geologia dell’Ambiente- periodico trimestrale della SIGEA (Società Italiana di Geologia Ambientale), Anno XIII n°4 (supplemento), Roma, p. 47-58.
- CAPELLI, G., MAZZA, R. & GAZZETTI, C., (a cura di) 2005. Strumenti e strategie per la tutela e l’uso compatibile della risorsa idrica nel Lazio- Gli acquiferi vulcanici. Quaderni di Tecniche di Protezione Ambientale n.78. Pitagora Editrice, 216pp., 4 tavv.f.t., 21 tavv.f.t. su CD-ROM allegato.
- CAPELLI, G., MAZZA, R., TAVIANI, S.; 2008. Acque sotterranee nella città di

- Roma (Groundwater in the city of Rome). *La Geologia di Roma dal Centro Storico alla Periferia, Parte Prima*. SELCA- Firenze, 443p, 221-245
- CARAPEZZA, M. L., BADALAMENTI, B., CAVARRA, L. & SCALZO, A. 2003. Gas hazard assessment in a densely inhabited area of Colli Albani Volcano (Cava dei Selci, Roma). *J. Volcanol. Geotherm. Res.* 123, 81-94.
- CARBONI, M. G., IORIO, D., 1997. Nuovi dati sul Plio-Pleistocene marino del sottosuolo di Roma. *Bollettino della Società Geologica Italiana* 116, 435–451.
- CINTI, F. R., MARRA, F., BOZZANO, F., CARA, F., DI GIULIO, G. and BOSCHI, E.; 2008. Chronostratigraphic study of the Grottaperfetta alluvial valley in the city of Rome (Italy): investigating possible interaction between sedimentary and tectonic processes. *Annals of Geophysics*, vol. 51, n. 5/6.
- COPPA, G., PEDICONI, L., AND BARDI, G., 1984. Acque e acquedotti a Roma.
- CORAZZA, A., LOMBARDI, L., 1995. Idrogeologia del centro Storico di Roma. In: Funicello R (ed) *La geologia di Roma. Il Centro Storico*. Mem Desc Carta Geol Ital 50: 179–208.
- CORAZZA A., LANZINI M., ROSA C., SALUCCI R.; 1999. Caratteri stratigrafici, idrogeologici e geotecnici delle alluvioni tiberine nel settore del centro storico di Roma. *Il Quaternario*, 12, 215-235.
- CORAZZA, A., GIORDANO, G., DE RITA, D.; 2005. Hydrogeology of the city of Rome. *Geological Society of America Special Paper* 408, pp113-116.
- CORAZZA, A., GIORDANO, G., and DE RITA, D., 2006. Hydrogeology of the city of Rome, in Heiken, G., ed., *Tuffs—Their properties, uses, hydrology, and resources: Geological Society of America Special Paper* 408, p. 113–118, doi: 10.1130/2006.2408(4.2).
- DI DOMENICANTONIO, A., CASSIANI, B., RUISI, M., TRAVERSA, P., 2009. *Quantitative Hydrogeology in the Tevere River Basin Management Planning (Central Italy)*
- FUNICIELLO, R., (ed), 1995. *La Geologia di Roma. Il Centro storico*. Mem Desc Carta Geol Ital 50: 550.

- FUNICIELLO, R., GIORDANO G., DE RITA, D., 2003. The Albano maar lake (Colli Albani Volcano, Italy): recent volcanic activity and evidence of pre-Roman Age catastrophic lahar events. *Journal of Volcanology and Geothermal Research*, 123, 43-61.
- FUNICIELLO, R., TESTA, O., CAMPOLUNGHÌ, M.P., LANZINI, M., CECILI, A., 2004. La struttura Geologica dell'area Romana e il Tevere—Atti del Convegno “Ecosistema Roma” 14/16 Aprile 2004. *Accademia Nazionale dei Lincei*.
- FUNICIELLO R., GIORDANO G. (ED.), 2005. Carta Geologica di Roma alla scala 1:10000 (18 tavole, 3 profili), vol. 1, Dipartimento Scienze Geologiche Università Roma TRE – Comune di Roma- APAT.
- FUNICIELLO, R., GIORDANO, G., MATTEI, M., 2008. Geological Map of Roma Municipality, scale 1:50.000, *La Geologia di Roma dal Centro Storico alla Periferia, Parte Prima*. SELCA- Firenze.
- GIORDANO, G., MAZZA, R., CAPELLI, G., FUNICIELLO, R., PAROTTO, M., 2004. Geological surveying in a metropolitan area: the southern suburbs of Rome. In: Pasquaré, G., Venturini, C., Gropelli, G. (Eds.), *Mapping Geology in Italy, A Cura Di*. Dipartimento Difesa del Suolo—Servizio Geologico d'Italia, pp. 113–122.
- HARBAUGH, A.W., 2005. MODFLOW-2005, the U.S. Geological Survey modular ground-water model—The ground-water flow process: U.S. Geological Survey Techniques and Methods 6–A16, variously paged.
- HILL, M.C. and TIEDEMAN, C.R. 2007. *Effective Groundwater Model Calibration with Analysis of Data, Sensitivities, Predictions, and Uncertainty*: Hoboken, New Jersey, Wiley Interscience, 455 p.
- LA VIGNA, F., HILL, M C., 2008. Rossetto R. Ground Water modeling of the Acque Albule hydrothermal system. Rome – Italy. *Hydropredict 2009*. Prague – Czech Republic, 2008.
- LA VIGNA, F., ROSSETTO, R., MAZZA, R., 2009. Ground water model calibration using geology information along with sensitivity analysis and estimation methods (UCODE-2005), the Acque Albule model, Rome.(Italy)

- MARRA, F., 1993. Stratigrafia ed assetto geologico-strutturale dell'area romana compresa tra il Tevere e Rio Galeria. *GeolRom* 29: 515–535
- MARRA, F., ROSA, C., 1995. Stratigrafia e assetto geologico dell'area romana. In: Funicello, R. (Ed.), *La geologia di Roma; il centro storico*. Vol. 50 of *Memorie Descrittive della Carta Geologica d'Italia*. Servizio Geologico d'Italia, pp. 49–118.
- MARRA, F., 2001. Strike-slip faulting and block rotation: a possible triggering mechanism for lava flows in the Alban Hills, *J. of Struct. Geol.*, 23 (1), 127-141.
- MCDONALD, M.G. AND HARBAUGH, A.W., 1988. A modular three-dimensional finite-difference ground-water flow model: U.S. Geological Survey Techniques of Water-Resources Investigations, book 6, chap. A1, 586 p.
- PARKHURST, D.L., KIPP, K.L., ENGESGAARD, PETER, AND CHARLTON, S.R., 2004. PHAST—A program for simulating ground-water flow, solute transport, and multicomponent geochemical reactions: U.S. Geological Survey Techniques and Methods 6–A8, 154 p.
- PAROTTO, M., 1990. “Geologia e idrogeologia del centro storico di Roma”. Progetto strategico Roma capitale. C.N.R. (1990)
- PISANI SARTORIO, G. And A.M. LIBERATI SILVERIO, eds. 1986. *Il trionfo dell'acqua: Acque e Acquedotti a Roma, IV.sec. a.C.-XX.sec.Rome*
- PREZIOSI, E., E, ROMANO., 2009. From a hydrostructural analysis to the mathematical modelling of regional aquifers. *Italian Journal of Engineering Geology and Environment*, 1, 183-198.
- RASPA, G., MOSCATELLI, M., STIGLIANO, F., PATERA, A., MARCONI, F., FOLLE, D., VALLONE, R., MANCINI, M., CAVINATO, G. P., MILLI, S., COIMBRA LEITE COSTA, J. F., 2009. Geotechnical characterization of the upper Pleistocene–Holocene alluvial deposits of Roma (Italy) by means of multivariate geostatistics: Cross-validation results
- SPITZ, K., MORENO, J.; 1996. *A Practical Guide to Groundwater and Solute Transport Modeling*. John Wiley & Sons, Inc., United States, 461 p.

- STRAMONDO, S., BOZZANO, F., MARRA, F., WEGMULLER, U., CINTI, F.R., MORO, M., SAROLI, M., 2008. Elsevier Inc. Subsidence induced by urbanization in the city of Rome detected by advanced InSAR technique and geotechnical investigations.
- TUCCIMEI, P., GIORDANO, G., TEDESCHI, M., 2006. CO2 release variations during the last 2000 years at the Colli Albani volcano (Roma, Italy) from speleothems studies. *Earth and Planetary Science Letters*, 243 (3-4), 449-462.
- VENTRIGLIA, U., 1971. *La geologia della città di Roma*. Amministrazione Provinciale di Roma, Roma, 417 pp.
- VENTRIGLIA, U., 1990. *Idrogeologia della Provincia di Roma*: Roma, Provincia di Roma. 255 p
- VENTRIGLIA, U.; 2002: *Geologia del Territorio del comune di Roma*. Amministrazione Provinciale di Roma, Roma, pp809.
- VIAROLI, S.; 2007: *Caratterizzazione idrogeologica dell'area di Valco S.Paolo (Roma)*. Università degli Studi Roma Tre, Facoltà di Scienze Matematiche Fisiche e Naturali, Saggio di laboratorio in Geologia Applicata, BSc. Thesis, unpublished.
- WINSTON, R.B., 2009, ModelMuse—A graphical user interface for MODFLOW–2005 and PHAST: U.S. Geological Survey Techniques and Methods 6–A29, 52 p., available only online at <http://pubs.usgs.gov/tm/tm6A29>.
- USER'S MANUAL OF ARCMAP 9.2 ArcGIS® (ESRI, Inc.)

CURRICULUM VITAE

Zeynep DEMİRAY was born on August 26, 1986 in Istanbul. After completing her education in Erenköy primary and Seyhan Anatolian high school, she enrolled in Kocaeli University Geological Engineering Department in 2003. She had graduated from the Geological Engineer Department of Kocaeli University with a Bachelor's of Science degree in 2007. She started her Master of Science education under division of Applied Geology in Geological Engineering Department of Çukurova University in 2007. She has been carrying on her MSc. education since 2007.